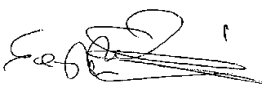




OPERATIONS REPORT

Issue 1/2018 rev. 2

Reporting period: January – June 2018

Authors			
Prepared by			
NAME		INSTITUTE	
Jari Hovila		FMI	
Contributions			
NAME		INSTITUTE	
Jari Hovila		FMI	
Axel Schmidt		DLR	
Pieter Valks		DLR	
Olaf Tuinder		KNMI	
Robert van Versendaal		KNMI	
Helge Jønch-Sørensen		DMI	
MariLiza Koukouli		AUTH	
Katerina Garane		AUTH	
Andy Delcloo		KMI	
Gaia Pinardi		BIRA-IASB	
Bavo Langerock		BIRA-IASB	
Wolfgang Steinbrecht		DWD	
Maya George		LATMOS	
Cathy Clerbaux		LATMOS	
Rosa Astoreca		ULB	
Daniel Hurtmans		ULB	
Pierre-François Coheur		ULB	
Carlos Vicente		EUMETSAT	
Approved by			
AC SAF Project Manager	Seppo Hassinen / FMI	10/12/2018	 Signature

Document change log

Revision	Date	Description of change
1	20/09/2018	Initial revision
2	10/12/2018	Required to be corrected by the Review Board of the AC SAF Operations Review 10: <ul style="list-style-type: none">- Sections 7.1, 7.3 and 7.7: Editorial changes- Section 7.5.1: Paragraph describing the contents of the quality monitoring images added

List of abbreviations

AC SAF	Satellite Application Facility on Atmospheric Composition Monitoring
ARP	Absorbing Aerosol Index from PMDs data product
ARP-A	Absorbing Aerosol Index from PMDs data product from Metop-A
ARP-A-R1	Reprocessed Absorbing Aerosol Index from PMDs data record from Metop-A
ARP-B	Absorbing Aerosol Index from PMDs data product from Metop-B
ARP-B-R1	Reprocessed Absorbing Aerosol Index from PMDs data record from Metop-B
ARS	Absorbing Aerosol Index data product
ARS-A	Absorbing Aerosol Index data product from Metop-A
ARS-A-R1	Reprocessed Absorbing Aerosol Index data record from Metop-A
ARS-B	Absorbing Aerosol Index data product from Metop-B
ARS-B-R1	Reprocessed Absorbing Aerosol Index data record from Metop-B
ATMOS	Atmospheric Parameters Measured by in-Orbit Spectroscopy (DLR data service)
ATO	Assimilated Total Ozone
AUTH	Aristotle University of Thessaloniki
BIRA-IASB	Belgian Institute for Space Aeronomy
BrO	Bromine Oxide
CDOP	Continuous Development and Operations phase
CO	Carbon Monoxide
DLR	German Aerospace Center
DMI	Danish Meteorological Institute
DWD	German Weather Service
ECMWF	European Centre for Medium-Range Weather Forecasts
EDC	EUMETSAT Data Centre
EDD	Erythematous Daily Dose
EOWEB	Earth Observation on the WEB
EPS	European Polar System
EUMETCast	EUMETSAT's primary dissemination mechanism for the near real-time delivery of satellite data and products
EUMETSAT	European Organisation for the Exploitation of Meteorological Satellites
FMI	Finnish Meteorological Institute
GOME	Global Ozone Monitoring Experiment
H ₂ O	Water Vapour
HCHO	Formaldehyde
KNMI	Royal Netherlands Meteorological Institute
L1b	Level 1b data product
L1c	Level 1c data product
L2	Level 2 data product
L3	Level 3 data product

LER	Lambertian-equivalent reflectivity data record
NHP	Near Real-time High-resolution Ozone Profile data product
NO2	Nitrogen Dioxide
NRT	Near Real-time
NTO	Near Real-time Total Column data product
NUV	Near Real-time UV index data product
O3	Ozone
O3M SAF	Satellite Application Facility on Ozone and Atmospheric Chemistry Monitoring
OHP	Offline High-resolution Ozone Profile data product
OEM	Optimal Estimation Method
OOP	Offline Ozone Profile data product
OPERA	Ozone Profile Retrieval Algorithm
OTO	Offline Total Column data product
OUV	Offline Surface UV data product
PDU	Product Dissemination Unit
PGE	Product Generation Element
PMD	Polarisation Measurement Device
RD	Reference Document
RMS	Root Mean Square
RMSE	Root Mean Square Error
SO2	Sulphur Dioxide
TOC	Total Ozone Column data product
TrOC	Tropospheric Ozone Column data product
TTrOC	Tropical Tropospheric Ozone Column data product
UMARF	Unified Meteorological Archive Facility
UTC	Coordinated Universal Time

TABLE OF CONTENTS

1.	INTRODUCTION	8
1.1.	SCOPE.....	8
1.2.	REPORTING PERIOD	8
1.2.1.	<i>Highlights</i>	8
1.3.	REFERENCE DOCUMENTS	8
1.4.	DEFINITION OF TERMS	11
1.5.	ACCURACY REQUIREMENTS OF AC SAF PRODUCTS	11
2.	PROCESSING CENTRE: FMI.....	14
2.1.	OFFLINE SURFACE UV	14
2.1.1.	<i>Availability.....</i>	14
2.1.2.	<i>Timeliness</i>	14
2.2.	SERVICES, MAIN EVENTS AND ANOMALIES	15
3.	PROCESSING CENTRE: DLR.....	18
3.1.	NRT AND OFFLINE TOTAL/TROPOSPHERIC TRACE GAS COLUMNS	18
3.1.1.	<i>Availability.....</i>	18
3.1.2.	<i>Timeliness</i>	20
3.2.	SERVICES, MAIN EVENTS AND ANOMALIES	22
4.	PROCESSING CENTRE: KNMI.....	24
4.1.	NRT AND OFFLINE HIGH-RESOLUTION OZONE PROFILES, ABSORBING AEROSOL INDEXES, TROPOSPHERIC OZONE (OZONE PROFILES).....	24
4.1.1.	<i>Availability.....</i>	24
4.1.2.	<i>Timeliness</i>	25
4.2.	SERVICES, MAIN EVENTS AND ANOMALIES	27
5.	PROCESSING CENTRE: DMI.....	30
5.1.	NRT CLEAR-SKY AND CLOUD-CORRECTED UV INDEX	30
5.1.1.	<i>Availability.....</i>	30
5.1.2.	<i>Timeliness</i>	30
5.2.	SERVICES, MAIN EVENTS AND ANOMALIES	31
6.	PROCESSING CENTRE: EUMETSAT	32
6.1.	NRT IASI CO AND SO2.....	32
6.1.1.	<i>Availability.....</i>	32
6.1.2.	<i>Timeliness</i>	32
6.2.	SERVICES, MAIN EVENTS AND ANOMALIES	33
7.	VALIDATION AND QUALITY MONITORING.....	35
7.1.	TOTAL OZONE COLUMN PRODUCTS.....	35
7.1.1.	<i>GOME-2A and GOME-2B GDP-4.8 total ozone column validation</i>	35
7.1.2.	<i>Validation website update.....</i>	40
7.1.3.	<i>Online quality monitoring.....</i>	45
7.2.	TROPOSPHERIC OZONE PRODUCTS	48
7.3.	TRACE GAS PRODUCTS.....	51
7.3.1.	<i>Online quality monitoring.....</i>	76
7.4.	OZONE PROFILE PRODUCTS.....	82
7.4.1.	<i>Online quality monitoring.....</i>	84
7.5.	AEROSOL PRODUCTS	86

7.5.1.	Online quality monitoring.....	86
7.6.	UV PRODUCTS.....	87
7.6.1.	Online quality monitoring.....	87
7.7.	IASI NRT PRODUCTS	88
8.	LIST OF AC SAF USERS.....	101
9.	UPDATES DURING THE REPORTING PERIOD.....	112
9.1.	SOFTWARE UPDATES	112
9.2.	HARDWARE UPDATES	112
9.3.	DOCUMENTATION UPDATES.....	112
10.	CHANGES AND USAGE STATISTICS OF THE WEB PORTAL	113
10.1.	CHANGES IN APPEARANCE AND CONTENT	113
10.2.	WEB PAGE STATISTICS.....	114
APPENDIX 1.....		116
APPENDIX 2.....		122

1. Introduction

1.1. Scope

The scope of this document is to summarise the operational activities concerning the products in operation and the associated services during the reporting period to see that the general requirements applicable to these services and products of the AC SAF [RD1-RD3] are fulfilled. Intended readers of this document are the members of AC SAF project team, Review Board of the annual Operations Review, AC SAF Steering Group and EUMETSAT OPS/WG as well as the users of the AC SAF products.

Operations Reports include information about product availability/timeliness, quality assurance, website usage, and delivery statistics. Main events, major anomalies and software/hardware updates are reported also. AC SAF Operations Report is published twice a year.

1.2. Reporting period

This Operations Report covers the period January – June 2018.

1.2.1. Highlights

New products

The following products were declared operational:

- IASI NRT SO₂ (O3M-57) from Metop-A&B

New data records

The following data records were released:

- NO₂ and H₂O climate data records (O3M-87, O3M-88) from Metop-A&B

1.3. Reference documents

Table 1.1. Operations Report reference documents

Reference	Title	Issued	Reporting period
RD1	Product Requirements Document (SAF/AC/FMI/RQ/PRD/001)	27/06/2017	N/A
RD2	Service Specification (SAF/AC/FMI/RQ/SESP/001)	19/04/2017	N/A
RD3	EUMETSAT Operational Services Specification (EUM/OPS/SPE/09/0810)	14/08/2015	N/A
RD4	EPS End User Requirements Document (EPS/MIS/REQ/93001)		N/A
RD5	O3M SAF Validation Report for NRT, offline and reprocessed total ozone columns	11/12/2015	January 2007 – December 2014

Reference	Title	Issued	Reporting period
RD6	AC SAF Validation Report for NRT, offline, reprocessed and level 3 total/tropospheric NO ₂ columns	10/11/2017	Metop-A: January 2007 – July 2015 Metop-B: January 2013 – July 2015
RD7	O3M SAF Validation Report for Metop-A NRT and offline coarse/high-resolution ozone profiles	20/02/2012	January 2007 – May 2011
RD8	O3M SAF Validation Report for Metop-B NRT and offline coarse/high-resolution ozone profiles	30/06/2013	December 2012 – April 2013
RD9	O3M SAF Validation Report for Metop-B NRT UV indexes	27/05/2013	May 2013
RD10	O3M SAF Validation Report for NRT, offline and reprocessed total SO ₂ columns	09/12/2015	January 2007 – December 2014
RD11	O3M SAF Validation Report for offline and reprocessed total BrO columns	09/12/2015	January 2007 – December 2014
RD12	O3M SAF Validation Report for NRT, offline and reprocessed total HCHO columns	30/10/2015	January 2007 – July 2015
RD13	O3M SAF Validation Report for offline and reprocessed total H ₂ O columns	30/10/2015	January 2007 – August 2015
RD14	O3M SAF Validation Report for NRT and offline aerosol products	25/06/2013	January 2007 – May 2013
RD15	O3M SAF Validation Report for Metop-B offline UV products	03/02/2015	June 2012 – May 2013
RD16	O3M SAF Validation Report for Metop-A reprocessed total ozone columns	19/02/2010	January 2007 – June 2009
RD17	AC SAF Validation Report for GOME-2 surface LER product	02/05/2017	N/A
RD18	O3M SAF Validation Report for offline tropospheric ozone columns (cloud slicing)	03/07/2015	January 2007 – December 2014
RD19	O3M SAF Validation Report for NRT and offline tropospheric ozone columns (ozone profiles)	09/09/2015	January 2007 – December 2014
RD20	O3M SAF Validation Report for NRT IASI CO	17/11/2015	September 2015 – November 2015

Reference	Title	Issued	Reporting period
RD21	AC SAF Validation Report for OClO data record	29/05/2017	January 2007 – September 2016
RD22	AC SAF Validation Report for NRT IASI SO2	17/11/2017	Metop-A: January 2007 – December 2013 June 2017 – October 2017 Metop-B: June 2017 – December 2017

Service Specification is available at https://acsaf.org/docs/AC_SAF_Service_Specification.pdf

Validation Reports are available at <https://acsaf.org/valreps.html>

1.4. Definition of terms

Availability is based on the definition in the EUMETSAT Operational Services Specification [RD3].

Product-specific clarifications:

- For NRT products, the monthly availability limit is 97.5 %. The availability is calculated as a “worst case scenario”:

$$\frac{\text{in time processed and disseminated L2 PDUs}}{\text{received L1b PDUs} + \text{missed L1b PDUs marked as “reception confirmed” in the EUMETCast sendlist}}$$

- For offline products, the availability is defined by the ratio of the number of in time processed, archived and quality-approved L2 products to the number of orbits for which L1b PDUs have been received per month. Availability limit for offline products is 95.5 %.
- NUV and OUV are daily L3 products, and availability is defined as the fraction of days in a month with products fulfilling the timeliness requirements.

Timeliness defines whether the product is near real time (NRT) product which is disseminated or ready for download in three hours from sensing at the latest or offline product which is available for download in two weeks after sensing at the latest, during system availability. System unavailability will in most cases not lead to loss of data but to delays with respect to the specified timeliness. In practice, timeliness of a product is determined by calculating the time from sensing to EUMETCast or archive upload. In the Operations Reports, the timeliness is presented as monthly average, minimum and maximum values.

Accuracy is defined as in the EPS End User Requirements Document [RD4]: the values of accuracy “represent RMS values” taking as reference the ‘true value’ measured by ground based instruments.

1.5. Accuracy requirements of AC SAF products

The following table lists all operational AC SAF products and their accuracy requirements as defined in [RD1].

Table 1.2. Accuracy requirements of AC SAF products

Product identifier	Product name	Product acronym	Threshold accuracy	Target accuracy	Means of quality assurance
O3M-01.1	NRT total O3	MAG-N-O3	20 %	4 % (SZA < 80°) 6 % (SZA > 80°)	Validation report
O3M-41.1		MBG-N-O3			
O3M-02.1	NRT total NO2	MAG-N-NO2	20 % of annual mean	8-15 % of annual mean	Online monitoring Validation report
O3M-50.1		MBG-N-NO2			
O3M-36.1	NRT tropospheric NO2	MAG-N-NO2TR	50 %	30 %	Online monitoring Validation report
O3M-52.1		MBG-N-NO2TR			
O3M-54.1	NRT total SO2	MAG-N-SO2	100 %	50 % (SZA < 70°)	Online monitoring Validation report
O3M-55.1		MBG-N-SO2			
O3M-176.0	NRT total HCHO	MAG-N-HCHO	100 %	50 % (polluted)	Online monitoring Validation report
O3M-177.0		MBG-N-HCHO			

Product identifier	Product name	Product acronym	Threshold accuracy	Target accuracy	Means of quality assurance
O3M-38	NRT high-resolution ozone profile	MAG-N-O3HRPR	30 % in stratosphere 70 % in troposphere	15 % in stratosphere 30 % in troposphere	Online monitoring Validation report
O3M-47		MBG-N-O3HRPR			
O3M-61.1	NRT absorbing aerorol index	MAG-N-AAI	1.0 index points	0.5 index points	Online monitoring Validation report
O3M-71.1		MBG-N-AAI			
O3M-62.1	NRT absorbing aerosol index from PMDs	MAG-N-AAIPMD	1.0 index points	0.5 index points	Online monitoring Validation report
O3M-72.1		MBG-N-AAIPMD			
O3M-91	NRT UV index, clear-sky	MBG-NUV_CLEAR	20 %	10 %	Online monitoring Validation report
O3M-92	NRT UV index, cloud-corrected	MBG-NUV_CLOUD	20 %	10 %	Online monitoring Validation report
O3M-181	NRT IASI CO	MAI-N-CO	25 % (normal conditions) 50 % (high pollution or low signal)	12 % (normal conditions) 20 % (high pollution or low signal)	Validation report
O3M-80		MBI-N-CO			
O3M-57	NRT IASI SO ₂	MxI-N-SO ₂	200 % (below 10 km) 100 % (above 10 km)	100 % (below 10 km) 35 % (above 10 km)	Validation report
O3M-06.1	Offline total O ₃	MAG-O-O ₃	20 %	3 % (SZA < 80°) 6 % (SZA > 80°)	Validation report
O3M-42.1		MBG-O-O ₃			
O3M-07.1	Offline total NO ₂	MAG-O-NO ₂	20 % of annual mean	8-15 % of annual mean	Online monitoring Validation report
O3M-51.1		MBG-O-NO ₂			
O3M-37.1	Offline tropospheric NO ₂	MAG-O-NO ₂ TR	50 %	30 %	Online monitoring Validation report
O3M-53.1		MBG-O-NO ₂ TR			
O3M-09.1	Offline total SO ₂	MAG-O-SO ₂	100 %	50 % (SZA < 70°)	Online monitoring Validation report
O3M-56.1		MBG-O-SO ₂			
O3M-08.1	Offline total BrO	MAG-O-BrO	50 %	30 %	Online monitoring Validation report
O3M-82.1		MBG-O-BrO			
O3M-10.1	Offline total HCHO	MAG-O-HCHO	100 %	50 % (polluted)	Online monitoring Validation report
O3M-58.1		MBG-O-HCHO			
O3M-12.1	Offline total H ₂ O	MAG-O-H ₂ O	25 %	10 %	Validation report
O3M-86.1		MAG-O-H ₂ O			
O3M-35	Tropical tropospheric ozone	MAG-O-O ₃ TR	50 %	25 %	Validation report
O3M-43		MBG-O-O ₃ TR	50 %	25 %	Validation report
O3M-39	Offline high-resolution ozone profile	MAG-O-O3HRPR	30 % in stratosphere 70 % in troposphere	15 % in stratosphere 30 % in troposphere	Online monitoring Validation report
O3M-48		MBG-O-O3HRPR			
O3M-172	NRT global tropospheric ozone	MAG-N-O3TROC	50 %	20 %	Validation report
O3M-174		MBG-N-O3TROC			
O3M-173	Offline global tropospheric ozone	MAG-O-O3TROC	50 %	20 %	Validation report
O3M-175		MBG-O-O3TROC			

Product identifier	Product name	Product acronym	Threshold accuracy	Target accuracy	Means of quality assurance
O3M-14.1	Offline absorbing aerosol index	MAG-O-AAI	1.0 index points	0.5 index points	Online monitoring Validation report
O3M-70.1		MBG-O-AAI			
O3M-63.1	Offline absorbing aerosol index from PMDs	MAG-O-AAIPMD	1.0 index points	0.5 index points	Online monitoring Validation report
O3M-73.1		MBG-O-AAIPMD			
O3M-95 – O3M-109	Offline surface UV	MBG-OUV_*	50 %	20 %	Online monitoring Validation report
O3M-40	Reprocessed total O3	MAG-RP1-O3	20 %	3% (SZA < 80°) 6% (SZA > 80°)	Validation Report
O3M-89.1	LER surface albedo	MAG-DS-LER	0.10	0.04	Validation Report
O3M-90		MBG-DS-LER			
O3M-119	OCIO data record	MxG-RP1-OCIO	100 %	50 %	Validation Report

Latest validation reports for all pre-operational and operational AC SAF products are listed in Section 1.3.

Online monitoring, when applicable, can be used to replace the regular validation reporting. Online monitoring results are found from dedicated sections “Online quality monitoring”, if the processing centre in question has such functionality.

2. Processing centre: FMI

2.1. Offline surface UV

OUV product consists of 15 sub-products which are listed in Table 2.1. Since they are all archived in the same file, single entries in the tables in the following sections represent them all.

Table 2.1. OUV sub-products

Product Identifier	Product Name	Product Acronym
O3M-95	Offline UV daily dose, erythemat (CIE) weighting	MBG-OUV_DD_CIE
O3M-96	Offline UV daily dose, plant response weighting	MBG-OUV_DD_PLANT
O3M-97	Offline UV daily dose, DNA damage weighting	MBG-OUV_DD_DNA
O3M-98	Offline UV Daily dose, vitamin D weighting	MBG-OUV_DD_VITD
O3M-99	Offline UV daily dose, UVA weighting	MBG-OUV_DD_UVA
O3M-100	Offline UV daily dose, UVB weighting	MBG-OUV_DD_UVB
O3M-101	Offline UV daily maximum dose rate, erythemat (CIE) weighting	MBG-OUV_MDSR_CIE
O3M-102	Offline UV daily maximum dose rate, plant response weighting	MBG-OUV_MDSR_PLANT
O3M-103	Offline UV daily maximum dose rate, DNA damage weighting	MBG-OUV_MDSR_DNA
O3M-104	Offline UV daily maximum dose, vitamin D weighting	MBG-OUV_MDSR_VITD
O3M-105	Offline UV daily maximum dose rate, UVA weighting	MBG-OUV_MDSR_UVA
O3M-106	Offline UV daily maximum dose rate, UVB weighting	MBG-OUV_MDSR_UVB
O3M-107	Offline UV Index	MBG-OUV_NOON_UVI
O3M-108	Offline daily maximum ozone photolysis rate	MBG-OUV_MPHR_O3
O3M-109	Offline daily maximum nitrogen dioxide photolysis rate	MBG-OUV_MPHR_NO2

2.1.1. Availability

For offline products, the availability requirement is 95.5 %. For OUV it is defined as the fraction of days in a month with product fulfilling the timeliness requirement.

Availability of OUV product during the reporting period is presented in Table 2.2. If the availability requirement has been violated, those values are marked with red colour, identified by numbers and reported in Table 2.7.

Table 2.2. Availability of OUV product during the reporting period

1/2018	2/2018	3/2018	4/2018	5/2018	6/2018
100 %	100 %	100 %	100 %	100 %	100 %

2.1.2. Timeliness

Timeliness indicates the elapsed time between sensing and product dissemination. Timeliness requirement is 15 days for offline products. If the requirement has been violated, those values are

marked with red colour. In addition, the violations are identified by numbers and reported in Table 2.7 if they have caused the availability values to drop below the allowed limits.

Note: timeliness violations are not listed as anomalies if the availability is above the limit.

The values in Table 2.3 indicate the elapsed times (days, hours and minutes in the format [ddT]hh:mm) from sensing to archive upload. In each cell, the values from top to bottom represent observed monthly average, minimum and maximum times.

Table 2.3. Timeliness of OUV product during the reporting period

1/2018	2/2018	3/2018	4/2018	5/2018	6/2018
ave: 03T05:38 min: 03T05:36 max: 03T06:36	ave: 03T14:20 min: 03T05:36 max: 12T10:06	ave: 03T06:25 min: 03T05:36 max: 04T06:41	ave: 03T05:36 min: 03T05:36 max: 03T05:36	ave: 03T05:36 min: 03T05:36 max: 03T05:36	ave: 03T05:36 min: 03T05:36 max: 03T05:36

2.2. Services, main events and anomalies

Table 2.4. FMI service statistics related to product archiving, ordering and AC SAF Helpdesk

Description of service / event	1/2018	2/2018	3/2018	4/2018	5/2018	6/2018
Product ordering ¹						
Number of users (WWW/EDC, cumulative)	206/64	208/67	212/68	219/71	223/73	227/74
Number of WWW orders	10	2	16	8	35	24
Number of ordered products	ARS: 1467 ARP: 94	ARP: 29	ARP: 280	ARP: 1164	OHP: 9104 ARS: 43 ARP: 6035 OUV: 366	OHP: 6859 ARS: 3597 ARP: 832 OUV: 2
Ordered data volume	ARS: 1.32 GB ARP: 585 MB	ARP: 179 MB	ARP: 1.76 GB	ARP: 7.16 GB	OHP: 2.26 TB ARS: 38.4 MB ARP: 37.5 GB OUV: 1.14 GB	OHP: 1.77 TB ARS: 3.27 GB ARP: 5.24 GB OUV: 251 kB
Number of EDC orders	10	7	1	10	3	1
Number of ordered products	OOP: 134 OHP: 276 ARS: 89 ARP: 32	OHP: 27 ARP: 27 OUV: 17	OOP: 19	OOP: 1235 OHP: 462 ARS: 28 ARP: 34	OHP: 20 ARS: 876	OUV: 879
Ordered data volume	OOP: 4.45 GB OHP: 69.5 GB ARS: 78.8 MB ARP: 180 MB	OHP: 6.79 GB ARP: 167 MB OUV: 812 MB	OOP: 713 MB	OOP: 40.8 GB OHP: 116 GB ARS: 25.5 MB ARP: 213 MB	OHP: 4.99 GB ARS: 729 MB	OUV: 36.5 GB
Number of bulk orders	0	0	0	0	0	0
Number of failed orders ²	0	0	0	0	0	0
Archive statistics ³						
Number of archived products (Metop-A)	OHP: 439 ARS: 439 ARP: 439	OHP: 396 ARS: 396 ARP: 396	OHP: 438 ARS: 438 ARP: 438	OHP: 425 ARS: 425 ARP: 425	OHP: 440 ARS: 440 ARP: 440	OHP: 425 ARS: 425 ARP: 425

Size of archived products (Metop-A)	OHP: 110 GB ARS: 391 MB ARP: 2.71 GB	OHP: 99.3 GB ARS: 352 MB ARP: 2.44 GB	OHP: 110 GB ARS: 389 MB ARP: 2.71 GB	OHP: 106 GB ARS: 378 MB ARP: 2.63 GB	OHP: 109 GB ARS: 394 MB ARP: 2.74 GB	OHP: 106 GB ARS: 381 MB ARP: 2.66 GB
Number of archived products (Metop-B)	OHP: 438 ARS: 438 ARP: 438 OUV: 31	OHP: 397 ARS: 397 ARP: 397 OUV: 28	OHP: 439 ARS: 439 ARP: 439 OUV: 31	OHP: 426 ARS: 426 ARP: 426 OUV: 30	OHP: 438 ARS: 438 ARP: 438 OUV: 31	OHP: 425 ARS: 425 ARP: 425 OUV: 30
Size of archived products (Metop-B)	OHP: 110 GB ARS: 398 MB ARP: 2.72 GB OUV: 1.48 GB	OHP: 99.8 GB ARS: 359 MB ARP: 2.45 GB OUV: 1.34 GB	OHP: 110 GB ARS: 399 MB ARP: 2.79 GB OUV: 1.48 GB	OHP: 107 GB ARS: 387 MB ARP: 2.68 GB OUV: 1.43 GB	OHP: 110 GB ARS: 400 MB ARP: 2.78 GB OUV: 1.48 GB	OHP: 106 GB ARS: 389 MB ARP: 2.70 GB OUV: 1.43 GB
GOME-2 L1b PDU rolling archive statistics ⁴						
PDUs archived / PDUs "reception confirmed" (Metop-A)	14875/14875 100 %	13439/13439 100 %	14879/14879 100 %	14358/14359 100 %	14845/14880 99.8 %	14389/14397 99.9 %
PDUs archived / PDUs "reception confirmed" (Metop-B)	14880/14880 100 %	13438/13438 100 %	14850/14850 100 %	14347/14347 100 %	14854/14880 99.8 %	14366/14380 99.9 %
Helpdesk statistics						
Number of emails	5	0	1	5	5	1
Number of email threads	2	0	1	2	2	1

¹ More detailed information about the orders is available in Appendix 1.

² Failed orders are detailed in Appendix 2.

³ Based on sensing start time

⁴ For Level 1b products, the availability is defined as the number of archived L1b PDUs divided by the number of L1b PDUs with status "reception confirmed" in the EUMETCast sendlist

Data archive statistics since 2008 are illustrated in Figure 2.1. Sudden increase in the cumulative amount of archived data in March 2017 is due to addition of reprocessed Metop-A aerosol products from 2007 onwards.

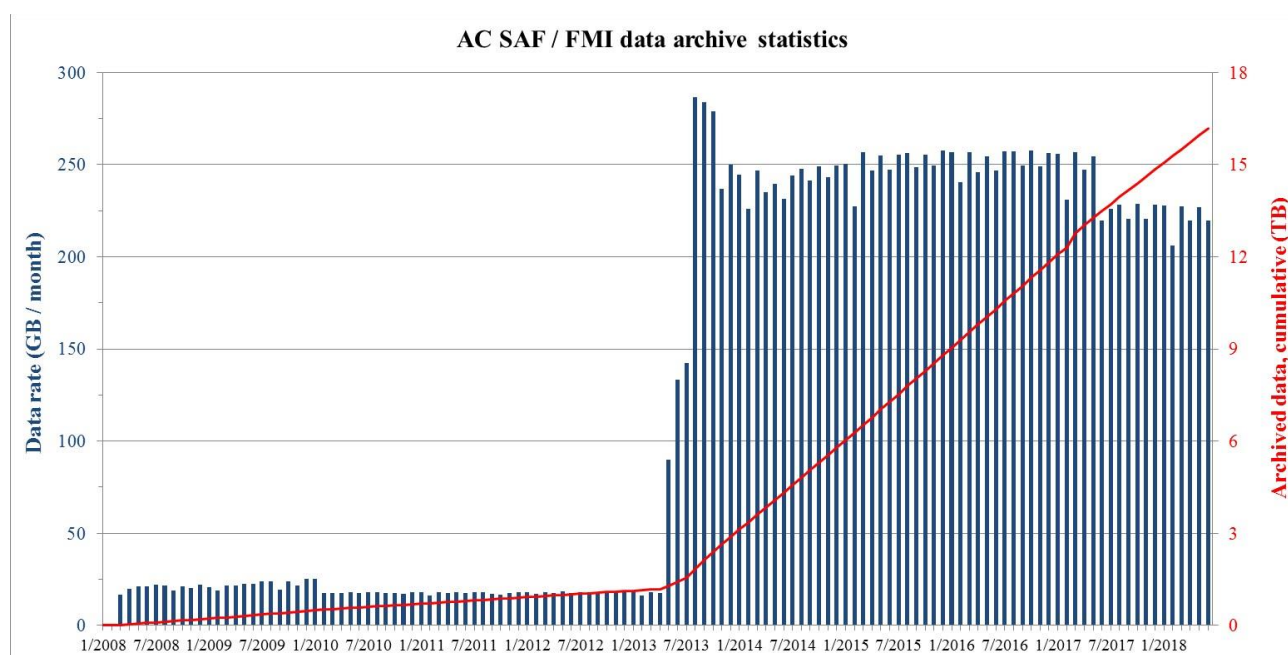


Figure 2.1. FMI data archive statistics: data rate and cumulative amount of data

Events affecting the data rate are presented in Table 2.5.

Table 2.5. Events affecting the FMI archive data rate

Date	Event	Data rate (GB/month)
03/2008	Archiving of OOP-A started	19.1 – 22.2
06/2009	Archiving of OUV-A started	19.2 – 23.8
11/2009	Archiving of ARS-A started	25.3
02/2010	Compression of OOP-A started	16.2 – 18.3
05/2013	Archiving of OHP-A started	133 – 142
08/2013	Archiving of OOP-B, OHP-B and ARS-B started	279 – 284
11/2013	Archiving of ARP-A and ARP-B started. KNMI implements shuffling algorithm in the hdf5 compression	226 – 250
03/2014	Archiving of OUV-A discontinued, archiving of OUV-B started	227 – 250
02/2015	OPERA algorithm update, tropospheric integrated profiles added	247-257
06/2017	Archiving of OOP-A and OOP-B discontinued	206-229

Table 2.6 lists the main events (product/service/hardware/software updates etc.) at FMI during the reporting period.

Table 2.6. Main events at FMI during the reporting period

Date	Description
	<i>Nothing to report.</i>

Table 2.7 lists the main local and external anomalies during the reporting period. Corrective and preventive actions should be provided also when applicable.

Table 2.7. Main local and external anomalies affecting FMI systems and performance during the reporting period

ID	Time period	Description
		<i>Nothing to report.</i>

3. Processing centre: DLR

3.1. NRT and offline total/tropospheric trace gas columns

3.1.1. Availability

For Level 1b products, the availability is defined as the number of L1b PDUs with status “reception confirmed”, i.e. EUMETSAT received these L1b PDUs through its EUMETCast reference receiving station, divided by the total number of L1b PDUs listed in the EUMETCast sendlist.

For NRT products, the availability requirement is 97.5 % and it is defined by the ratio of the number of in time processed and disseminated products to the number of received input products (L1b PDUs) with status “reception confirmed” in the EUMETCast sendlist per month. Missed input products are thereby considered to be always potentially useful for L2 processing (worst case scenario), although only about 50 % of disseminated L1b PDUs are usually useful.

For offline products, the availability requirement is 95.5 % and it is defined by the ratio of the number of in time processed, archived and quality-approved L2 products to the number of orbits for which input products (L1b PDUs) have been received per month.

Table 3.1 and Table 3.2 present the availability statistics of DLR products. If the availability requirements have been violated, those values are marked with red colour, identified by numbers and reported in Table 3.7.

Table 3.1. Availability of Metop-A total and tropospheric trace gas column products during the reporting period

Product Identifier	Product Name	1/2018	2/2018	3/2018	4/2018	5/2018	6/2018
L1b	PDUs received / PDUs “reception confirmed”	14809/14875 99.6 %	13432/13439 99.9 %	14875/14879 100 %	14357/14359 100 %	14871/14880 99.9 %	14394/14397 100 %
O3M-01.1	NRT total O3	99.6 %	100 %	100 %	100 %	99.9 %	100 %
O3M-02.1	NRT total NO2						
O3M-36.1	NRT tropospheric NO2						
O3M-54.1	NRT total SO2						
O3M-176.0	NRT total HCHO						
O3M-06.1	Offline total O3	99.3 %	99.5 %	99.9 %	99.8 %	99.3 %	99.8 %
O3M-07.1	Offline total NO2						
O3M-08.1	Offline total BrO						
O3M-09.1	Offline total SO2						
O3M-10.1	Offline total HCHO						
O3M-12.1	Offline total H2O						
O3M-37.1	Offline tropospheric NO2						
O3M-35	Offline tropical tropospheric ozone	100 %	100 %	100 %	100 %	100 %	100 %

Table 3.2. Availability of Metop-B total and tropospheric trace gas column products during the reporting period

Product Identifier	Product Name	1/2018	2/2018	3/2018	4/2018	5/2018	6/2018
L1b	PDU received / PDUs "reception confirmed"	14836/14880 99.7 %	13428/13438 99.9 %	14848/14850 100 %	14346/14347 100 %	14880/14880 100 %	14375/14380 100 %
O3M-01.1	NRT total O3	99.7 %	99.9 %	100 %	100 %	100 %	100 %
O3M-02.1	NRT total NO2						
O3M-36.1	NRT tropospheric NO2						
O3M-54.1	NRT total SO2						
O3M-177.0	NRT total HCHO						
O3M-06.1	Offline total O3	99.6 %	99.5 %	99.1 %	99.3 %	99.3 %	98.1 %
O3M-07.1	Offline total NO2						
O3M-08.1	Offline total BrO						
O3M-09.1	Offline total SO2						
O3M-10.1	Offline total HCHO						
O3M-12.1	Offline total H2O						
O3M-37.1	Offline tropospheric NO2						
O3M-43	Offline tropical tropospheric ozone, cloud slicing	100 %	100 %	100 %	100 %	100 %	100 %

3.1.2. Timeliness

Timeliness indicates the elapsed time between sensing and product dissemination. Timeliness requirements are 3 hours for NRT products and 15 days for offline products. If the requirements have been violated, those values are marked with red colour. In addition, the violations are identified by numbers and reported in Table 3.7 if they have caused the availability values to drop below the allowed limits.

Note: timeliness violations are not listed as anomalies if the availability is above the limit.

The values in Table 3.3 and Table 3.4 indicate the elapsed times (days, hours and minutes in the format [ddT]hh:mm) from sensing to EUMETCast (NRT) or archive (offline) upload. In each cell, the values from top to bottom represent observed monthly average, minimum and maximum times.

Table 3.3. Timeliness of Metop-A total and tropospheric trace gas column products during the reporting period

Product Identifier	Product Name	1/2018	2/2018	3/2018	4/2018	5/2018	6/2018
O3M-01.1	NRT total O3	ave: 01:40 min: 01:14 max: 02:44	ave: 01:41 min: 00:43 max: 01:55	ave: 01:38 min: 00:32 max: 02:26	ave: 01:37 min: 00:34 max: 02:02	ave: 01:35 min: 00:34 max: 02:24	ave: 01:35 min: 00:36 max: 02:00
O3M-02.1	NRT total NO2						
O3M-36.1	NRT tropospheric NO2						
O3M-54.1	NRT total SO2						
O3M-176.0	NRT total HCHO						
O3M-06.1	Offline total O3	ave: 01T07:27 min: 01T01:10 max: 08T01:26	ave: 01T03:46 min: 01T01:09 max: 13T07:43	ave: 01T12:05 min: 01T01:09 max: 07T19:55	ave: 01T01:44 min: 01T01:09 max: 02T04:33	ave: 01T05:45 min: 01T01:09 max: 10T16:04	ave: 01T03:06 min: 01T01:09 max: 08T07:45
O3M-07.1	Offline total NO2						
O3M-08.1	Offline total BrO						
O3M-09.1	Offline total SO2						
O3M-10.1	Offline total HCHO						
O3M-12.1	Offline total H2O						
O3M-37.1	Offline tropospheric NO2						
O3M-35	Offline tropical tropospheric ozone, cloud slicing	N/A	N/A	N/A	N/A	N/A	N/A

Table 3.4. Timeliness of Metop-B total and tropospheric trace gas column products during the reporting period

Product Identifier	Product Name	1/2018	2/2018	3/2018	4/2018	5/2018	6/2018
O3M-01.1	NRT total O3	ave: 00:57 min: 00:38 max: 02:01	ave: 00:56 min: 00:31 max: 01:48	ave: 01:04 min: 00:30 max: 02:18	ave: 01:04 min: 00:30 max: 01:53	ave: 00:57 min: 00:31 max: 02:00	ave: 00:57 min: 00:30 max: 01:51
O3M-02.1	NRT total NO2						
O3M-36.1	NRT tropospheric NO2						
O3M-54.1	NRT total SO2						
O3M-177.0	NRT total HCHO						
O3M-06.1	Offline total O3	ave: 01T06:55 min: 01T01:12 max: 05T04:55	ave: 01T03:48 min: 01T01:11 max: 13T06:44	ave: 01T12:09 min: 01T01:12 max: 05T17:47	ave: 01T01:35 min: 01T01:11 max: 01T04:35	ave: 01T04:50 min: 01T01:12 max: 08T13:28	ave: 01T03:11 min: 01T01:11 max: 02T14:01
O3M-07.1	Offline total NO2						
O3M-08.1	Offline total BrO						
O3M-09.1	Offline total SO2						
O3M-10.1	Offline total HCHO						
O3M-12.1	Offline total H2O						
O3M-37.1	Offline tropospheric NO2						
O3M-43	Offline tropical tropospheric ozone, cloud slicing	N/A	N/A	N/A	N/A	N/A	N/A

3.2. Services, main events and anomalies

Table 3.5. DLR service statistics related to product archiving and ordering

Description of service / event	1/2018	2/2018	3/2018	4/2018	5/2018	6/2018
Archive statistics ²						
Number of archived products (cumulative) – according to product insertion time	168048	169800	174637	178810	182725	183579
Size of archived products (TB, cumulative)	7.300	7.401	7.683	7.908	8.139	8.189
Number of missing orbit products – according to sensing time	0	2	1	1	1	0
Number of archived products with good/poor/error ³ quality assessed per month – according to product insertion time	873/0/4	792/0/1	879/0/9	845/2/5	912/0/3	841/2/11
Number of UMARF uploads – according to product upload date	879	797	880	1599 ⁴	933	861
Online Access ¹						
Number of searches in the GOME.TC collection	107	124	154	70	76	85
Number of ATMOS subscribers	173	174	180	183	187	190
Number of ATMOS downloads	81054	0	0	97880	140353	330961
Downloaded data volume (GB)	114	0	0	241	441	3222
Product ordering						
Number of successful UMARF orders	0	2	1	1	0	1
Number of successful EOWEB orders	0	10	7	7	0	0
Delivered data volume (GB)	0	1868	14.3	10.2	0	0

¹ NTO product and OTO product is stored at the DLR for external search and download

² O3MOTO product (collection GOME.TC, Metop missions) is archived and available to non-NRT users

³ good: max. 2 PDUs missing, poor/error: more than 2 PDUs missing

⁴ Re-ingestion of O3MOTO metadata was required due to accidental clean-up of metadata queue in EDC

Table 3.6 lists the main events (product/service/hardware/software updates etc.) at DLR during the reporting period.

Table 3.6. Main events at DLR during the reporting period

Date	Event
	<i>Nothing to report.</i>

Table 3.7 lists the main and external local anomalies at DLR during the reporting period. Corrective and preventive actions should be provided also when applicable.

Table 3.7. Main local and external anomalies affecting DLR systems and performance during the reporting period

ID	Time period	Description
		<i>Nothing to report.</i>

4. Processing centre: KNMI

4.1. NRT and offline high-resolution ozone profiles, absorbing aerosol indexes, tropospheric ozone (ozone profiles)

4.1.1. Availability

For Level 1b products, the availability is defined as the number of unique L1b PDUs received either via EUMETCast Satellite or EUMETCast Terrestrial (demonstrational dissemination service), divided by the number of L1b PDUs not marked as “not sent” in the EUMETCast Satellite sendlist. This approximation presumes that all PDUs marked as “sent not confirmed” are still available via EUMETCast Terrestrial.

For NRT products, the availability requirement is 97.5 % and it is defined by the ratio of the number of in time processed and disseminated products to the number of received input products (L1b PDUs) with status “reception confirmed” in the EUMETCast sendlist per month. Missed input products are thereby considered to be always potentially useful for L2 processing (worst case scenario), although only about 50 % of disseminated L1b PDUs are usually useful.

For offline products, the availability requirement is 95.5 % and it is defined by the ratio of the number of in time processed, archived and quality-approved Level 2 products to the number of orbits for which input products (L1b PDUs) have been received per month.

Table 4.1 and Table 4.2 present the availability statistics of KNMI products. If the availability requirements have been violated, those values are marked with red colour, identified by numbers and reported in Table 4.9.

Tropospheric ozone products are included in the ozone profile products and have the same statistics. The same applies to scattering aerosol index products which are included in the absorbing aerosol index products.

Table 4.1. Availability of Metop-A L1b PDUs, ozone profile products and aerosol products during the reporting period

Product Identifier	Product Name	1/2018	2/2018	3/2018	4/2018	5/2018	6/2018
EUMETCast							
L1b	PDUs received / sent	14877/14875 100 %	13440/13440 100 %	14880/14880 100 %	14365/14392 99.8 %	14880/14880 100 %	14400/14400 100 %
O3M-38	NRT high-resolution ozone profile	100 %	100 %	100 %	99.6 %	100 %	100 %
O3M-61	NRT absorbing aerosol index	100 %	100 %	100 %	99.7 %	100 %	100 %
O3M-62	NRT absorbing aerosol index from PMDs	100 %	100 %	100 %	99.7 %	100 %	100 %
WMO/GTS							
O3M-38	NRT high-resolution ozone profile	100 %	100 %	100 %	100 %	100 %	100 %

Product Identifier	Product Name	1/2018	2/2018	3/2018	4/2018	5/2018	6/2018
FMI archive							
O3M-39	Offline high-resolution ozone profile	100 %	100 %	100 %	100 %	100 %	100 %
O3M-14	Offline absorbing aerosol index	100 %	100 %	100 %	100 %	100 %	100 %
O3M-63	Offline absorbing aerosol index from PMDs	100 %	100 %	100 %	100 %	100 %	100 %

Table 4.2. Availability of Metop-B L1b PDUs, ozone profile products and aerosol products during the reporting period

Product Identifier	Product Name	1/2018	2/2018	3/2018	4/2018	5/2018	6/2018
EUMETCast							
L1b	PDUs received / sent	14880/14880 100 %	13440/13440 100 %	14850/14850 100 %	14380/14398 99.9 %	14880/14880 100 %	14380/14380 100 %
O3M-47	NRT high-resolution ozone profile	100 %	100 %	100 %	99.7 %	100 %	100 %
O3M-71	NRT absorbing aerosol index	100 %	100 %	100 %	99.7 %	100 %	100 %
O3M-72	NRT absorbing aerosol index from PMDs	100 %	100 %	100 %	99.7 %	100 %	100 %
WMO/GTS							
O3M-47	NRT high-resolution ozone profile	100 %	100 %	100 %	100 %	100 %	100 %
FMI archive							
O3M-48	Offline high-resolution ozone profile	100 %	100 %	100 %	100 %	100 %	100 %
O3M-70	Offline absorbing aerosol index	100 %	100 %	100 %	100 %	100 %	100 %
O3M-73	Offline absorbing aerosol index from PMDs	100 %	100 %	100 %	100 %	100 %	100 %

4.1.2. Timeliness

Timeliness indicates the elapsed time between sensing and product dissemination. Timeliness requirements are 3 hours for NRT products and 15 days for offline products. If the requirements have been violated, those values are marked with red colour. In addition, the violations are

identified by numbers and reported in Table 4.9 if they have caused the availability values to drop below the allowed limits.

Note: timeliness violations are not listed as anomalies if the availability is above the limit.

The values in Table 4.3 and Table 4.4 indicate elapsed times (days, hours and minutes in the format [ddT]hh:mm) from sensing to EUMETCast (NRT) or archive upload (offline). In each cell, the values from top to bottom represent observed monthly average, minimum and maximum times.

Tropospheric ozone products are included in the ozone profile products and have the same statistics.

Table 4.3. Timeliness of Metop-A ozone profile and aerosol products during the reporting period

Product Identifier	Product Name	1/2018	2/2018	3/2018	4/2018	5/2018	6/2018
EUMETCast							
O3M-38	NRT high-resolution ozone profile	ave: 02:18 min: 01:00 max: 02:56	ave: 02:15 min: 00:41 max: 02:58	ave: 02:08 min: 00:32 max: 02:49	ave: 02:08 min: 00:33 max: 03:11	ave: 02:06 min: 00:37 max: 02:52	ave: 02:01 min: 00:37 max: 02:47
O3M-61	NRT absorbing aerosol index	ave: 01:40 min: 00:59 max: 01:59	ave: 01:40 min: 00:40 max: 02:01	ave: 01:35 min: 00:31 max: 01:57	ave: 01:36 min: 00:32 max: 02:30	ave: 01:33 min: 00:33 max: 02:07	ave: 01:34 min: 00:34 max: 02:04
O3M-62	NRT absorbing aerosol index from PMDs	ave: 01:41 min: 00:59 max: 02:00	ave: 01:40 min: 00:40 max: 02:01	ave: 01:36 min: 00:32 max: 01:58	ave: 01:36 min: 00:32 max: 02:30	ave: 01:34 min: 00:34 max: 02:07	ave: 01:34 min: 00:34 max: 02:04
WMO/GTS							
O3M-38	NRT high-resolution ozone profile	ave: 02:19 min: 01:01 max: 02:57	ave: 02:16 min: 00:42 max: 02:59	ave: 02:09 min: 00:33 max: 02:50	ave: 02:09 min: 00:34 max: 03:12	ave: 02:07 min: 00:38 max: 02:53	ave: 02:02 min: 00:38 max: 02:48
FMI archive							
O3M-39	Offline high-resolution ozone profile	ave: 08:33 min: 07:34 max: 01T04:00	ave: 08:16 min: 07:27 max: 08:57	ave: 08:10 min: 07:24 max: 08:58	ave: 08:27 min: 07:27 max: 02T02:51	ave: 08:23 min: 07:30 max: 20:48	ave: 08:20 min: 07:33 max: 09:03
O3M-14	Offline absorbing aerosol index	ave: 08:21 min: 07:15 max: 01T03:54	ave: 08:04 min: 07:15 max: 08:39	ave: 07:59 min: 07:18 max: 08:42	ave: 08:15 min: 07:21 max: 02T03:15	ave: 08:12 min: 07:21 max: 20:36	ave: 08:08 min: 07:21 max: 08:48
O3M-63	Offline absorbing aerosol index from PMDs	ave: 08:25 min: 07:30 max: 01T03:52	ave: 08:10 min: 07:30 max: 08:50	ave: 08:03 min: 07:18 max: 08:48	ave: 08:21 min: 07:29 max: 02T02:56	ave: 08:18 min: 07:27 max: 20:31	ave: 08:14 min: 07:30 max: 08:59

Table 4.4. Timeliness of Metop-B ozone profile and aerosol products during the reporting period

Product Identifier	Product Name	1/2018	2/2018	3/2018	4/2018	5/2018	6/2018
EUMETCast							
O3M-47	NRT high-resolution ozone profile	ave: 01:18 min: 00:50 max: 02:32	ave: 01:18 min: 00:30 max: 02:47	ave: 01:23 min: 00:30 max: 02:32	ave: 01:22 min: 00:30 max: 02:31	ave: 01:15 min: 00:32 max: 02:30	ave: 01:16 min: 00:32 max: 02:30
O3M-71	NRT absorbing aerosol index	ave: 00:56 min: 00:37 max: 01:54	ave: 00:55 min: 00:30 max: 02:47	ave: 01:01 min: 00:29 max: 02:17	ave: 01:01 min: 00:30 max: 02:00	ave: 00:55 min: 00:30 max: 01:51	ave: 00:55 min: 00:28 max: 01:49
O3M-72	NRT absorbing aerosol index from PMDs	ave: 00:56 min: 00:37 max: 01:55	ave: 00:55 min: 00:30 max: 01:55	ave: 01:02 min: 00:29 max: 02:18	ave: 01:02 min: 00:30 max: 02:00	ave: 00:55 min: 00:30 max: 01:51	ave: 00:55 min: 00:28 max: 01:50
WMO/GTS							
O3M-47	NRT high-resolution ozone profile	ave: 01:19 min: 00:51 max: 02:33	ave: 01:19 min: 00:31 max: 02:48	ave: 01:24 min: 00:30 max: 02:33	ave: 01:23 min: 00:31 max: 02:32	ave: 01:16 min: 00:33 max: 02:31	ave: 01:17 min: 00:33 max: 02:31
FMI archive							
O3M-48	Offline high-resolution ozone profile	ave: 07:57 min: 07:03 max: 01T02:57	ave: 08:13 min: 07:00 max: 02T03:24	ave: 07:57 min: 07:00 max: 02T03:15	ave: 07:46 min: 06:48 max: 02T03:11	ave: 07:38 min: 06:51 max: 19:49	ave: 08:01 min: 06:51 max: 02T03:08
O3M-70	Offline absorbing aerosol index	ave: 07:51 min: 06:59 max: 01T02:56	ave: 08:08 min: 07:02 max: 02T03:14	ave: 07:50 min: 06:53 max: 02T03:10	ave: 07:41 min: 06:44 max: 02T02:56	ave: 07:34 min: 06:47 max: 21:18	ave: 07:56 min: 06:47 max: 02T03:22
O3M-73	Offline absorbing aerosol index from PMDs	ave: 07:50 min: 06:56 max: 01T02:55	ave: 08:08 min: 06:56 max: 02T03:10	ave: 07:51 min: 06:52 max: 02T03:04	ave: 07:42 min: 06:46 max: 02T02:31	ave: 07:34 min: 06:44 max: 21:13	ave: 07:56 min: 06:47 max: 02T03:25

4.2. Services, main events and anomalies

Tropospheric ozone products are included in the ozone profile products and have the same statistics.

Table 4.5. Number of products sent to FMI archive¹

Product Identifier	Product Name	Metop satellite	1/2018	2/2018	3/2018	4/2018	5/2018	6/2018
O3M-39	Offline high-resolution ozone profile	A	439	396	438	425	440	425
O3M-48		B	438	397	439	426	438	425
O3M-14	Offline absorbing aerosol index	A	439	396	438	425	440	425
O3M-70		B	438	397	439	426	438	425
O3M-63	Offline absorbing aerosol index from PMDs	A	439	396	438	425	440	425
O3M-73		B	438	397	439	426	438	425

Table 4.6. Number of products stored locally at KNMI²

Product Identifier	Product Name	Metop satellite	1/2018	2/2018	3/2018	4/2018	5/2018	6/2018
O3M-38	NRT high-resolution ozone profile	A	8104	7322	8093	7760	8009	7735
O3M-47		B	8385	7585	8359	7986	8186	7895
O3M-61	NRT absorbing aerosol index	A	8104	7322	8093	7760	8009	7735
O3M-71		B	8385	7585	8359	7986	8186	7895
O3M-62	NRT absorbing aerosol index from PMDs	A	8104	7322	8093	7760	8009	7735
O3M-72		B	8385	7585	8359	7986	8186	7895
O3M-39	Offline high-resolution ozone profile	A	439	396	438	425	440	425
O3M-48		B	438	397	439	426	438	425
O3M-14	Offline absorbing aerosol index	A	439	396	438	425	440	425
O3M-70		B	438	397	439	426	438	425
O3M-63	Offline absorbing aerosol index from PMDs	A	439	396	438	425	440	425
O3M-73		B	438	397	439	426	438	425

Table 4.7. EUMETCast and WMO/GTS uploads³

Product Identifier	Product Name	Metop satellite	1/2018	2/2018	3/2018	4/2018	5/2018	6/2018
O3M-38	NRT high-resolution ozone profile	A	8104/8104	7322/7322	8039/8039	7759/7758	8009/8009	7735/7735
O3M-47		B	8385/8385	7585/7585	8359/8359	7986/7986	8186/8186	7895/7895
O3M-61	NRT absorbing aerosol index	A	8104	7322	8093	7760	8009	7735
O3M-71		B	8385	7585	8359	7986	8186	7895
O3M-62	NRT absorbing aerosol index from PMDs	A	8104	7322	8093	7760	8009	7735
O3M-72		B	8385	7585	8359	7986	8186	7895

¹ Products are archived in HDF5 format.

² Products are stored for 3 years (in HDF5 and BUFR formats).

³ NRT high-resolution ozone profile is disseminated via EUMETCast and WMO/GTS in BUFR format. NRT absorbing aerosol index and NRT absorbing aerosol index from PMDs are disseminated only via EUMETCast (in HDF5 and BUFR formats).

Table 4.8 lists the main events (product/service/hardware/software updates etc.) at KNMI during the reporting period.

Table 4.8. Main events at KNMI during the reporting period

Date	Description
	<i>Nothing to report.</i>

Table 4.9 lists the main local and external anomalies at KNMI during the reporting period. Corrective and preventive actions should be provided also when applicable.

Table 4.9. Main local and external anomalies affecting KNMI systems and performance during the reporting period

ID	Time period	Description
		<i>Nothing to report.</i>

5. Processing centre: DMI

5.1. NRT clear-sky and cloud-corrected UV index

5.1.1. Availability

NUV product is required to be produced every day, either on the basis of new GOME ATO input or in the case of ATO delivery failure based on back-up total ozone data (ECMWF or climatology). Availability requirement is 97.5 % and it is defined as the fraction of days in a month when NUV product is delivered to all users on time.

Table 5.1 presents the availability statistics of DMI products. If the requirement is violated, those values are marked with red colour, identified by numbers and reported in Table 5.5.

Table 5.1. Availability of NRT UV products during the reporting period

Product Identifier	Product Name	1/2018	2/2018	3/2018	4/2018	5/2018	6/2018
O3M-91	NRT UV index, clear-sky	100 %	100 %	100 %	100 %	100 %	100 %
O3M-92	NRT UV index, cloud-corrected						

5.1.2. Timeliness

Timeliness requirement for NUV says that the final NUV product is to be delivered to users no later than two hours after receiving the ATO input and not later than 04:00 UTC. Processing is started at 02:45 UTC thus the maximum processing time allowed is 1h 15m. If timeliness requirement is violated, those values are marked with red colour. In addition, the violations are identified by numbers and reported in Table 5.5 if they have caused the availability values to drop below the allowed limits.

Days where no products are produced or could be delivered to users (as indicated in Table 5.1) are not included in Table 5.2.

Note: timeliness violations are not listed as anomalies if the availability is above the limit.

The values in Table 5.2 indicate elapsed processing times (hours, minutes and seconds in the format [hh:]mm:ss). In each cell, the values from top to bottom represent observed monthly average, minimum and maximum processing times.

Table 5.2. Timeliness of NRT UV products during the reporting period

Product Identifier	Product Name	1/2018	2/2018	3/2018	4/2018	5/2018	6/2018
O3M-91	NRT UV index, clear-sky	ave: 07:53 min: 07:44 max: 08:05	ave: 08:03 min: 07:51 max: 08:18	ave: 08:04 min: 07:48 max: 08:15	ave: 07:52 min: 07:44 max: 08:04	ave: 07:55 min: 07:43 max: 10:26	ave: 07:57 min: 07:42 max: 09:07
O3M-92	NRT UV index, cloud-corrected						

5.2. Services, main events and anomalies

Table 5.3. Number of products stored locally at DMI¹

Description of service / event	1/2018	2/2018	3/2018	4/2018	5/2018	6/2018
Storage statistics						
Number of stored products	62	56	62	60	62	60
Size of stored products (MB)	77.5	70.0	77.5	75.0	77.5	75.0

¹ NUV products are stored at the DMI at least until the end of the Metop programs.

Table 5.4 lists the main events (product/service/hardware/software updates etc.) at DMI during the reporting period.

Table 5.4. Main events at DMI during the reporting period

Date	Event
	<i>Nothing to report.</i>

Table 5.5 lists the main local and external anomalies at DMI during the reporting period. Corrective and preventive actions should be provided also when applicable.

Table 5.5. Main local and external anomalies affecting DMI systems and performance during the reporting period

ID	Time period	Description
		<i>Nothing to report.</i>

6. Processing centre: EUMETSAT

6.1. NRT IASI CO and SO₂

6.1.1. Availability

For Level 1c products, the availability is defined as the number of available PDUs divided by the number of maximum expected PDUs.

For NRT products, the availability requirement is 97.5 % and it is defined by the ratio of the number of in time processed and disseminated products to the number of maximum expected input products (L1c PDUs) per month.

Table 6.1 and Table 6.2 present the availability statistics of EUMETSAT products. If the availability requirements have been violated, those values are marked with red colour, identified by numbers and reported in Table 6.8.

Note that in the frame of this product processing centre being the CAF (Central Application Facility - Darmstadt), the L1c data is directly available to the algorithm, i.e., its availability is not dependable of EUMETCast dissemination. Furthermore, since there is no relay of information from *Satellite* processing centres, the L2 product availability in the following tables concern the end-to-end availability as they were recorded in the EUMETSAT Reference Receiving Stations.

Table 6.1. Availability of Metop-A L1c PDUs and IASI NRT products during the reporting period

Product Identifier	Product Name	1/2018	2/2018	3/2018	4/2018	5/2018	6/2018
L1c	PDUs available / PDUs expected	14853 / 14880	13333 / 13440	14886 / 14880	14303 / 14400	14870 / 14880	14236 / 14400
L1c	Availability	99.8 %	99.2 %	100 %	99.3 %	99.9 %	98.9 %
O3M-181	NRT IASI CO	98.0 %	98.5 %	98.8 %	99.0 %	99.3 %	98.7 %
O3M-57	NRT IASI SO ₂				99.0 %	99.3 %	98.7 %

Table 6.2. Availability of Metop-B L1c PDUs and IASI NRT products during the reporting period

Product Identifier	Product Name	1/2018	2/2018	3/2018	4/2018	5/2018	6/2018
L1c	PDUs available / PDUs expected	14865 / 14880	13402 / 13440	14823 / 14880	14298 / 14400	14682 / 14880	12602 / 14400
L1c	Availability	99.9 %	99.7 %	99.6 %	99.3 %	98.7 %	87.5 % (1),(2)
O3M-80	NRT IASI CO	98.1 %	99.3 %	98.4 %	98.8 %	98.1 %	86.9 % (1),(2)
O3M-57	NRT IASI SO ₂				98.8 %	98.1 %	86.9 % (1),(2)

6.1.2. Timeliness

Timeliness indicates the elapsed time between sensing and product dissemination. Timeliness requirement is 3 hours for NRT products. If the requirements have been violated, those values are

marked with red colour. In addition, the violations are identified by numbers and reported in Table 6.8 if they have caused the availability values to drop below the allowed limits.

Note: timeliness violations are not listed as anomalies if the availability is above the limit.

The values in Table 6.3 and Table 6.4 indicate elapsed times (hours and minutes in the format hh:mm) from sensing to EUMETCast Reference Receiving Station, i.e., end-to-end timeliness. In each cell, the values from top to bottom represent observed monthly average, minimum and maximum times.

Table 6.3. Timeliness of Metop-A IASI NRT products during the reporting period

Product Identifier	Product Name	1/2018	2/2018	3/2018	4/2018	5/2018	6/2018
O3M-181	NRT IASI CO	ave: 01:23 min: 00:36 max: 01:57	ave: 01:23 min: 00:43 max: 02:12	ave: 01:22 min: 00:42 max: 01:58	ave: 01:23 min: 00:44 max: 02:06	ave: 01:23 min: 00:43 max: 01:57	ave: 01:23 min: 00:43 max: 02:10
O3M-57	NRT IASI SO2				ave: 01:23 min: 00:44 max: 02:06	ave: 01:23 min: 00:43 max: 01:57	ave: 01:23 min: 00:43 max: 02:10

Table 6.4. Timeliness of Metop-B IASI NRT products during the reporting period

Product Identifier	Product Name	1/2018	2/2018	3/2018	4/2018	5/2018	6/2018
O3M-80	NRT IASI CO	ave: 00:51 min: 00:29 max: 01:52	ave: 00:51 min: 00:30 max: 01:51	ave: 00:57 min: 00:31 max: 02:13	ave: 00:55 min: 00:32 max: 01:53	ave: 00:51 min: 00:23 max: 02:10	ave: 00:51 min: 00:31 max: 02:09
O3M-57	NRT IASI SO2				ave: 00:55 min: 00:32 max: 01:53	ave: 00:51 min: 00:23 max: 02:10	ave: 00:51 min: 00:31 max: 02:09

6.2. Services, main events and anomalies

Table 6.5. Number of products stored locally at EUMETSAT¹

Product Identifier	Product Name	Metop satellite	1/2018	2/2018	3/2018	4/2018	5/2018	6/2018
O3M-181	NRT IASI CO	A	14603	13252	14720	14305	14788	14252
O3M-80		B	14612	13354	14656	14291	14603	12535
O3M-57	NRT IASI SO2	A				14305	14788	14252
		B				14290	14603	12534

Table 6.6. EUMETCast uploads²

Product Identifier	Product Name	Metop satellite	1/2018	2/2018	3/2018	4/2018	5/2018	6/2018
O3M-181	NRT IASI CO	A	14582	13248	14707	14264	14781	14236
O3M-80		B	14597	13345	14644	14256	14595	12521
O3M-57	NRT IASI SO2	A				14265	14780	14237
		B				14256	14595	12521

¹ PDUs are concatenated back to orbit based products before being stored

² NRT IASI products are disseminated via EUMETCast (in BUFR format)

Table 6.7 lists the main events (product/service/hardware/software updates etc.) at EUMETSAT during the reporting period.

Table 6.7. Main events at EUMETSAT during the reporting period

Date	Description
18 April	Metop-A and Metop-B NRT IASI SO2 products become available to users via EUMETCast in BUFR format with the “Operational” status. Since June 2017, the product had been disseminated over EUMETCast as “Demonstrational”. For clarity and readability purposes, the April 2018 values in tables 6.x refer to entire month.

Table 6.8 lists the main local and external anomalies at EUMETSAT during the reporting period. Corrective and preventive actions should be provided also when applicable.

Table 6.8. Main local and external anomalies affecting EUMETSAT systems and performance during the reporting period

ID	Time period	Description
1	23 May - 28 June	Several instances of Metop-B IASI instrument in “Standby refuse” mode due to Single Event Transient most likely caused by radiation impacts to the power converters supplying the IASI DPCs / FMU and DMC. Corrective action: Mode transition issued. Preventive action: Try to detect “Standby refuse” mode earlier so that mode transition can be issued sooner.
2	27 June - 2 July	Planned maintenance. Metop-B IASI instrument decontamination.

7. Validation and quality monitoring

This section describes the validation status and validation/quality monitoring activities during the reporting period. Reference documents are listed in Section 1.3 and accuracy requirements in Section 1.5.

7.1. Total ozone column products

Table 7.1. Validation status of total ozone column products

Product Identifier	Product Name	Accuracy	Reference	Validating Institute
O3M-01.1	NRT total O3	Fulfil threshold accuracy requirement	RD5	AUTH
O3M-41.1				
O3M-06.1	Offline total O3	Fulfil threshold accuracy requirement	RD5	AUTH
O3M-42.1				

Validation results can be found in more detail on the AC SAF validation & quality assessment website at http://lap3.physics.auth.gr/eumetsat/validation/near_real and <http://lap3.physics.auth.gr/eumetsat/validation/offline>

7.1.1. GOME-2A and GOME-2B GDP-4.8 total ozone column validation

This summary presents the validation activities for total ozone products (TOCs), reported by the GOME-2/Metop-A and GOME-2/Metop-B instruments. Members of the Laboratory of Atmospheric Physics of the Aristotle University of Thessaloniki, Thessaloniki, Greece, LAP/AUTH, (<http://lap.physics.auth.gr/index.asp?lang=en>) involved in the validation activities include Professor, Dr. Dimitris Balis, Research Associate, Dr. MariLiza Koukouli and Research Associate, Dr. Katerina Garane.

During the reporting period, the operational validation of offline total ozone products continued as per previous periods.

7.1.1.1 Update of database for reference ground-based data

The validation database was brought up-to-date with the current satellite and ground-based data and covers the period January 2007 to June 2018, based on the last date of the ground based data availability. For the nominal validation the TOCS employed are those reported to the World Ozone and Ultraviolet Radiation Data Centre [<http://www.woudc.org>]. WOUDC is one of the World Data Centres which are part of the Global Atmosphere Watch (GAW) programme of the World Meteorological Organization (WMO). Total ozone columns from Brewer, Dobson and M-124 instruments are employed in the validation sequence. For the quality of the reference ground-based data, used for the validation of the total ozone products, updated information were extracted from recent inter-comparisons and calibration records. This continuously updated selection of ground-based measurements has already been used numerous times in the validation and analysis of global total ozone records such as the inter-comparison between the OMI/Aura TOMS and OMI/Aura DOAS algorithms [Balis *et al.*, 2007a], the validation of ten years of GOME/ERS-2 ozone record [Balis *et al.*, 2007b], the validation of the updated version of the OMI/Aura TOMS algorithm [Antón *et al.*, 2009], the GOME-2/Metop-A validation [Loyola *et al.*, 2011; Koukouli *et al.*, 2012], the GOME-2/Metop-B validation [Hao *et al.*, 2014] and the evaluation of the European Space

Agency's Ozone Climate Change Initiative project [O₃-CCI] TOCs [Koukouli *et al.*, 2015, Garane *et al.*, 2018]. In all the aforementioned works, LAP/AUTH assumes the leading role in the validation efforts. The number of WOUDC ground-based stations used in the full operational periods of the two instruments, alongside the mean difference between ground- and space-based TOC estimates is given in Table 7.2.

7.1.1.2 GOME-2A and GOME-2B GDP-4.8 TOC validation | The Dobson comparisons

GOME-2A and GOME-2B OTO data based on GDP-4.8 for the period January 2007 to June 2018 have been downloaded, quality assured and pre-processed in order to perform the validation strategies. The GDP-4.8 algorithm is the latest version of the GDP-4.x suite of algorithms that have been used for the operational processing of GOME-2 total ozone columns.

This period's satellite-to-ground-based measurements comparisons were performed and were added to the existing time series. The majority of the quality-assured ground-based Brewer and Dobson TOCs are reported to the WOUDC repository between 3 and 6 months after measurement which accounts for the last couple of months missing from the comparative plots shown below. This is a common reporting feature, quite unavoidable.

The plots shown in Figure 7.1 show the status of the two missions since the beginning of each individual mission. The time-series of the monthly mean percentage differences between GOME-2A GDP-4.8 (blue line) and GOME-2B GDP-4.8 (orange line) against the Dobson Northern Hemisphere stations are shown in the upper left panel and against the Dobson Southern Hemisphere stations in the upper right panel. The latitudinal dependency of the differences for the Dobson network is shown at the bottom panel.

The data shown in this Figure are not common data points, it is hence unavoidable that some of the differences seen in Figure 7.1, bottom panel, are sampling differences and not real inter-satellite deviations. Those may be perused from the upper panel where the time series are shown.

Focusing on the monthly mean time series, both for the Northern [left] as well as the Southern Hemisphere [right], the differences appear well-stable in time and within 0 – 2 % to the ground network, depending on the season. This seasonality in the differences between satellite and ground-based Dobson observations is a well-known feature which appears in most operational and scientific satellite TOC comparisons, see for e.g. the validation of the OMI/Aura products [Balis *et al.*, 2007a], the GOME/ERS-2 product [Balis *et al.*, 2007b] and even the recent GOME/ERS-2, SCIAMACHY/Envisat and GOME-2/Metop-A ESA products [Koukouli *et al.*, 2015, Garane *et al.*, 2015]. The reasons have to do with the treatment of the variability of the stratospheric temperature and how that affects the ozone absorption coefficients used in the different algorithms [Fragkos *et al.*, 2013; Serdyuchenko *et al.*, 2014]. Hence, when the assumed stratospheric temperature deviates strongly from what is assumed by the algorithms, which is usually the case during the winter months, the differences between ground and satellite increase. See the recent work of Koukouli *et al.*, 2016, and discussion therein, on this topic.

In the right upper panel of Figure 7.1, a deviation from the normal seasonality is observed for the last six months of 2017 and the beginning of 2018 in the Northern Hemisphere, which comes mainly from the 20°S – 40°S belt where stations such as Melbourne (lat: -37.47; lon: 144.58) and Cachoeira-Paulista (lat: -22.68; lon: - 45.00) are located and their rather unstable behavior dominate the statistics, since the data availability from other stations is limited for the time being.

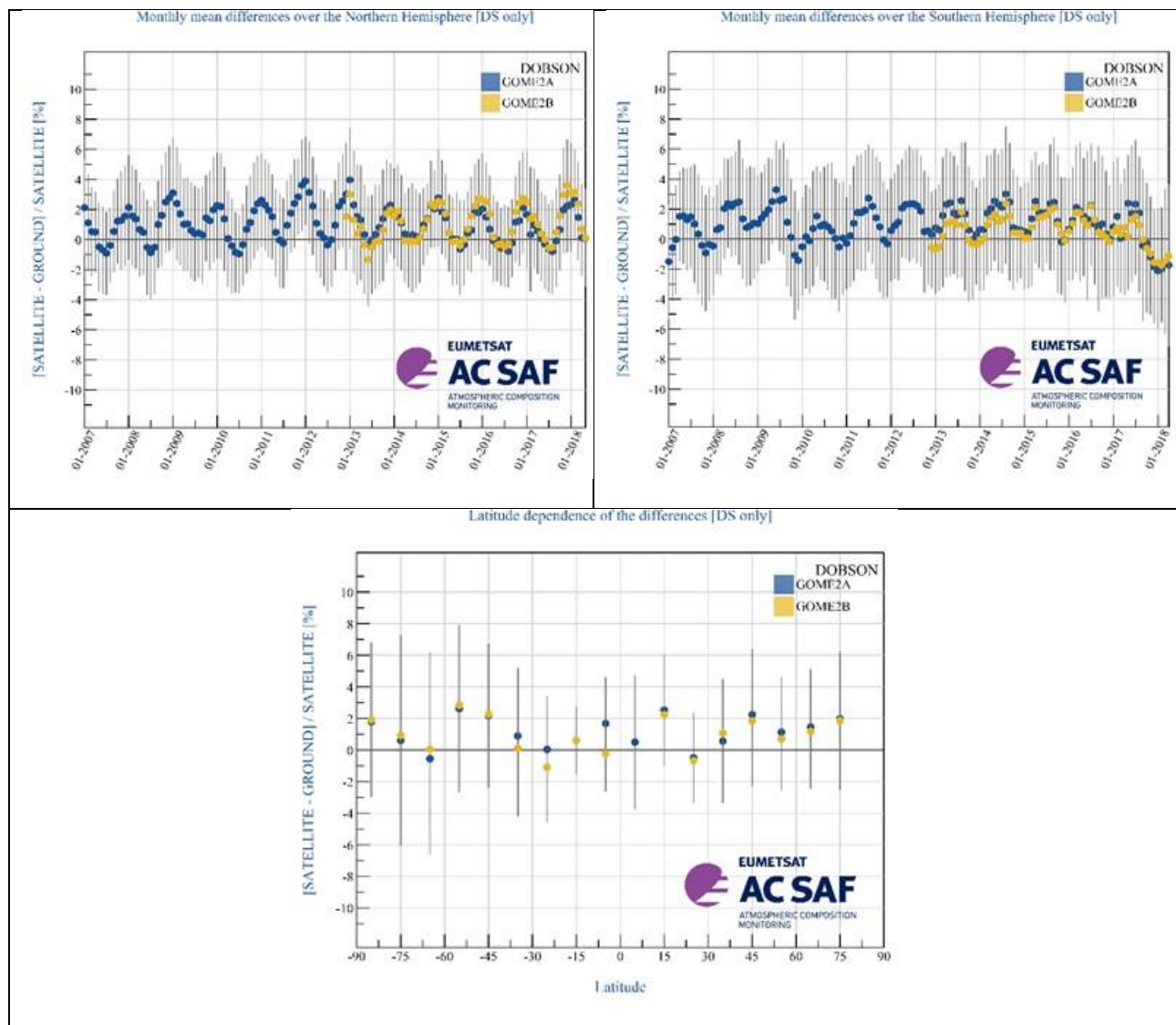


Figure 7.1. Time-series of the monthly mean percentage differences between GOME-2A GDP-4.8 (blue line) and GOME-2B GDP-4.8 (orange line) against the Dobson Northern Hemisphere stations (upper left panel) and the Dobson Southern Hemisphere stations (upper right panel). The latitudinal dependency of the differences for the Dobson network are shown at the bottom panel.

The plots shown in Figure 7.2 are as per Figure 7.1 but for the common points between the two sensors, hence the temporal span is limited to the beginning of year 2013 onwards. There appear to be periods where the two instruments deviate in both the NH [upper left] and the SH [upper right]; for the NH, a >1% difference is seen for year 2013 as well as from mid-2015 to mid-2016 which manifests as over-estimation in the former and under-estimation in the latter period. For the SH, the 2013 differences are observed, again at the ~1% difference level, extending up until the mid-2014. From the latitudinal variability plot, Figure 7.2 bottom panel, it can be seen that the Antarctic regions, southwards of -65°S show an over-estimation of GOME-2B whereas for the rest of the planet GOME-2A shows an over-estimation.

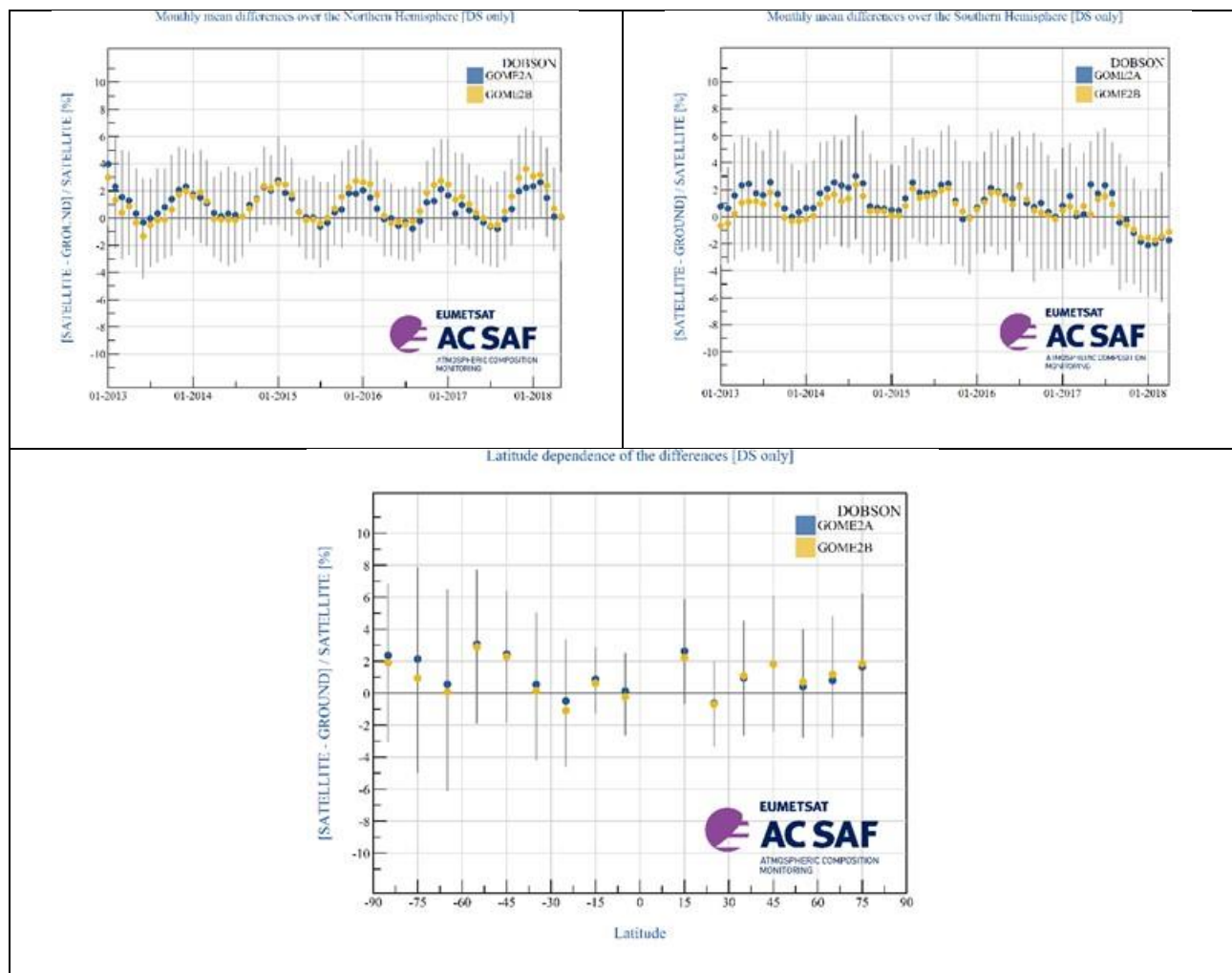


Figure 7.2. Time-series of the monthly mean percentage differences between GOME-2A GDP-4.8 (blue line) and GOME-2B GDP-4.8 (orange line) against the Dobson Northern Hemisphere stations (upper left panel) and the Dobson Southern Hemisphere stations (upper right panel). The latitudinal dependency of the differences for the Dobson network is shown at the bottom panel.

7.1.1.3 GOME-2A and GOME-2B GDP-4.8 TOC validation | The Brewer comparisons

In Figure 7.3, left panel, the time series of the comparisons between GOME-2A and GOME-2B and Brewer TOCs are shown for the Northern Hemisphere. In the right panel, the latitudinal variability of the differences is presented. Zooming into the common period between 2013 and June 2017 [Figure 7.4] a very similar behaviour is observed in the left panel, as per Figure 7.2 left panel for the Dobson comparisons.

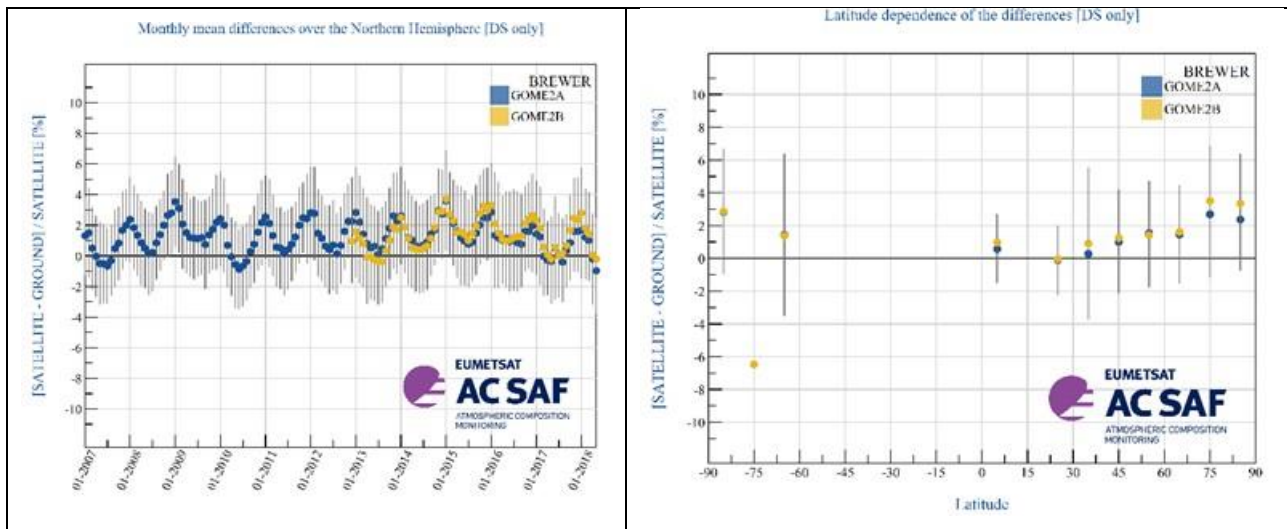


Figure 7.3. Time-series of the monthly mean percentage differences between GOME-2A GDP-4.8 (blue line) and GOME-2B GDP-4.8 (orange line) against the Brewer reported TOCs between January 2007 and June 2018; left panel, the NH time series and right panel, the latitudinal dependency of the differences.

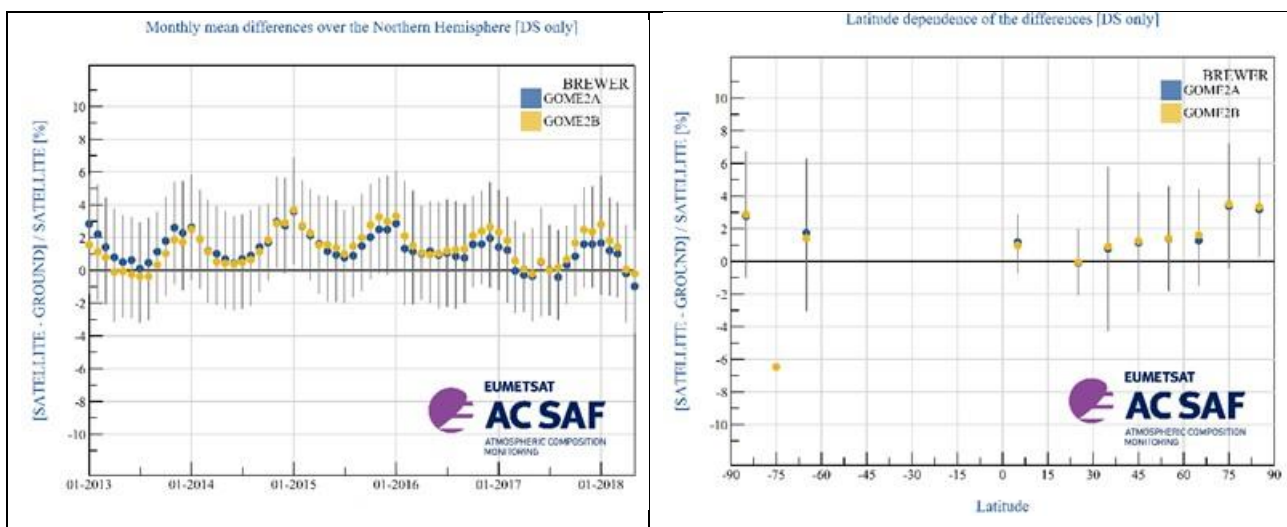


Figure 7.4. Time-series of the monthly mean percentage differences between GOME-2A GDP-4.8 (blue line) and GOME-2B GDP-4.8 (orange line) against the Brewer reported TOCs between January 2013 and June 2018; left panel, the NH time series and right panel, the latitudinal dependency of the differences.

7.1.1.4 GOME-2A and GOME-2B GDP-4.8 TOC validation | Tables of statistics

In Table 7.2, the summary statistics for the comparisons presented in Figure 7.1, top left and right panels, for the Dobson stations, as well as Figure 7.3, left panel only, for the Brewer stations, are enumerated. The number of individual daily common observations for the Dobsons hence apply to the entire Globe whereas the Brewer comparisons depict only the NH. As can be noted, the relative differences between GOME-2A and GOME-2B against Brewer and Dobson stations are very stable, with an average mean difference of 1 ± 5 %.

Table 7.2. Summary statistics for the January 2007 [or January 2013] to June 2018 period, applicable to Figure 7.1 top panels and Figure 7.3, left panel, based on GOME-2A & GOME-2B OTO data and WUDC Brewer & Dobson observations.

		Brewer	Dobson
GOME-2/Metop-A 01/2007 – 06/2018	# stations:	72	68
	# obs:	154140	116260
	mean:	$1.02 \pm 5.16 \%$	$0.90 \pm 4.65 \%$
GOME-2/Metop-B 01/2013 – 06/2018	# stations:	61	63
	# obs:	69304	53807
	mean:	$1.09 \pm 4.46 \%$	$0.72 \pm 4.41 \%$

7.1.2. Validation website update

The AC SAF Ozone Validation & Quality Assessment Website is currently available at <http://lap3.physics.auth.gr/eumetsat/> however is still under-going quality control and fine-tuning after its launch on the initiation of the AC SAF project in 1 March 2017.

The validation webpages host the validation results of GOME-2A GDP-4.8 and GOME-2B GDP-4.8 near real-time and offline data and they are available until 31/07/2018 and 19/08/2018, respectively. In Figure 7.5 example statistics about the website traffic are shown for the period 1 January 2018 – 30 June 2018 as extracted from Google Analytics.

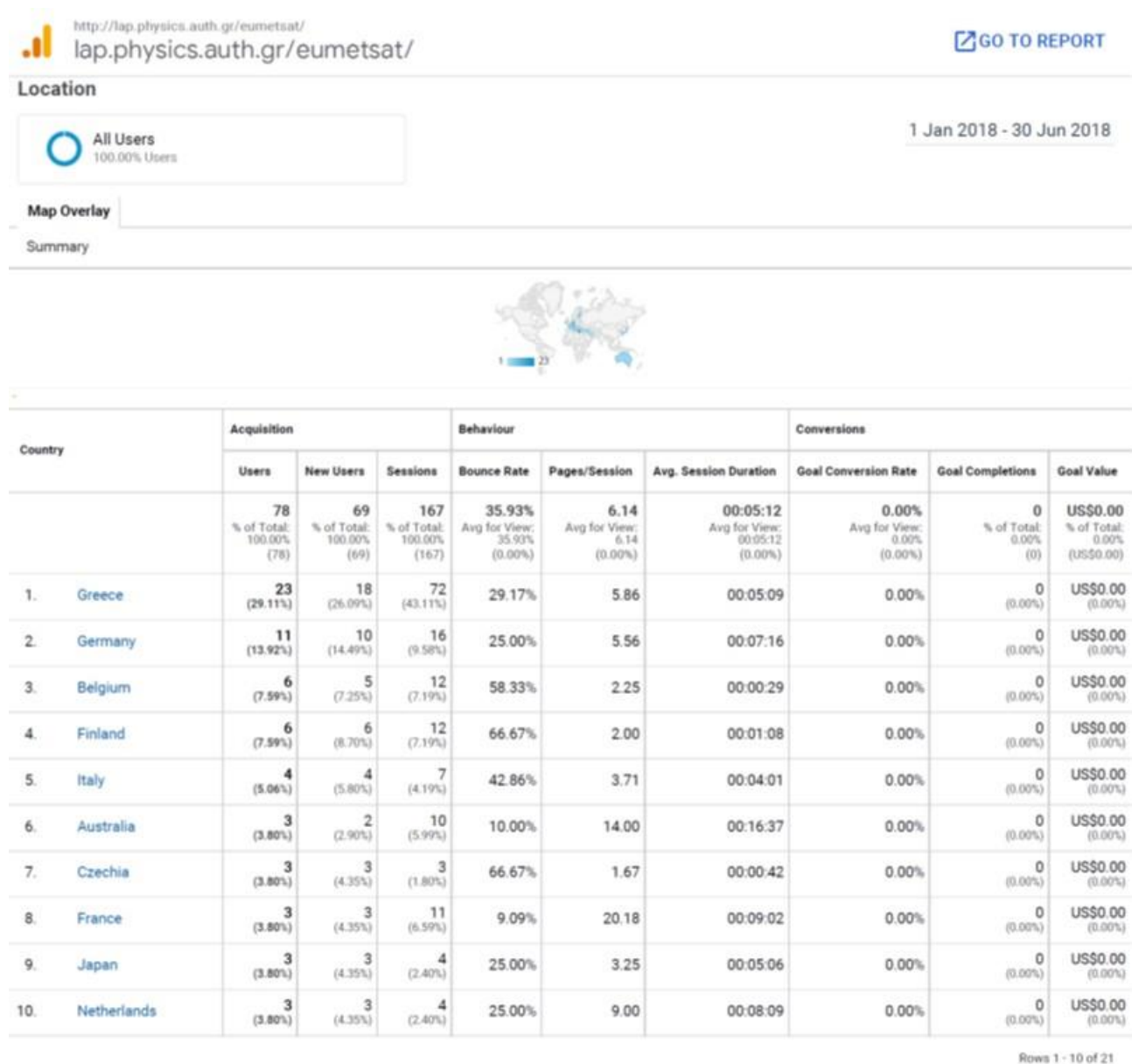


Figure 7.5. The global demographics of the visitors to the AC SAF validation website.

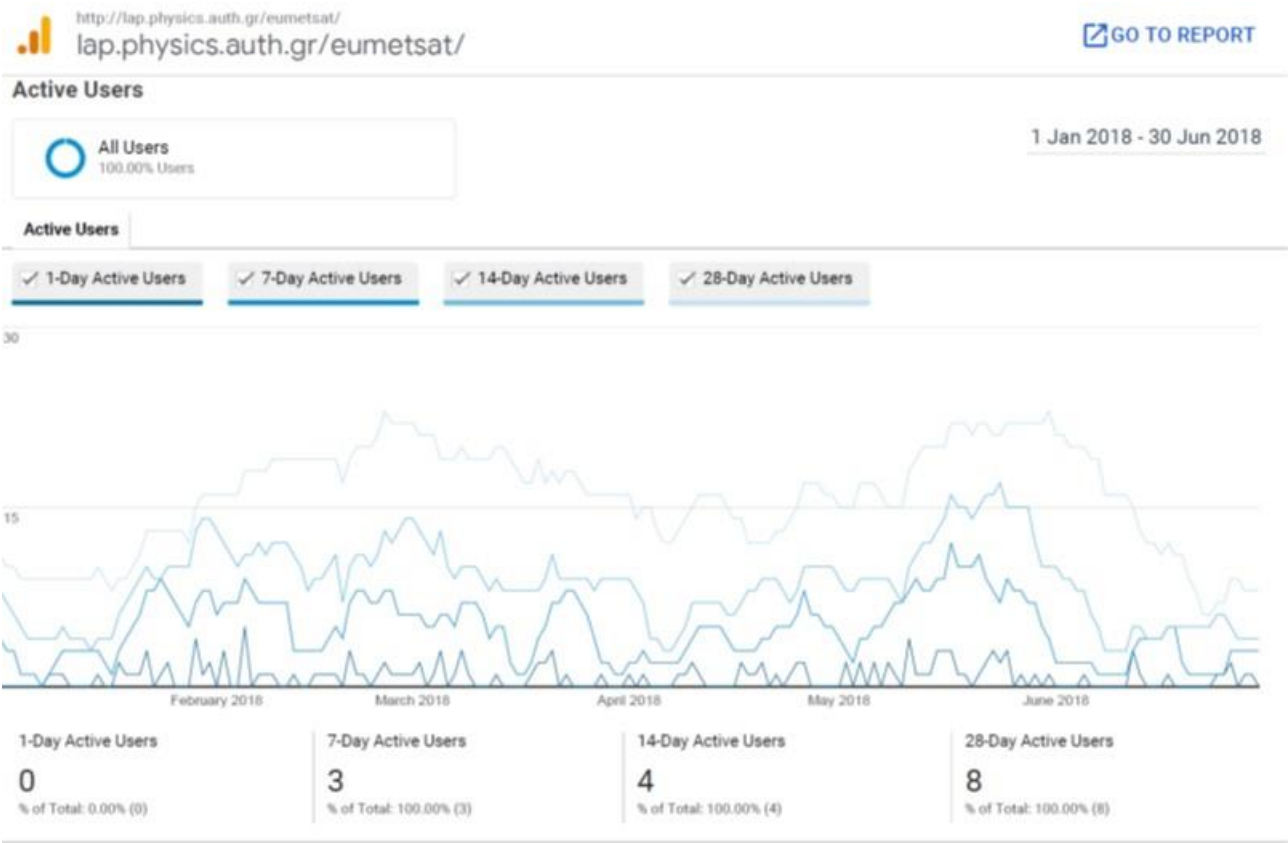


Figure 7.6. The activity of the users of the AC SAF validation web pages.

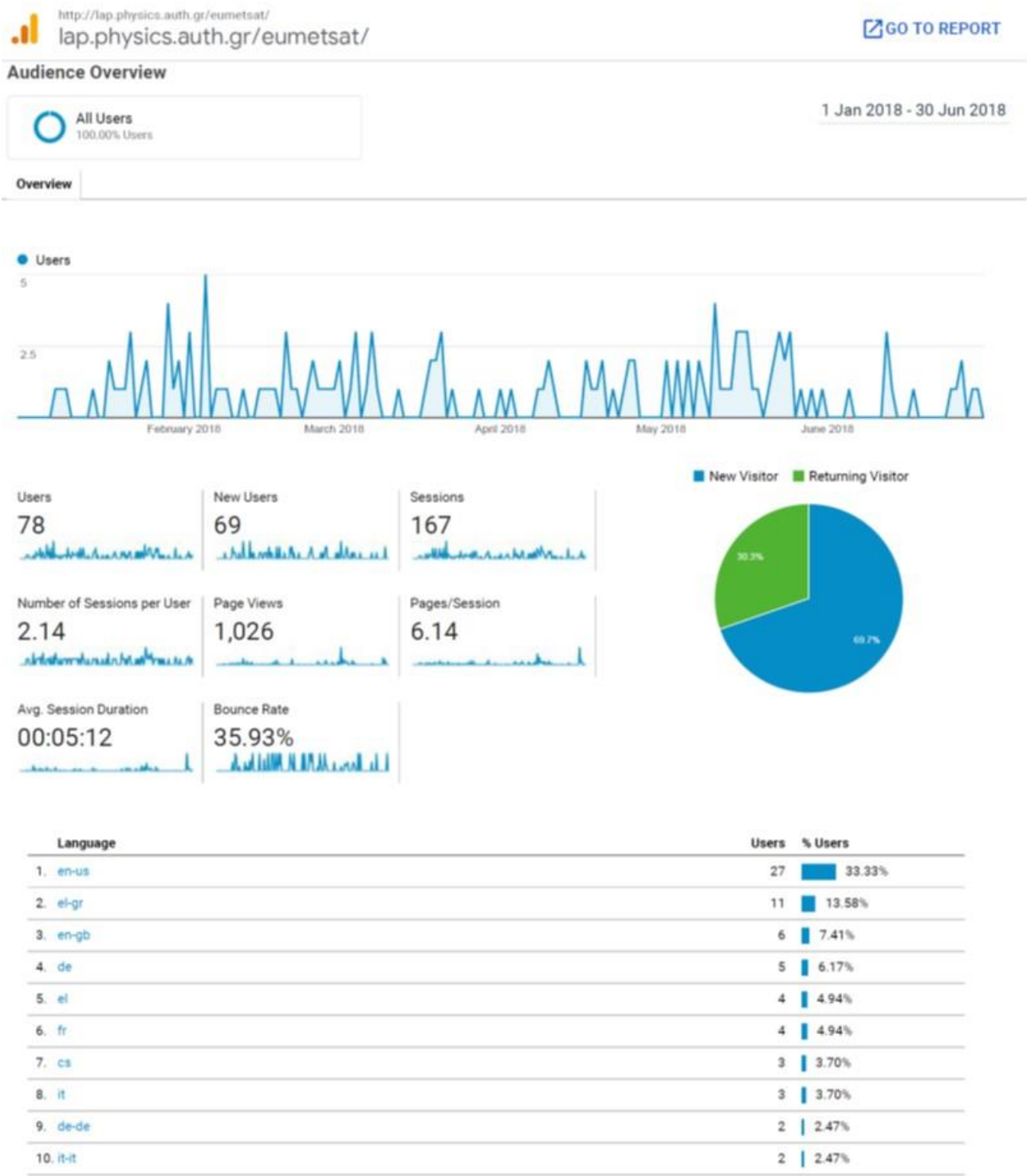


Figure 7.7. From top to bottom: daily number of visiting sessions, percentage of website visitors and average session duration and provenance of website visitors per country of origin.

References:

- Antón, M., Loyola, D., López, M., Vilaplana, J. M., Bañón, M., Zimmer, W., and Serrano, A.: Comparison of GOME-2/MetOpA total ozone data with Brewer spectroradiometer data over the Iberian Peninsula, *Annales Geophysicae*, 27, 1377–1386, 2009.
<https://doi.org/10.5194/angeo-27-1377-2009>
- Balis, D., Kroon M., Koukouli, M.E., Brinksma, E. J., Labow, G., Veefkind, J. P., and McPeters, R. D.: Validation of Ozone Monitoring Instrument total ozone column measurements using Brewer and Dobson spectrophotometer ground-based observations, *J. Geophys. Res.*, 112, D24S46, 2007a.
<https://doi.org/10.1029/2007JD008796>
- Balis, D., Lambert, J-C., Van Roozendael, M., Spurr, R., Loyola, D., Livschitz, Y., Valks, P., Amiridis, V., Gerard, P., Granville, J., and Zehner, C.: Ten years of GOME/ERS-2 total ozone data – The new GOME data processor (GDP) version 4: 2. Ground-based validation and comparisons with TOMS V7/V8, *J. Geophys. Res.*, vol. 112, D07307, 2007b.
<https://doi.org/10.1029/2005JD006376>
- Fragkos, K., Bais, A. F., Balis, D., Meleti, C., and Koukouli, M. E.: The effect of three different absorption cross-sections and their temperature dependence on total ozone measured by a mid-latitude Brewer spectrophotometer, *Atmos. Ocean*, 53, 2015.
<https://doi.org/10.1080/07055900.2013.847816>
- Hao, N., Koukouli, M. E., Inness, A., Valks, P., Loyola, D. G., Zimmer, W., Balis, D. S., Zyrichidou, I., Van Roozendael, M., Lerot, C., and Spurr, R. J. D.: GOME-2 total ozone columns from MetOp-A/MetOp-B and assimilation in the MACC system, *Atmos. Meas. Tech.*, 7, 2937–2951, 2014.
<https://doi.org/10.5194/amt-7-2937-2014>
- Koukouli, M. E., Balis, D. S., Loyola, D., Valks, P., Zimmer, W., Hao, N., Lambert, J.-C., Van Roozendael, M., Lerot, C., and Spurr, R. J. D.: Geophysical validation and long-term consistency between GOME-2/MetOp-A total ozone column and measurements from the sensors GOME/ERS-2, SCIAMACHY/ENVISAT and OMI/Aura, *Atmos. Meas. Tech.*, 5, 2169–2181, 2012.
<https://doi.org/10.5194/amt-5-2169-2012>
- Koukouli, M. E., Lerot, C., Granville, J., Goutail, F., Lambert, J.-C., Pommereau, J.-P., Balis, D., Zyrichidou, I., Van Roozendael, M., Coldewey-Egbers, M., Loyola, D., Labow, G., Frith, S., Spurr, S., and Zehner, C.: Evaluating a new homogeneous total ozone climate data record from GOME/ERS-2, SCIAMACHY/Envisat and GOME-2/MetOp-A, *J. Geophys. Res. Atmos.*, 120, 12296–12312, 2015.
<https://doi.org/10.1002/2015JD023699>
- Koukouli, M. E., Zara, M., Lerot, C., Fragkos, K., Balis, D., van Roozendael, M., Allart, M. A. F., and van der A, R. J.: The impact of the ozone effective temperature on satellite validation using the Dobson spectrophotometer network, *Atmos. Meas. Tech.*, 9, 2055–2065, 2016.
<https://doi.org/10.5194/amt-9-2055-2016>
- Loyola, D. G., Koukouli, M. E., Valks, P., Balis, D. S., Hao, N., Van Roozendael, M., Spurr, R. J. D., Zimmer, W., Kiemle, S., Lerot, C., and Lambert, J.-C.: The GOME-2 total column ozone product: Retrieval algorithm and ground-based validation, *J. Geophys. Res.*, 116, 2011.
<https://doi.org/10.1029/2010JD014675>

Serdyuchenko, A., Gorshelev, V., Weber, M., Chehade, W., and Burrows, J. P.: High spectral resolution ozone absorption cross-sections – Part 2: Temperature dependence, *Atmos. Meas. Tech.*, 7, 625–636, 2014.

<https://doi.org/10.5194/amt-7-625-2014>

Garane, K., Lerot, C., Coldewey-Egbers, M., Verhoelst, T., Koukouli, M. E., Zyrichidou, I., Balis, D. S., Danckaert, T., Goutail, F., Granville, J., Hubert, D., Keppens, A., Lambert, J.-C., Loyola, D., Pommereau, J.-P., Van Roozendaal, M., and Zehner, C.: Quality assessment of the Ozone_cci Climate Research Data Package (release 2017) – Part 1: Ground-based validation of total ozone column data products, *Atmos. Meas. Tech.*, 11, 1385–1402, 2018.

<https://doi.org/10.5194/amt-11-1385-2018>

7.1.3. Online quality monitoring

Before the CDOP-3, the online quality monitoring of the total ozone column products by DLR was limited to the generation of orbital and daily quick look maps of the total ozone columns from GOME-2A, GOME-2B, as well as composite maps. An example is shown below in Figure 7.8.

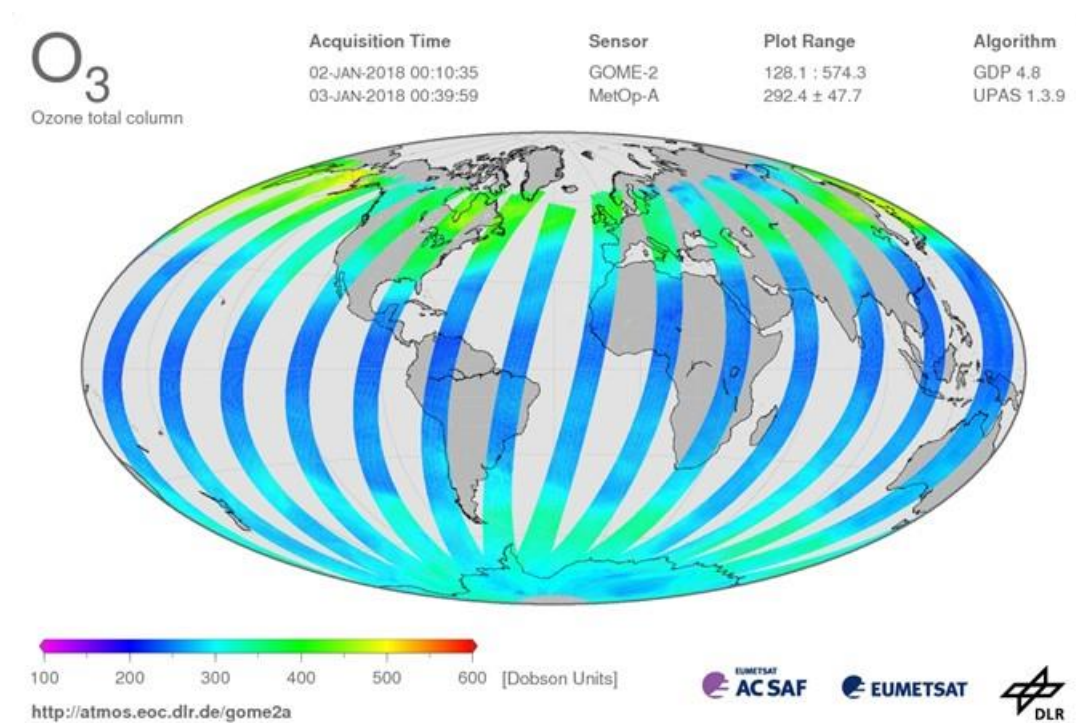


Figure 7.8. Example of daily GOME-2A total ozone map (January 2, 2018)

A new online quality monitoring tool for the operational GOME-2 L2 total ozone and other trace gas column products has been developed by DLR at the end of the CDOP-2. The QA tool generates daily distribution maps and time series of DOAS fitting residual (RMS), slant column densities (SCDs) and vertical column densities (VCDs) for global and selected regions to do the online quality monitoring. Figure 7.9 shows the distribution of total ozone RMS and the numbers of pixels on January 2, 2018. Most of the total ozone RMS are between 0.001 - 0.002 and the maximum is smaller than 0.01 and there are 170519 measurements in total. The constant ozone VCDs in the South Pacific Ocean between 1 - 31 January 2018, as shown in Figure 7.11, indicate that there are probably no (major) issues with the data quality in this month (a sudden change in the average ozone column in the tropical southern Pacific would be an indication of a problem with the GOME-2 data).

This information indicates that there are no data quality issue of ozone DOAS fitting on this day. The similar distribution maps of SCDs and VCDs can provide more information of data quality related to DOAS fitting and AMF calculations (see Figure 7.10 and other examples for other trace gases in Section 7.3.1).

In addition, the time-series of key parameters (RMS, SCDs and VCDs) are investigated for a subset of geo-locations where natural or anthropogenic variations are minimum to assess the overall consistency and possible changes with time. The time span and latitude and longitude of regions can be selected by the users, for example the Southern Pacific Ocean (25°S - 15°S and 150°W - 110°W) and the Sahara desert (20°N - 30°N and 0°E - 30°E).

The online quality monitoring tool will be implemented in the operational AC SAF processing environment in 2018/2019.

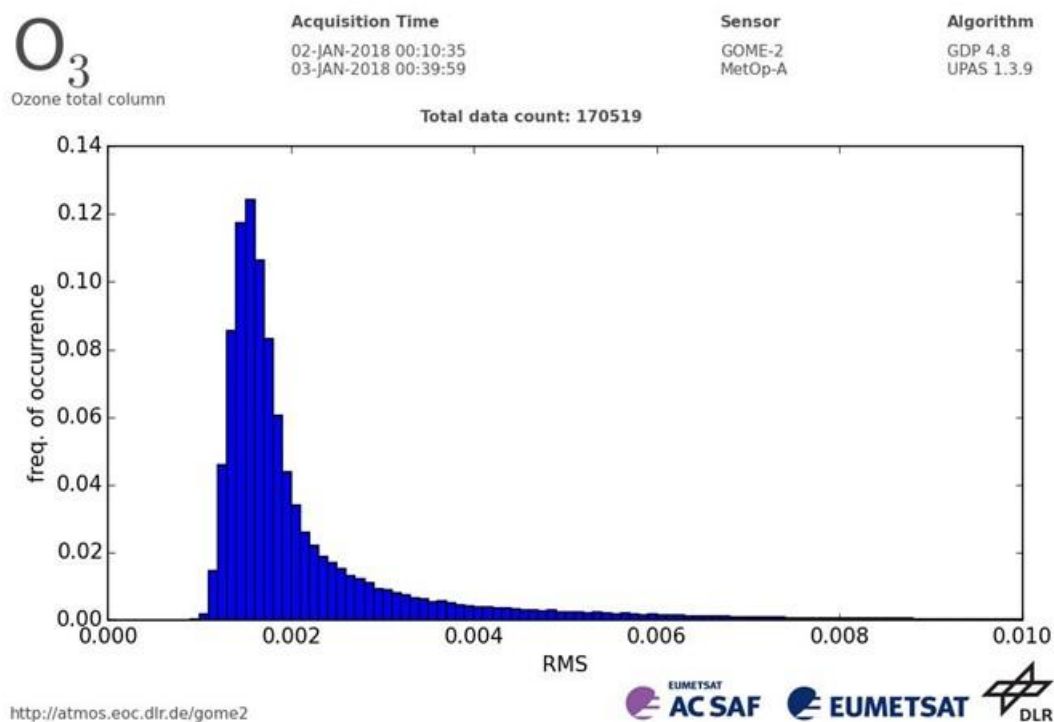


Figure 7.9. Daily distribution map of total ozone DOAS fitting residual (RMS) on January 2, 2018 using global GOME-2A data.

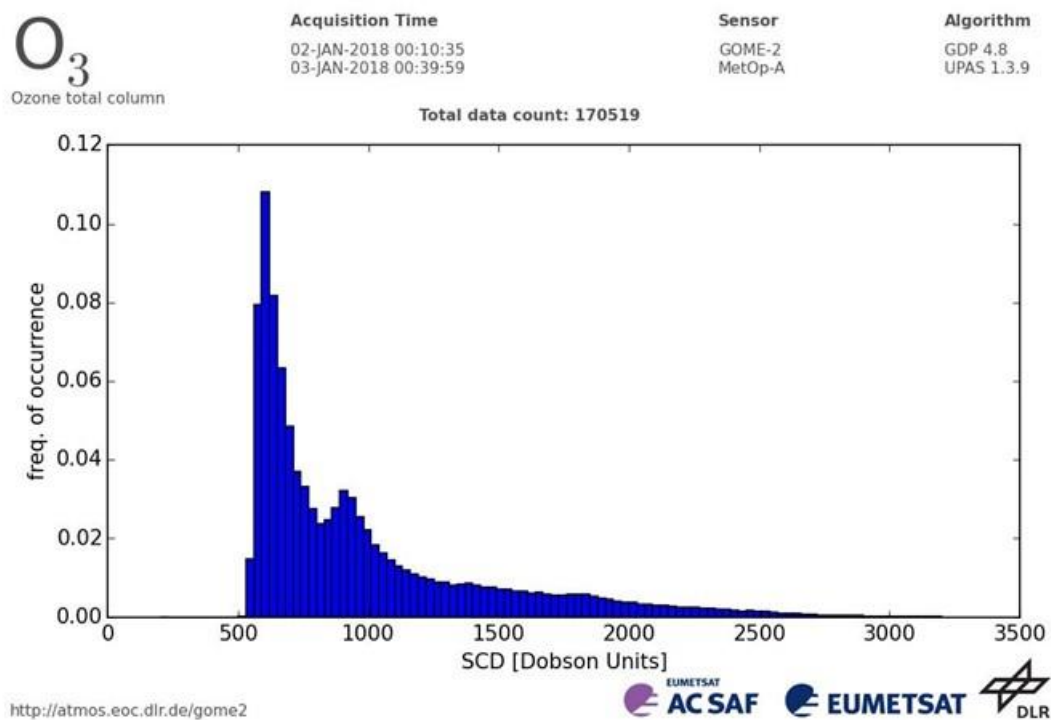


Figure 7.10. Daily distribution map of ozone SCDs on January 2, 2018 using global GOME-2A data.

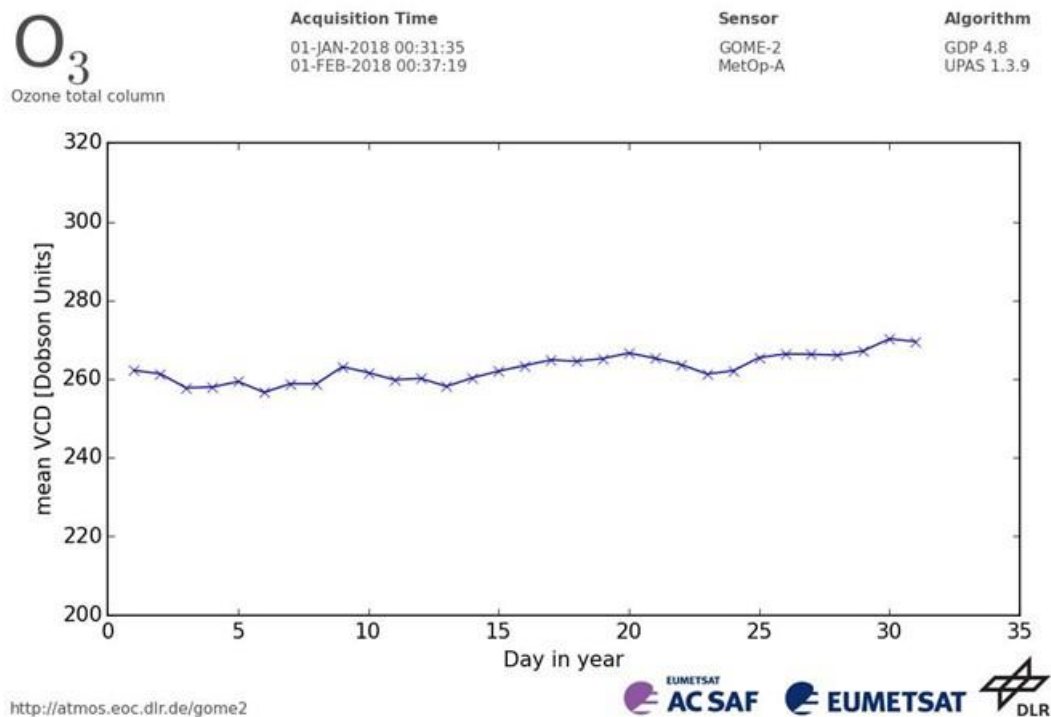


Figure 7.11. The time-series of total ozone VCDs in the South Pacific Ocean, 1 - 31 January 2018.

More information about quality monitoring of the operational GOME-2 total ozone columns by other AC SAF and external partners is available at the following websites:

<https://acsaf.org> → Product info → QM websites

http://lap3.physics.auth.gr/eumetsat/validation/near_real

<http://lap3.physics.auth.gr/eumetsat/validation/offline>

<http://www.temis.nl/o3msaf/vod/>

<https://www.ecmwf.int/en/forecasts/charts/obstat/?facets=Parameter,Ozone;Instrument,GOME2>

7.2. Tropospheric ozone products

Table 7.3. Validation status of tropospheric ozone products

Product Identifier	Product Name	Accuracy	Reference	Validating Institute
O3M-35	Offline tropical tropospheric ozone	Fulfil target accuracy requirement	RD18	KMI
O3M-43				
O3M-172	NRT global tropospheric ozone	Fulfil target accuracy requirement	RD19	KMI
O3M-174				
O3M-173	Offline global tropospheric ozone	Fulfil target accuracy requirement	RD19	KMI
O3M-175				

Validation activities summary for global tropospheric ozone:

This summary contains validation results of the GOME-2A and GOME-2B high resolution (HR) tropospheric ozone column products, retrieved by the Ozone Profile Retrieval Algorithm (OPERA) at KNMI. It covers the time period July 2017 - June 2018. Validation results are shown from two TrOC products, i.e. the tropopause related product and a fixed altitude TrOC product. The TrOC products are derived from the daily operational ozone profile product.

Since these TrOC products are derived from the OPERA ozone profile product, OPERA averaging kernel smoothing has been applied to the ground based reference profiles before calculating comparison statistics. This AVK smoothing is expected to reduce the vertical smoothing difference error between satellite and ground based measurements. The outcome is summarized at the end of this section.

This summary was made available by Dr. Andy Delcloo from KMI. More information on how these values are extracted is available in the validation report

(https://acsaf.org/docs/vr/Validation_Report_O3Tropo_Sep_2015.pdf). The collocation data used are the same as for the ozone profiles (Figure 7.43).

The statistics on the accuracy of the GOME-2A and GOME-2B HR tropospheric ozone column products (tropopause related) for different latitude belts, validated against $X_{\text{AVK-sonde}}$, are shown in Table 7.4 and Table 7.5.

Table 7.4. Relative Differences (RD) and standard deviation (STDEV) are shown (in percent) together with the Absolute Difference (DU) on the accuracy of the GOME-2A HR tropospheric ozone column products (tropopause related) for five different latitude belts, validated against $X_{AVK-sonde}$

	GOME-2A HR			
July 2017 - June 2018	RD (%)	STDEV (%)	AD (DU)	STDEV (DU)
Northern Polar Region	-19.4	16.2	-5.9	5.4
Northern Mid-Latitudes	-36.9	22.3	-13.3	8.6
Tropical region	-40.3	24.2	-11.5	8.0
Southern Mid-Latitudes	-19.8	19.6	-5.0	5.4
Southern Polar Region	-25.4	8.0	-6.9	4.8

Table 7.5. Relative Differences (RD) and standard deviation (STDEV) are shown (in percent) together with the Absolute Difference (DU) on the accuracy of the GOME-2B HR tropospheric ozone column products (tropopause related) for five different latitude belts, validated against $X_{AVK-sonde}$

	GOME-2B HR			
July 2017 - June 2018	RD (%)	STDEV (%)	AD (DU)	STDEV (DU)
Northern Polar Region	45.9	47.2	13.3	14.2
Northern Mid-Latitudes	45.0	63.3	11.4	19.1
Tropical region	-37.8	33.9	-10.6	10.9
Southern Mid-Latitudes	35.5	47.7	7.9	11.6
Southern Polar Region	30.7	59.0	5.8	10.9

The statistics on the accuracy of the GOME-2A and GOME-2B HR tropospheric ozone column products (fixed altitude) for different latitude belts, validated against $X_{AVK-sonde}$, are shown in Table 7.6 and Table 7.7.

Table 7.6. Relative Differences (RD) and standard deviation (STDEV) are shown (in percent) together with the Absolute Difference (DU) on the accuracy of the GOME-2A HR tropospheric ozone column products (fixed altitude) for five different latitude belts, validated against $X_{AVK-sonde}$

	GOME-2A HR			
July 2017 - June 2018	RD (%)	STDEV (%)	AD (DU)	STDEV (DU)
Northern Polar Region	-14.2	11.8	-2.4	2.1
Northern Mid-Latitudes	-34.0	21.1	-6.2	4.2
Tropical region	-54.5	27.8	-6.6	4.4
Southern Mid-Latitudes	-16.2	16.0	-1.9	2.0
Southern Polar Region	-17.7	7.7	-2.0	0.9

Table 7.7. Relative Differences (RD) and standard deviation (STDEV) are shown (in percent) together with the Absolute Difference (DU) on the accuracy of the GOME-2B HR tropospheric ozone column products (fixed altitude) for five different latitude belts, validated against X_{AVK-sonde}

July 2017 - June 2018	GOME-2B HR			
	RD (%)	STDEV (%)	AD (DU)	STDEV (DU)
Northern Polar Region	22.6	23.7	3.7	4.0
Northern Mid-Latitudes	23.6	33.3	3.2	5.5
Tropical region	-43.0	39.2	-5.3	5.7
Southern Mid-Latitudes	18.8	25.8	2.3	3.2
Southern Polar Region	26.1	53.2	2.5	5.0

The tropospheric ozone column (TrOC) product has the following user requirements:

- Threshold accuracy: within 50 %
- Target accuracy: within 20 %
- Optimal accuracy: within 15 %

Besides the tropopause related altitude GOME-2B HR TrOC products for Northern mid-latitudes, all the products are within the threshold accuracy. However, most of the products don't meet the target accuracy anymore. The GOME-2A products are clearly affected by the degradation on its sensor. This results in a significant underestimation of the retrieved tropospheric ozone concentrations.

The elevated relative difference values and standard deviations for the GOME2-B products can be explained by an issue found in the retrieval of the ozone profile product. KNMI (personal communication, Olaf Tuinder) reported that there seems to be an issue with the choice of the wavelength range, used for this ozone profile product on GOME-2B. The necessary modifications will soon be implemented in the operational chain during the next software update.

Validation activities summary for tropical tropospheric ozone:

This summary contains validation results of the GOME-2A and GOME-2B tropical tropospheric ozone column (TTrOC) products, using the cloud slicing method. The tropospheric ozone retrieval is based on the GOME-2 ozone columns as derived by the GOME Data Processor (GDP, version 4.8) and covers the tropical latitude belt (20°S - 20°N). This product is available on a monthly basis and has a resolution of 1.25° latitude x 2.5° longitude.

The tropical tropospheric ozone column (TTrOC) product has the following user requirements:

- Threshold accuracy: within 50 %
- Target accuracy: within 25 %
- Optimal accuracy: within 15 %

This summary was made available by Dr. Andy Delcloo from KMI. More information on how these values are extracted is available in the validation report

(https://acsaf.org/docs/vr/Validation_Report_OTTO_O3Tropo_Jul_2015.pdf) The collocation data used are the same as for the ozone profiles (Figure 7.43).

The time period covered is January 2015 - December 2017 for GOME-2A and GOME-2B offline TTrOC products.

In Table 7.8 and Table 7.9, the statistics on the accuracy of the GOME-2A and GOME-2B tropical tropospheric ozone column products for different stations under consideration are shown, showing some general statistics for the GOME-2A dataset. It is shown that most of the stations are within the target accuracy (20 %). The correlation varies between 0.4 and 0.9 with an RMSE between 2.2 and 8.3 DU. There is also an offset present between GOME-2A and GOME-2B as described in the validation report. These TTrOC products still fulfill the user requirements.

Table 7.8. Relative Differences (RD), standard deviation (STDEV), correlation, bias and RMSE are shown on the accuracy of the GOME-2A TTrOC product for the time period January 2015 - December 2017

Station	RD (%)	STDEV (%)	Correlation	Bias (DU)	RMSE (DU)
Paramaribu	14.80	13.46	0.90	2.82	3.89
Alajuela	46.25	23.15	0.60	6.87	7.59
Samoa	9.83	27.79	0.39	1.18	4.96
Kuala Lumpur	7.39	12.65	0.78	1.27	2.54
Nairobi	31.97	16.10	0.72	5.95	6.51
Natal	15.73	12.09	0.89	3.80	4.67
Hilo	24.64	25.95	0.75	5.58	8.32

Table 7.9. Relative Differences (RD), standard deviation (STDEV), correlation, bias and RMSE are shown on the accuracy of the GOME-2B TTrOC product for the time period January 2015 - December 2017

Station	RD (%)	STDEV (%)	Correlation	Bias (DU)	RMSE (DU)
Paramaribu	3.16	14.50	0.85	0.73	2.73
Alajuela	29.32	21.91	0.66	4.42	5.45
Samoa	-10.71	27.68	0.35	-1.86	5.33
Kuala Lumpur	-7.40	13.43	0.65	-1.61	2.99
Nairobi	17.54	12.05	0.80	3.25	3.84
Natal	4.64	12.55	0.87	1.09	3.06
Hilo	19.36	24.12	0.76	4.60	7.27

7.3. Trace gas products

Table 7.10. Validation status of trace gas products

Product Identifier	Product Name	Accuracy	Reference	Validating Institute
O3M-02.1	NRT total NO ₂	Fulfils threshold accuracy requirement	RD6	BIRA-IASB
O3M-50.1				

Product Identifier	Product Name	Accuracy	Reference	Validating Institute
O3M-36.1	NRT tropospheric NO ₂	Fulfil threshold accuracy requirement	RD6	BIRA-IASB
O3M-52.1				
O3M-54.1	NRT total SO ₂	Fulfil threshold accuracy requirement	RD10	BIRA-IASB
O3M-55.1				
O3M-176.0	NRT total HCHO	Fulfil threshold accuracy requirement	RD12	BIRA-IASB
O3M-177.0				
O3M-07.1	Offline total NO ₂	Fulfil threshold accuracy requirement	RD6	BIRA-IASB
O3M-51.1				
O3M-37.1	Offline tropospheric NO ₂	Fulfil threshold accuracy requirement	RD6	BIRA-IASB
O3M-53.1				
O3M-09.1	Offline total SO ₂	Fulfil threshold accuracy requirement	RD10	BIRA-IASB
O3M-56.1				
O3M-08.1	Offline total BrO	Fulfil threshold accuracy requirement	RD11	BIRA-IASB
O3M-82.1				
O3M-10.1	Offline total HCHO	Fulfil target accuracy requirement	RD12	BIRA-IASB
O3M-58.1				
O3M-12.1	Offline total H ₂ O	Fulfil threshold accuracy requirement	RD13	DLR
O3M-86.1				

Validation activities summary:

This summary presents validation activities for offline total and tropospheric NO₂, total HCHO, total BrO and SO₂ data products of GOME-2/Metop-A/B as performed at BIRA-IASB.

The authors of this summary are Gaia Pinardi (for tropospheric NO₂, HCHO and SO₂ validation), Jean-Christopher Lambert and José Granville (for total NO₂ validation), François Hendrick (for BrO validation) and Jeroen van Gent (for quality assessment).

Validation exercises are performed following the protocols described in the original Metop-A and Metop-B validation reports (<http://cdop.aeronomie.be/validation/valid-reports>), and the results presented in this report are based on updates of the correlative datasets with the last available - and sometimes improved - versions. While illustrations at a few stations are included in this report, all the updated figures are reported on the BIRA-IASB validation server (<http://cdop.aeronomie.be/validation/valid-results>).

Update of database for reference data

The validation database was updated with ground-based BIRA-IASB MAXDOAS NO₂ and HCHO data, BIRA-IASB ZenithSky BrO data at Harestua, NDACC UVVIS ZenithSky NO₂ data, Xianghe MAXDOAS SO₂ data and Xianghe DirectSun NO₂ and SO₂ data, in order to cover as much as possible of the period until end of June 2018.

ZenithSky NO₂ total columns are downloaded from the NDACC Data Host Facility (where data have to be uploaded maximum 2 years after acquisition) and from the SAOZ rapid delivery web facility; the ground-based data are then quality assessed and post-processed at BIRA-IASB in preparation for the data comparisons.

The BIRA-IASB MAXDOAS ground-based dataset are automatically retrieved with an improved version of the bePRO profiling algorithm (Clémer *et al.*, 2010; Hendrick *et al.*, 2014, Vlemmix *et al.*, 2015) developed within the EU FP7 NORS and QA4ECV projects (aiming at rapid delivery of improved NO₂ and HCHO profiles). Datasets are available at the following ground-based stations: OHP (from June 2007 to July 2014 with the geometrical approximation, and since August 2014 to March 2017 with the profiling tool; after that period the instrument had a fatal failure and the data are thus not included in this report), Beijing (from June 2008 to April 2009), Xianghe (since March 2010), Uccle (from April 2011 to March 2016 with a miniMAXDOAS instrument (Uccle-miniDOAS) and since end of January 2017 with a scientific grade MAXDOAS: Uccle-SG), Bujumbura (from November 2013 to July 2017; since then the instrument had a power failure and thus no new data are included in this report) and LePort, on Reunion Island (from April 2016 to 10 January 2018 when the instrument has been dismantled due to a cyclone). The instrument in Reunion Island has been reinstalled just before the summer on the Mado site, but no data are available for this report.

Ground-based BrO columns are derived at Harestua from vertical profiles retrieved by applying an OEM (Optimal Estimation Method)-based profiling technique to zenith-sky measurements at sunrise (Hendrick *et al.*, 2007).

Xianghe SO₂ MAXDOAS profiles dataset has been extended following Wang *et al.* (2014) until June 2018.

Status of GOME-2A & GOME-2B tropospheric NO₂

Comparisons with ground-based MAXDOAS instruments is performed similarly as in previous validation reports

(https://acsaf.org/docs/vr/Validation_Report_NTO_OTD_DR_NO2_GDP48_Nov_2015.pdf).

Since operation report 2/2016 the ground-based NO₂ MAXDOAS data have been filtering for clouds, using the cloud discrimination method described in Gielen *et al.* (2014) and removing thick clouds. This has been found to remove large peaks in tropospheric NO₂ in winter period, which was leading to large relative differences, i.e. in the Xianghe comparisons. However, work performed in the second half of 2017 lead to the conclusion that for the special case of Xianghe (and more generally all potential sites in Eastern China) the NO₂ and aerosol are tightly linked to each other. So filtering for clouds (or equivalently low aerosol content since MAXDOAS cloud filters are sensitive to aerosols) is equivalent to filtering for clean conditions having both low NO₂ and low aerosol content. Since both satellite and MAXDOAS measurements are sensitive to this, it should not affect too much the validation results, but it affects clearly the sampling of the comparison cases and the range of NO₂ columns. This has been showed by Richter *et al.* in a presentation at the DOAS workshop 2017, and since last operation report (2/2017) we thus come back to show validation results keeping the “high aerosol load” cases (i.e. without MAXDOAS cloud filtering, e.g. in Figure 7.12 for GOME-2A). For the sake of continuity, since the last operation reports, the figures with and without the cloud filtering have been kept in the webserver cdop.aeronomie.be validation results that was slightly re-styled.

Of the six BIRA-IASB stations, only two have data until end of June 2018 (Xianghe and Uccle-SG). Figure 7.12 and Figure 7.13 show examples of results at the Xianghe station (China), showing daily and monthly time-series and scatter plot and mean absolute and relative differences

for GOME-2A. Monthly mean differences are calculated for every year and for the whole time-series in order to see the evolution in time of the bias. Table 7.11 report the differences and the standard deviations at the three stations, and the figures for the other stations can be found on the BIRA-IASB validation web server: <http://cdop.aeronomie.be/validation/valid-results?gas=12&platform=0&instrumentType=1&station=0&instrument=7>

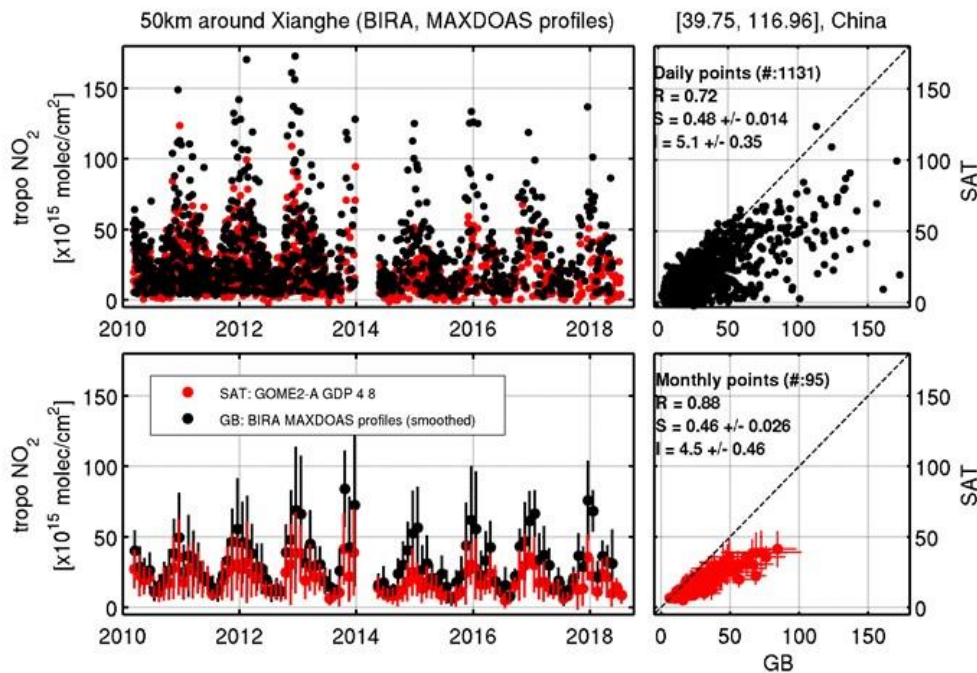


Figure 7.12. Time-series and scatter plots of GOME-2A GDP-4.8 and MAXDOAS tropospheric NO₂ columns above Xianghe, from March 2010 to end June 2018. The upper panels present the daily comparisons while the lower panels present the monthly mean comparisons.

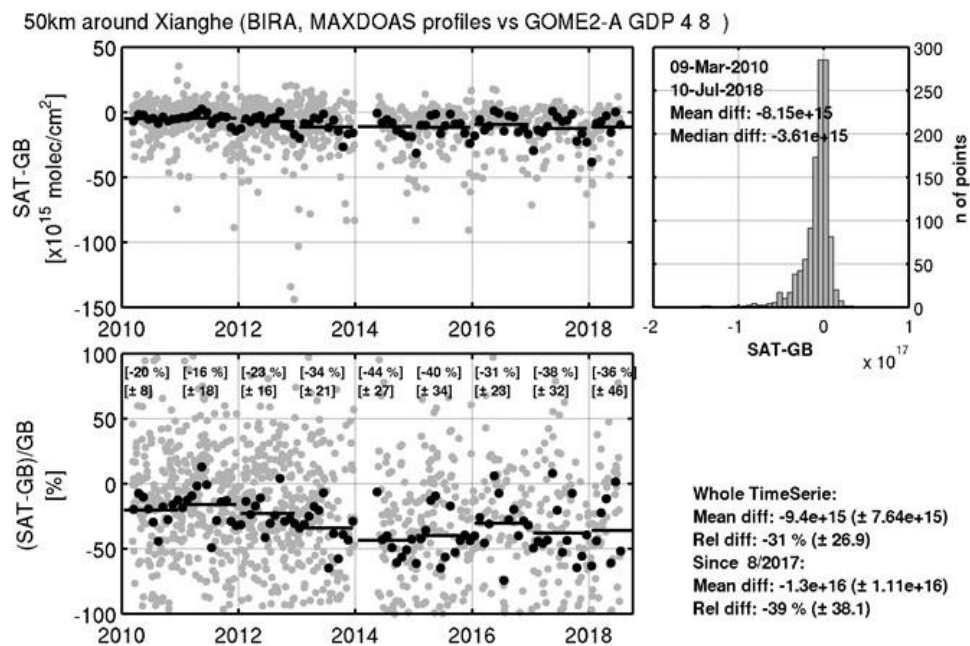


Figure 7.13. Time-series of GOME-2A GDP-4.8 minus MAXDOAS tropospheric NO₂ columns above Xianghe, from March 2010 to end of end June 2018. The upper panel on the left presents the absolute

values (daily points in grey and monthly means in black) and the lower left panel the relative values. Yearly values for the mean and standard deviation are given as inset. The panel on the right presents the histogram of the absolute differences with as inset the mean and median values of the daily points' differences.

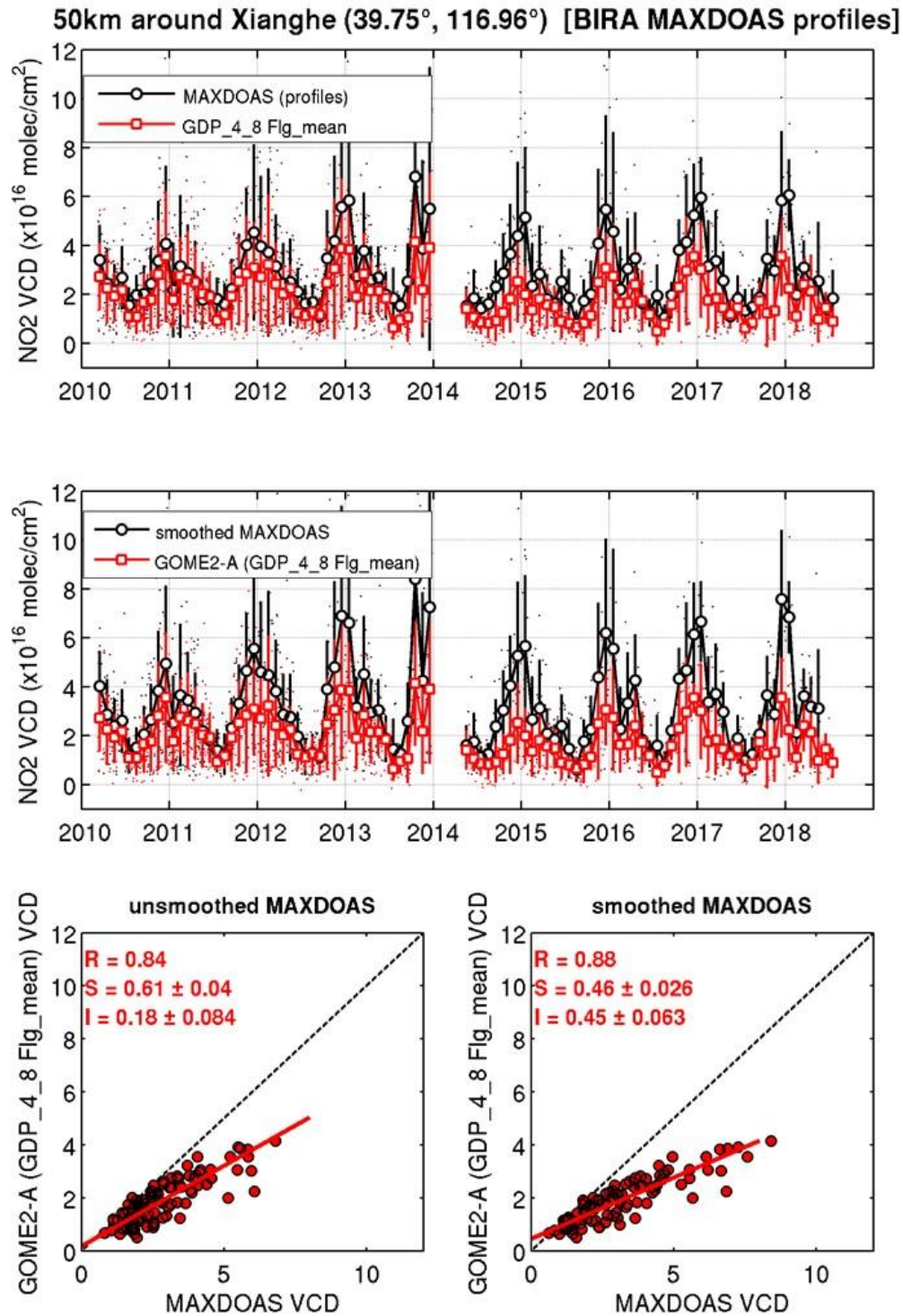


Figure 7.14. Illustration for the Xianghe MAXDOAS versus GOME-2A GDP-4.8 tropospheric NO₂ comparisons, of the application of the satellite averaging kernels on MAXDOAS profiles.

As already discussed in the previous operation report, the selection of (all or only cloud free) MAXDOAS points does not have a big impact on the monthly mean scatter plot in Xianghe (similar correlation and slopes, especially for the monthly mean values), but has an impact on the differences, which are smaller when filtering for the MAXDOAS clouds, that samples smaller NO₂ conditions (Richter *et al.*, 2017, DOAS workshop). The differences are within the target accuracy requirement of 30 % in polluted conditions, and close to the optimal accuracy of 20 % when filtering the MAXDOAS for clouds, but are about 30-40 % for Xianghe (see Table 7.11) when we don't filter the MAXDOAS for clouds. Moreover, the differences seem to show an increase in time, with larger oscillations from year to year and a decrease after 2013 that could be related to the smaller pixels after the swath change, and/or the GOME-2A degradation effect. This trend is not seen in the GOME-2B comparisons or in the comparisons with other BIRA-IASB stations, but none of the other comparisons has a time-series as long as in that case (more than 8 years). Table 7.11 allows to investigate both the comparison stability issue (comparing results of mid 2017-mid 2018 to the whole time-series), and the issue of meeting the requirements (target accuracy requirement of 30 % in polluted conditions and optimal accuracy of 20 %). Results in Table 7.11 show that the results at the Xianghe station are close to the target accuracy. Beijing, Bujumbura and Uccle are known exception (Pinardi *et al.*, 2014; NO₂ Validation Report 2015). The results in Reunion show a behaviour comparable to the Bujumbura case: the MAXDOAS instrument is located in a city, contaminated by local pollution while the satellite instrument is smearing out the NO₂ content within the satellite pixel. In term of stability most of the stations report coherent differences over time and the results does not differ largely for GOME-2A and GOME-2B, except maybe Xianghe (-39 % difference wrt. GOME-2A and -30 % difference wrt. GOME-2B).

Improvements of the NO₂ retrievals is investigated by DLR and BIRA (Liu *et al.*, 2018, in review) and validation results performed on the future GDP-4.9 GOME-2 data show reduced differences, e.g., from -29 % to -6 % on data from Xianghe from 03/2010 to 11/2016.

Table 7.11. Averaged Absolute Differences (AD, in 10^{15} molec/cm²), Relative Differences (RD, in %) and standard deviation (STDEV) on the accuracy of GOME-2A and GOME-2B tropospheric NO₂ product when comparing to MAXDOAS data (NOT cloud filtered). Values for the last 12 months are given, and the values for the whole time-series are reported in brackets for comparison. Results for both the original comparisons and for the smoothed comparisons are reported. Only Uccle-SG and Xianghe have been updated in this report.

	GOME-2A			GOME-2B		
	AD ($\times 10^{15}$)	RD (%)	STDEV (%)	AD ($\times 10^{15}$)	RD (%)	STDEV (%)
Beijing (06/208 to 4/2009)	[-21]	[-60]	[12]	-	-	-
Beijing smoothed	[-18]	[-53]	[26]	-	-	-
Bujumbura (11/2013 to 7/2017)	-3.6 [-3.7]	-88 [-89]	12.5 [24]	-3.8 [-3.5]	-88 [-88]	20 [24]
Bujumbura smoothed	-2.7 [-2.5]	-84 [-85]	31 [34]	-2.4 [-2.2]	-83 [-82]	23 [32]
OHP (8/2014 to 3/2017)	-1.3 [-1]	-52 [-47]	53 [39]	-1.2 [-0.8]	-47 [-34]	55 [43]
OHP smoothed	-1 [-1]	-49 [-46]	35 [31]	-1.2 [-0.8]	-47 [-34]	58 [47]
Reunion (4/2016 to 12/2017)	-1.5 [-1.6]	-84 [-86]	29 [28]	-1.4 [-1.4]	-83 [-84]	25 [25]
Reunion smoothed	-0.5 [-0.5]	-62 [-67]	29 [31]	-0.41 [-0.42]	-59 [-60]	22 [25]
Uccle minDOAS (4/2011 to 3/2016)	-4.2 [-6.2]	-41 [-52]	32 [33]	-3.9 [-5.6]	-43 [-54]	18 [29]
Uccle minDOAS smoothed	-4.8 [-7.4]	-44 [-56]	35 [36]	-4.4 [-6.5]	-45 [-57]	21 [30]
Uccle SG (since 2/2017)	-5.1 [-5.5]	-49 [-51]	26 [29]	-4.4 [-4.5]	-52 [-50]	28 [28]
Uccle SG smoothed	-5.9 [-6.3]	-53 [-55]	23 [29]	-5.1 [-5.4]	-56 [-55]	23 [28]
Xianghe (since 3/2010)	-13 [-9.4]	-39 [-31]	38 [27]	-7.8 [-8.3]	-30 [-27]	23 [29]
Xianghe smoothed	-19 [-12]	-47 [-34]	40 [33]	-12 [-11]	-37 [-29]	25 [36]

Smoothing the MAXDOAS profiles with the satellite averaging kernels is not always reducing the mean comparison differences (e.g. for Xianghe as illustrated in Figure 7.14), with an impact of ~10-20 % depending on the station. This is mostly related e.g. in Xianghe, to smoothed MAXDOAS columns being larger than the originals in winter time (as seen in Figure 7.15) and it has been shown at the last PT meeting (May 2018) that this is related to the specific shape of the GOME-2 averaging kernels and the MAXDOAS profiles. The sensitivity of the satellite, with typically AK=1 at smaller height in winter, leads to a larger impact of the peaked MAXDOAS

profiles and thus larger columns after smoothing of MAXDOAS NO₂ profiles. Two examples, are shown here:

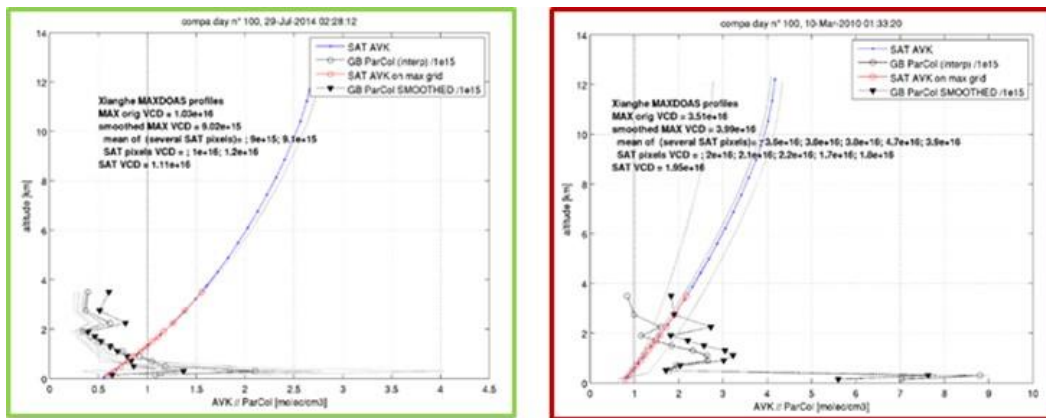


Figure 7.15. Illustration of the application of GOME-2 AVK to MAXDOAS profiles in Xianghe for a case in summer (left) and in winter (right), showing respectively the decrease and increase of the MAXDOAS column after smoothing.

Status of GOME-2A & GOME-2B total (stratospheric) NO₂

Quality assessment of the GOME-2 NO₂ total (stratospheric) column data is regularly carried out using ground-based reference measurements collected from about 20 Zenith-Sky DOAS UV-visible instruments performing network operation in the framework of the Network for the Detection of Atmospheric Composition Change (NDACC). The NO₂ column validation protocol has already been described in previous AC SAF validation reports; it includes the selection of GOME-2/NDACC co-located data pairs based on the air-mass matching technique, a model-based photochemical correction compensating for significant local time differences during high latitude summer, and a cloud-based filtering of NO₂ data over polluted stations aiming at the removal of pollution-affected pixels. Ground-based data retrieved with real-time processing using NO₂ absorption cross-sections at room temperature instead of stratospheric temperature, which produces a negative systematic bias of 15-20 %, thus a seasonally varying bias in absolute values, are also removed. Thanks to this strict protocol, data comparisons can be carried out within a residual uncertainty of maximum $2\text{--}3 \times 10^{14}$ molec.cm⁻² combining both the ground-based data uncertainty and comparison errors, which is indicated by the shaded area on the pole-to-pole graphs.

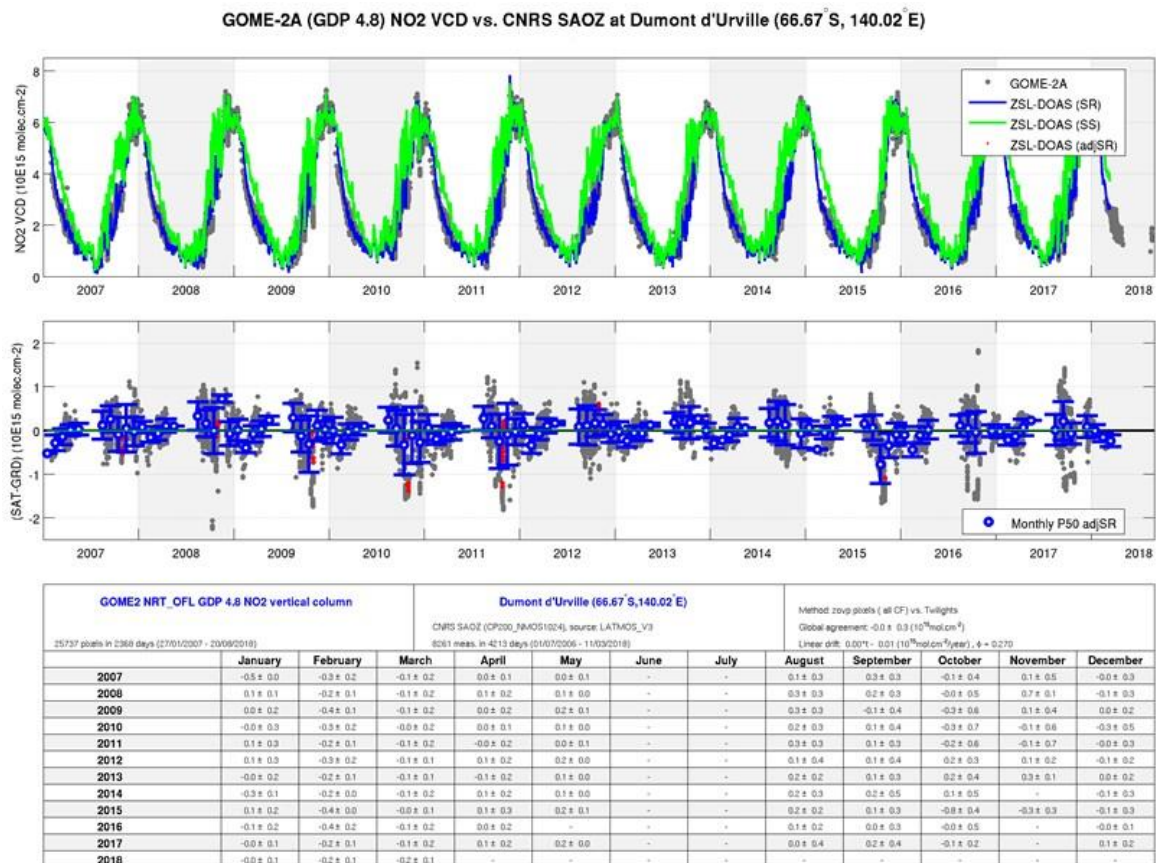


Figure 7.16. Comparison of NO₂ column data measured at the NDACC Antarctic station of Dumont d'Urville by GOME-2A (GDP-4.8) and by the CNRS/LATMOS DOAS UV-visible zenith-sky spectrometer. Top: time series of NO₂ column data; centre: time series of NO₂ column difference; bottom (table): monthly median values (and its 1 σ scatter) of the difference between GOME-2A GDP-4.8 and the NDACC NO₂ column data.

Figure 7.16 illustrates the comparison of NO₂ column data at the NDACC station of Dumont d'Urville, a station located on the Antarctic polar circle and in a pristine environment without any known NO₂ emission. Comparison results at this station are representative of the validation of purely stratospheric data series, at moderate and large solar zenith angle, and over the full range of NO₂ stratospheric column values from 10^{14} molec/cm² (wintertime denoxification episodes) up to 7×10^{15} molec/cm² (complete depletion of N₂O₅ into NO₂ during polar midnight Sun). On a monthly median basis, and over the 12 years of GOME-2A operation, the target bias of $3\text{--}5 \times 10^{14}$ molec/cm² has never been exceeded, except occasionally in October when the station is overpassed frequently by the border of the polar vortex, thus when atmospheric variability adds significant mismatch noise to the data comparison.

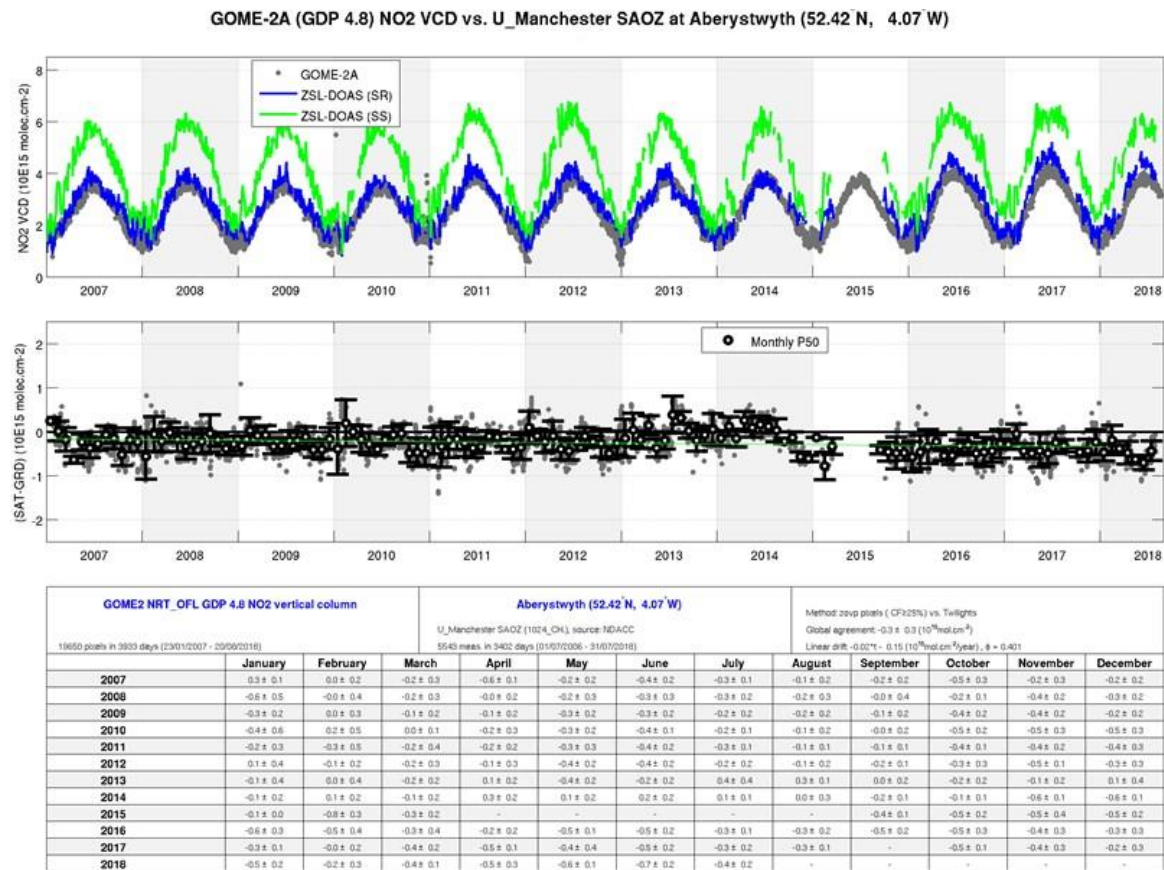


Figure 7.17. Same as Figure 7.16 but at the NDACC station of Aberystwyth by GOME-2A (GDP-4.8) and by the U. Manchester DOAS UV-visible zenith-sky spectrometer. Top: time series of NO₂ column data; centre: time series of NO₂ column difference; bottom (table): monthly median values (and its 1 σ scatter) of the difference between GOME-2A GDP-4.8 and the NDACC NO₂ column data.

Figure 7.17 and Figure 7.18 illustrate similar results obtained at the mid-latitude station of Aberystwyth in Wales and the sub-tropical station of Izana on Tenerife Island, thus in occasional presence of pollution and over a wider range of solar zenith angle. Again, the target bias of $3\text{--}5 \times 10^{14}$ molec/cm² has rarely been exceeded, except in very few cases, e.g. in 2015 at Aberystwyth before an interruption of the ground-based instrument operation.

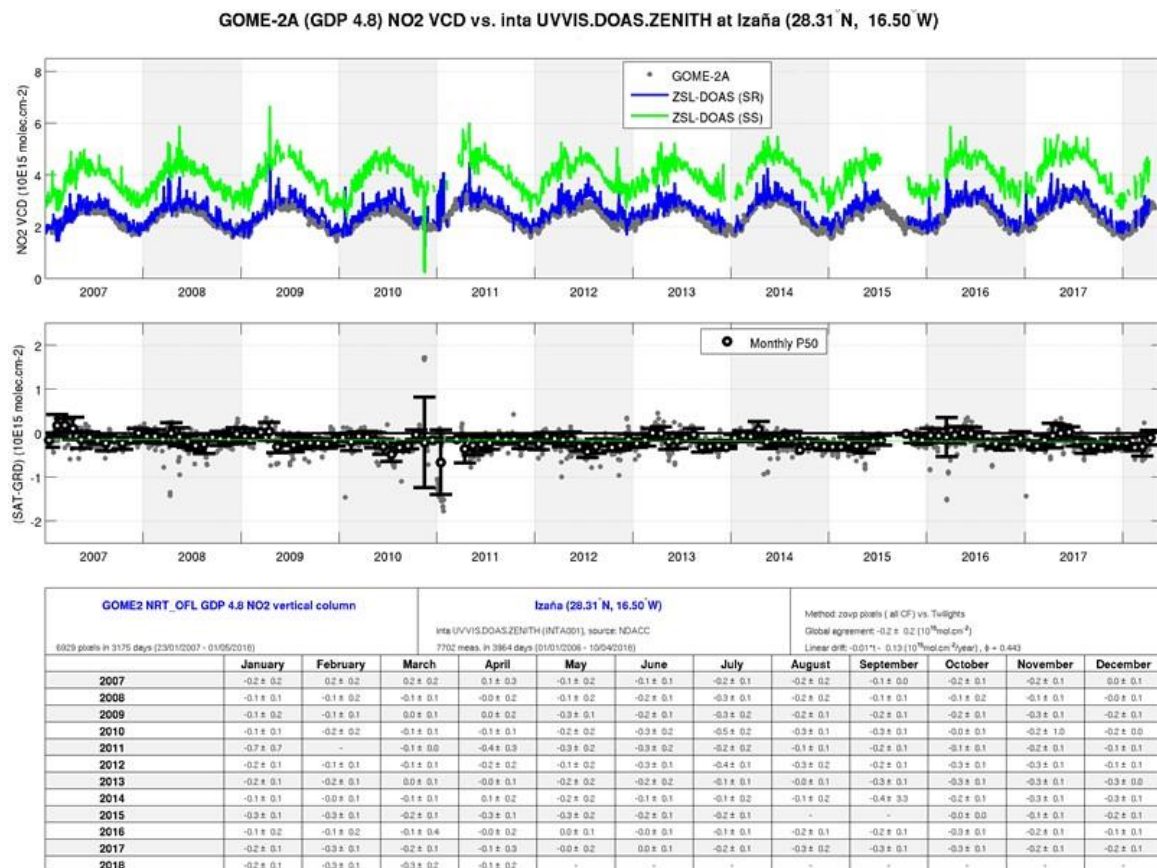


Figure 7.18. Same as Figure 7.16 and Figure 7.17, but at the NDACC tropical station of Izaña on Tenerife Island by GOME-2A (GDP-4.8) and by the INTA DOAS UV-visible zenith-sky spectrometer. **Top:** time series of NO₂ column data; **centre:** time series of NO₂ column difference; **bottom (table):** monthly median values (and its 1σ scatter) of the difference between GOME-2A GDP-4.8 and the NDACC NO₂ column data.

Finally, Figure 7.19 reports from pole to pole the median value of the systematic bias between GOME-2 and NDACC/UVVIS data, covering the entire GOME-2A/B operational time-series until July 2018. This graph shows that at almost all stations the target bias of $3\text{--}5 \times 10^{14}$ molec/cm² in unpolluted conditions is achieved for both the GOME-2A and GOME-2B GDP-4.8 NO₂ column data. This figure also confirms the slight difference already noticed in previous validation reports between the biases observed respectively in the Southern and Northern hemispheres. Averaging median differences separately over the Northern and Southern Hemispheres concludes to an inter-hemispheric bias of about $2\text{--}3 \times 10^{14}$ molec/cm².

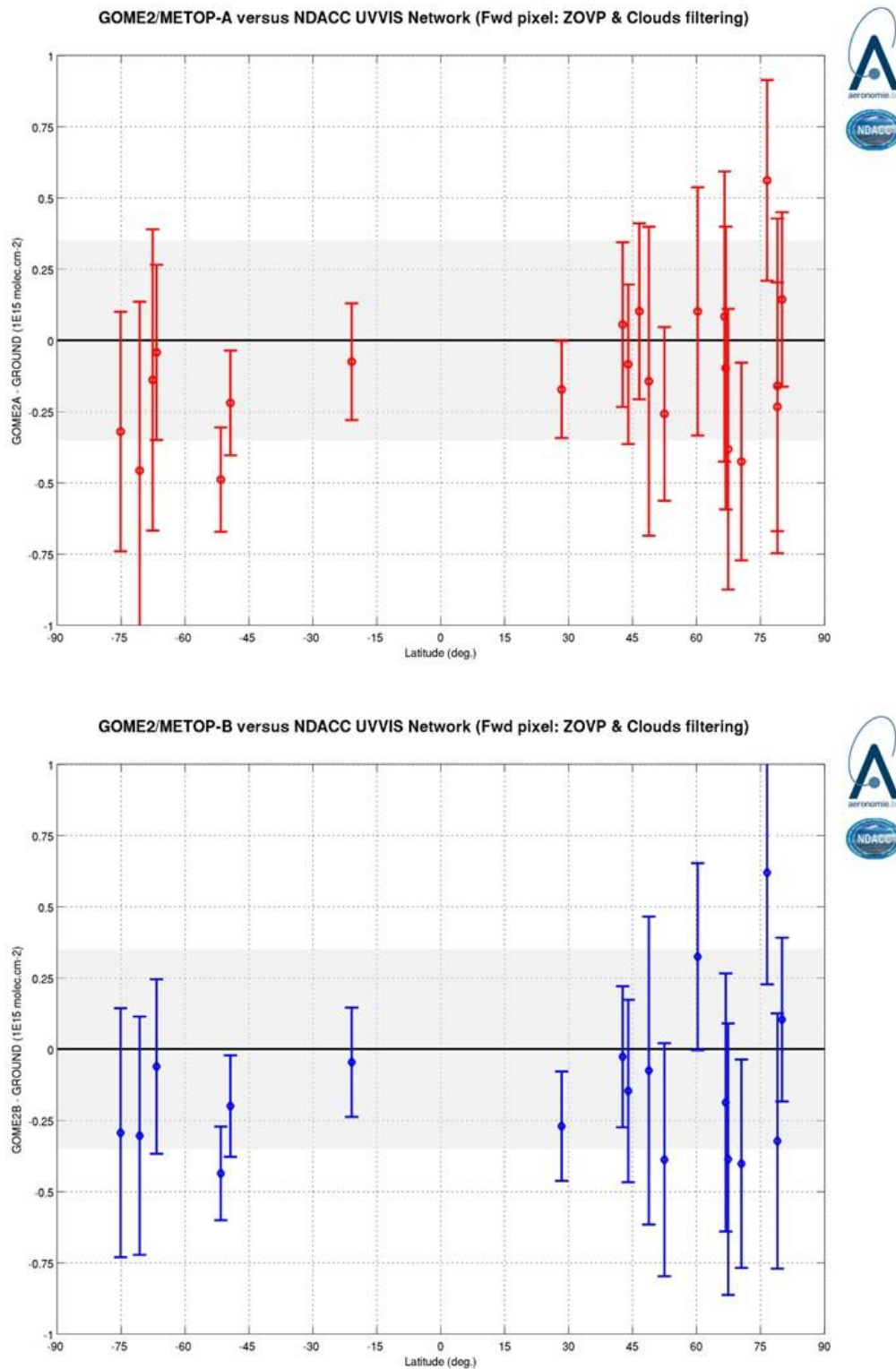


Figure 7.19. From pole to pole, median absolute difference at about 20 NDACC station between NO_2 column data reported by GOME-2A/B (top/bottom) GDP-4.8 and by ground-based ZenithSky-DOAS UV-visible spectrometers.

Status of GOME-2A & GOME-2B total HCHO

This validation exercise is an extension of what is presented in the HCHO GDP-4.8 validation report

(https://acsaf.org/docs/vr/Validation_Report_NTO_OTO_DR_HCHO_GDP48_Oct_2015.pdf), relying on correlative observations from MAX-DOAS instruments operated by BIRA-IASB at Xianghe, Bujumbura, Uccle (miniDOAS and SG), OHP and Reunion. Only data from Xianghe and Uccle-SG are available for the last 6 months' time-period. Step-by-step verification of the operational data with respect to the GOME-2 scientific algorithm v14 over predefined emission regions could not be extended, due to unavailability of the scientific algorithm.

The satellite and ground-based data selections are as in the validation report, and the updated comparisons figures until end of June 2018 can be found on the BIRA validation web server:

<http://cdop.aeronomie.be/validation/valid-results?gas=2&platform=0&instrumentType=0&station=0®ion=0&instrument=7>

An illustration of the results for Xianghe is shown in Figure 7.20 for the time-series and the scatter plots of both original comparisons and when smoothing MAXDOAS profiles with satellite averaging kernels, while Figure 7.21 presents the absolute and relative differences. Mean bias values and correlation coefficients are summarized in Table 7.12.

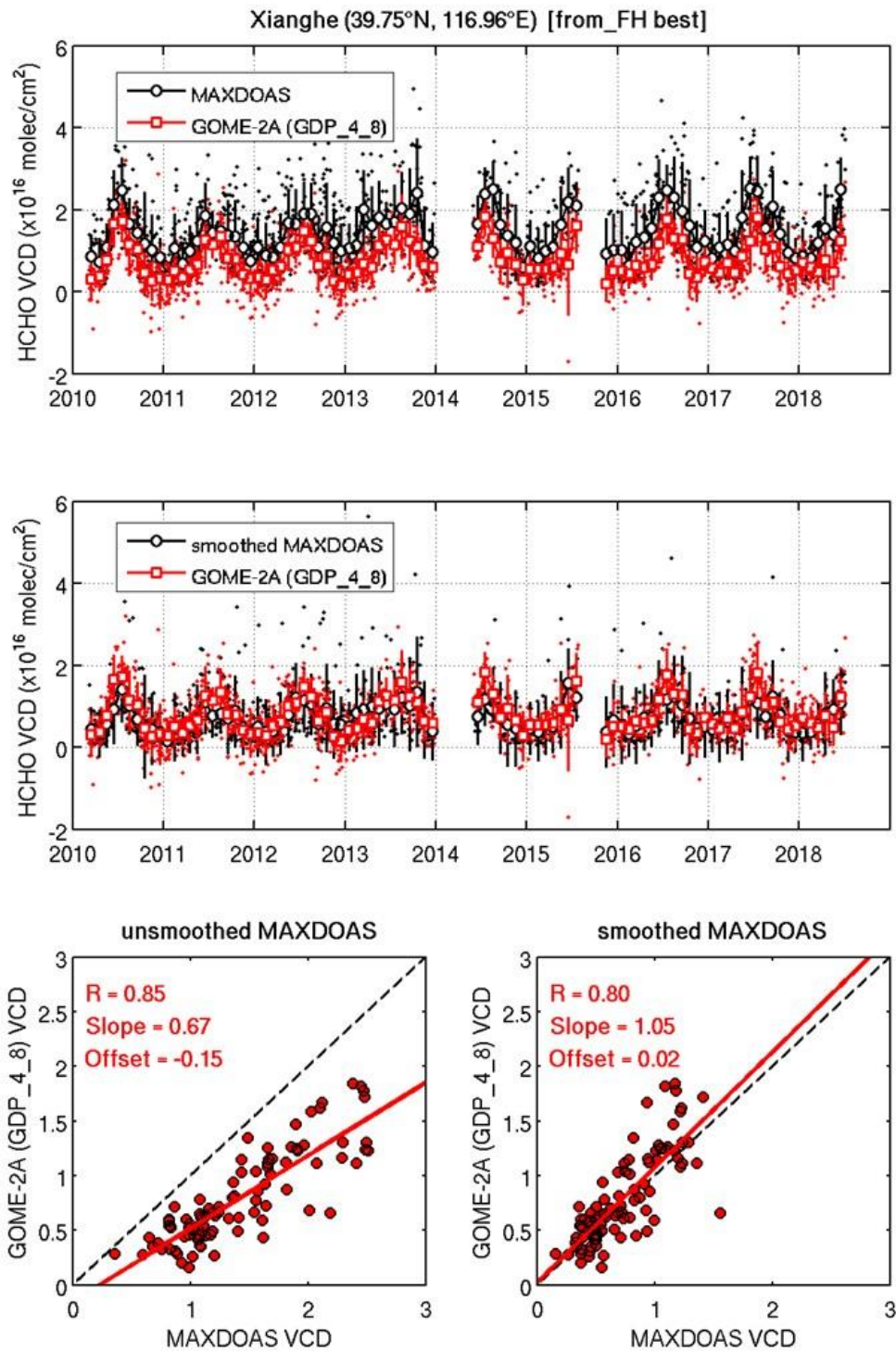


Figure 7.20. Comparison between GOME-2 GDP-4.8 and MAX-DOAS HCHO VCDs at Xianghe.

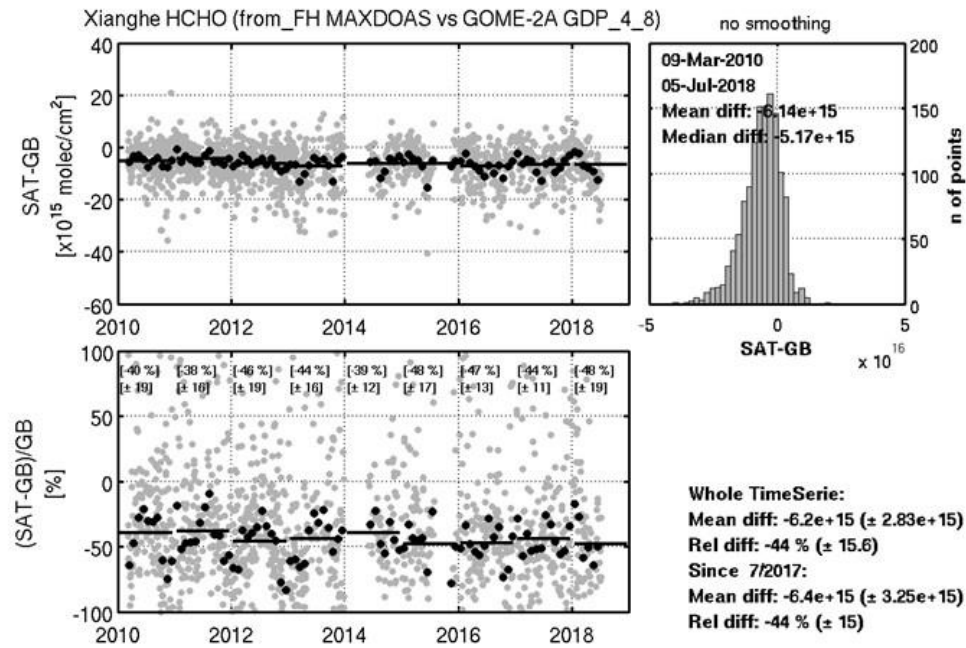


Figure 7.21. Time-series of HCHO GOME-2A GDP-4.8 minus MAXDOAS tropospheric columns above Xianghe, from March 2010 to mid-2018. The upper panel on the left presents the absolute values (daily points in grey and monthly means in black) and the lower left panel the relative values. Yearly values for the mean and standard deviation are given as inset. The panel on the right presents the histogram of the absolute differences with as inset the mean and median values of the daily points' differences.

Table 7.12. Summary of the mean biases (in 10^{15} molec/cm²) between GOME-2A/B and MAX-DOAS HCHO VCDs. The values in parentheses correspond to the mean relative biases and R is the correlation coefficients and S the slope of the linear regression of the monthly mean points. Only Uccle-SG and Xianghe have been updated in this report.

	GOME-2A	GOME-2B
BUJUMBURA (3.0°S, 29.0°E) (11/2013 to 07/2017)	-6.3 ± 2.4 (-44 ± 10) R=0.83, S=0.46	-4.4 ± 2.2 (-32 ± 10) R=0.88, S=0.52
With smoothing	-1.6 ± 2.4 (-17 ± 24) R=0.50, S=0.43	0.3 ± 2.0 (3.2 ± 25) R=0.72, S=0.65
OHP	-0.1 ± 2.5 (1.7 ± 40) R=0.42, S=0.29	0.3 ± 1.1 (4.2 ± 21) R=0.90, S=0.75
With smoothing	0.9 ± 2.3 (16 ± 42) R=0.39, S=0.32	1.0 ± 1.0 (17 ± 22) R=0.86, S=1.01
REUNION (20.9°S, 55.3°E) since 4/2016	-0.3 ± 1.0 (-10 ± 43) R=0.66, S=1.23	1.1 ± 0.8 (39 ± 26) R=0.80, S=1.56
With smoothing	1.1 ± 1.1 (71 ± 99) R=0.59, S=1.56	2.6 ± 0.1 (180 ± 56) R=0.78, S=2.83

UCCLE-miniDOAS (50.8°N, 4.3°E) (4/2011 to 5/2015)	-0.5 ± 2.6 (-8.3 ± 49) R=0.21, S=0.25	-0.6 ± 1.6 (-9.4 ± 29) R=0.76, S=0.89
With smoothing	0.8 ± 2.7 (14 ± 81) R=0.11, S=0.13	-0.4 ± 1.7 (7.1 ± 34) R=0.73, S=0.88
UCCLE-SG (50.8°N, 4.3°E) since 02/2017	1.5 ± 1.6 (32 ± 51) R=0.60, S=0.52	-0.2 ± 2.2 (4.7 ± 64) R=0.76, S=1.19
With smoothing	2.6 ± 1.4 (77 ± 83) R=0.62, S=0.70	1.5 ± 2.3 (43 ± 95) R=0.76, S=1.67
XIANGHE (39.7°N, 117.0°E) since 3/2010	-6.2 ± 2.8 (-44 ± 16) R=0.85, S=0.67	-7.6 ± 2.1 (-50 ± 16) R=0.91, S=0.81
With smoothing	0.6 ± 2.5 (8.3 ± 33) R=0.80, S=1.05	0.5 ± 2.3 (6.4 ± 31) R=0.90, S=1.48

The results confirm that both satellite instruments capture well the HCHO VCD seasonality. In Reunion the signal is very small (less than $\sim 0.5 \times 10^{16}$ molec/cm²) and is more difficult to have firm conclusions. In Uccle and OHP, the signal from GOME-2A is quite noisy, and the results are better with GOME-2B, which is probably related to GOME-2A degradation. A significant bias exists between GOME-2A/B and MAX-DOAS observations at the four stations (up to 50 %), but as already shown in the GDP-4.8 validation report and here for Xianghe, this bias can be significantly reduced when smoothing the MAX-DOAS profiles with the satellite column averaging kernels (see also values with smoothing in Table 7.12).

Monthly mean differences are calculated for every year and for the whole time-series in order to see the evolution in time of the bias. The differences are overall quite coherent over time and no specific issues are identified in the first half of 2018, as can be see e.g. in Figure 7.21 for the Xianghe station (China), showing daily and monthly mean absolute and relative differences for GOME-2A. A mean bias of -44 % is found for 7/2017 - 6/2018 before any smoothing, consistent with the -44 % bias found over the whole time-series, as can be seen in Figure 7.21. The difference figures for the other stations can also be found on the BIRA validation web server.

Status of GOME-2A & GOME-2B total BrO

GOME-2A and GOME-2B total columns of BrO from GDP-4.8 Operational Product are compared to ground-based UV-visible zenith-sky measurements at Harestua, Norway (60°N, 11°E). As done in previous validation report

(https://acsaf.org/docs/vr/Validation_Report_OTO_DR_BrO_GDP48_Dec_2015.pdf), the ground-based columns are derived from vertical profiles retrieved by applying an OEM (Optimal Estimation Method) -based profiling technique to zenith-sky measurements at sunrise (Hendrick *et al.*, 2007).

The sensitivity of these measurements to the troposphere is increased by using a fixed reference spectrum corresponding to clear-sky noon summer conditions for the spectral analysis. In order to ensure the photochemical matching between satellite and ground-based observations, sunrise ground-based columns have been photochemically converted to the satellite overpass SZAs using a stacked box photochemical model (Hendrick *et al.*, 2007 and 2008).

Comparison results (150 km overpasses) for GOME-2A and GOME-2B are shown in Figure 7.22 and Figure 7.23. For both GOME-2 instruments (A and B), two different products are involved in the verification exercise: the standard product provided in the DLR data files ('vcd_corr') and obtained using a stratospheric AMF and a second product derived by dividing the SCDs ('scd_corr') by total AMFs calculated from retrieved GB tropospheric and stratospheric profiles.

Mean biases values between GOME-2B and ground-based data are of $-17 \pm 11 \%$ and $-15 \pm 11 \%$ when using stratospheric and total AMFs, respectively. Corresponding values for GOME-2A are $-10 \pm 11 \%$ and $-16 \pm 13 \%$. GOME-2A/B BrO columns are thus within the target accuracy (30 %) and also within the optimal accuracy (15 %) once the tropospheric content is taken into account in the comparison. It is worthy to note that the level of agreement between GOME-2A and ground-based observations is lower when using total AMFs from summer 2015 (see Figure 7.22), which is an indication of a possible drift in GOME-2A BrO total column data. This feature is currently under investigation.

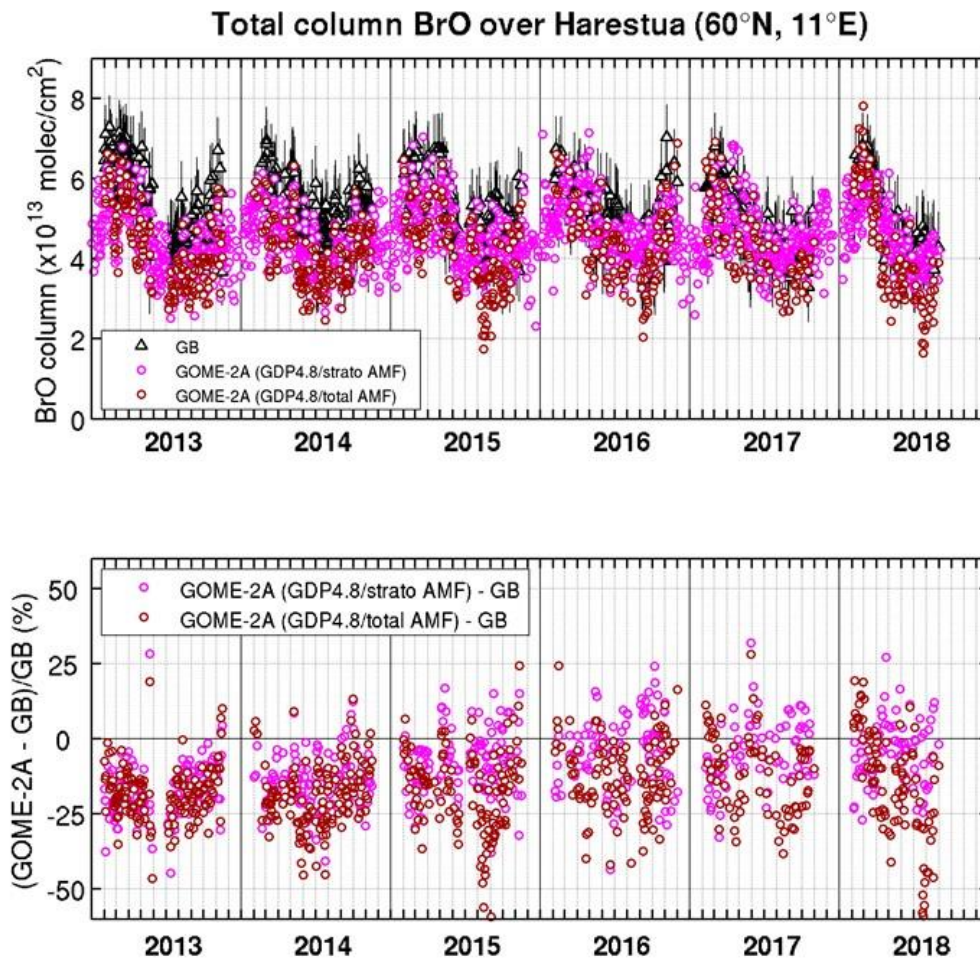


Figure 7.22. Comparison between GOME-2A GDP-4.8 and ground-based total BrO columns at Harestua (60°N, 11°E). The relative differences appear in the lower plot.

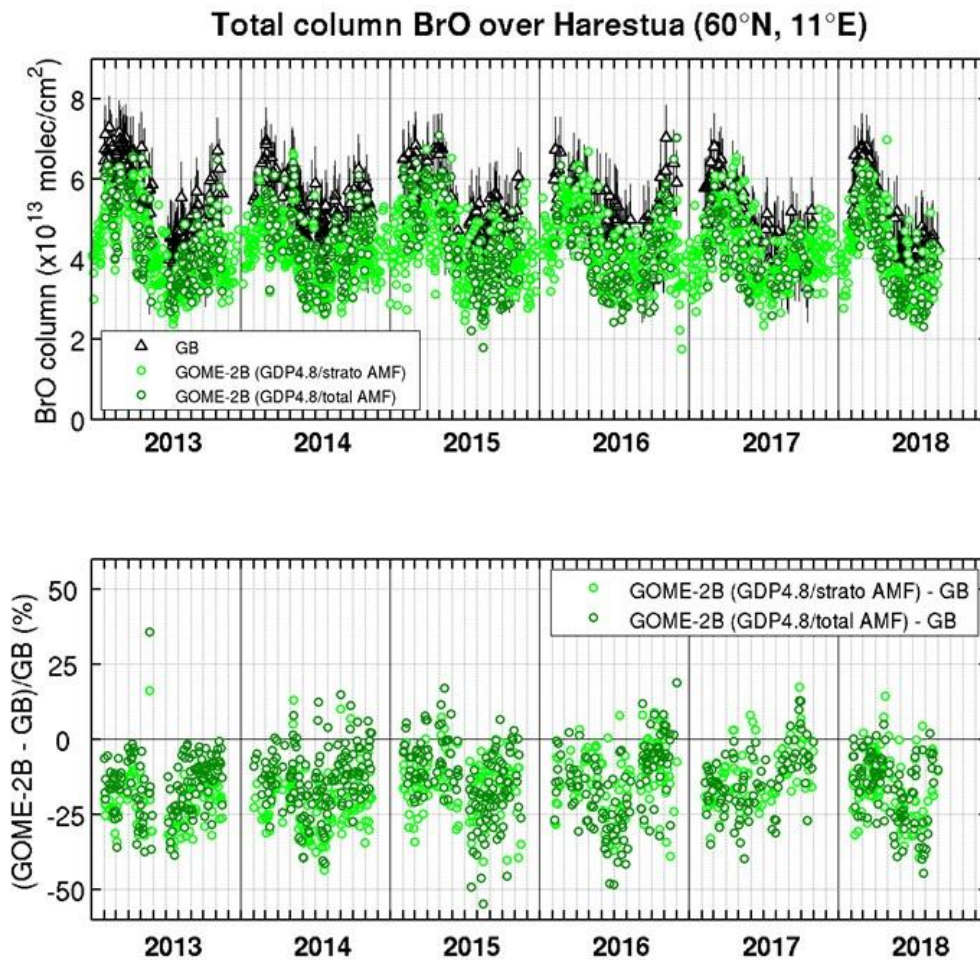


Figure 7.23. Comparison between GOME-2B GDP-4.8 and ground-based total BrO columns at Harestua (60°N, 11°E). The relative differences appear in the lower plot.

Status of GOME-2A & GOME-2B SO₂

GOME-2 SO₂ GDP-4.8 data are used for the near-real-time observation of volcanic activity within the SACS service. The Support to Aviation Control Service (SACS) hosted by the Royal Belgian Institute for Space Aeronomy aims at supporting the Volcanic Ash Advisory Centers, like Toulouse VAAC and London VAAC. This is achieved by delivering near real-time data of SO₂ and aerosols derived from satellite measurements regarding volcanic emissions by UV-VIS (OMI, GOME-2A, GOME-2B, OMPS) and infrared (AIRS, IASI-A, IASI-B) instruments. In case of volcanic eruptions, notifications are sent out by email to interested parties. The SACS notification archive service gathers all the notifications; the results for the first half of 2018 can be found here:

<http://sacs.aeronomie.be/alert/Archive/index.php?Year=2018&Month=08&Day=28&InstruGOME2=2&InstruGOME2b=3&InstruOMI=1&InstruIASI=4&InstruIASIb=5&InstruAIRS=6&monthly=0>

In the first half of 2018, SACS reported 11 cases where the maximum SO₂ detected by UVvis instruments was larger than 10 DU. Corresponding SACS regions are shown below (Figure 7.24 - Figure 7.33). In most of the cases, the importance of GOME-2 measurements is clear, with IR instruments having no sensitivity to degassing plumes (such as for Hawaii, e.g. 02/06/2018, Figure 7.30, Figure 7.31 and Figure 7.32) or cases where OMI missed the plume due to the row gap (Figure 7.28, Figure 7.31 and Figure 7.33). When several instruments see the volcanic plume, a general coherence of the GOME-2 signal with the others is seen, considering the overpass time

difference. Only the cases of 21 February and 9 March (Figure 7.24 and Figure 7.25) the GOME-2 signal is too noisy to detect the Peru spot, only seen by OMI.

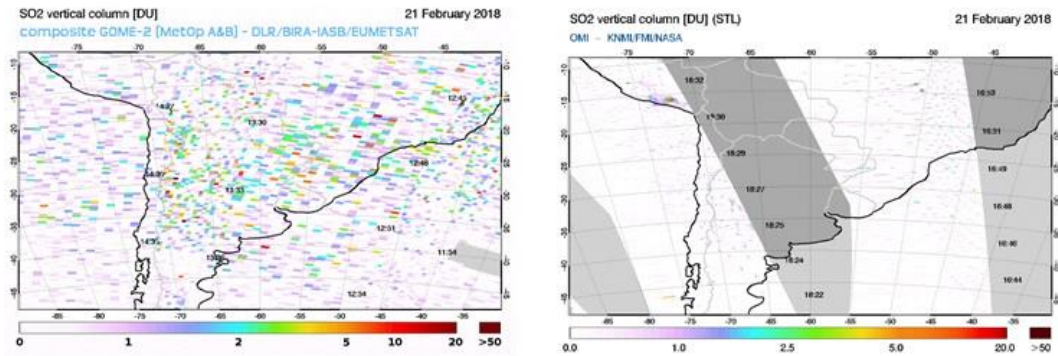


Figure 7.24. Illustration of the SACs region 404 for 21 February 2018 as seen by GOME-2A and GOME-2B (composite), and OMI instruments.

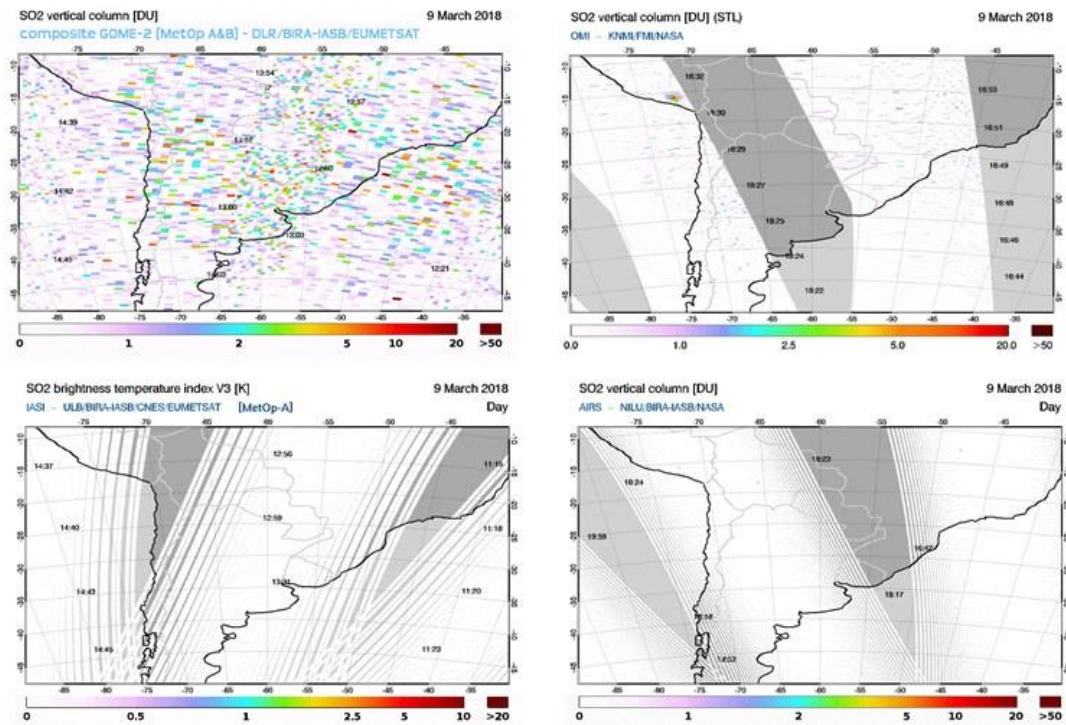


Figure 7.25. Illustration of the SACs region 404 for 9 March 2018 as seen by GOME-2A and GOME-2B (composite), OMI, IASI-A, and AIRS instruments.

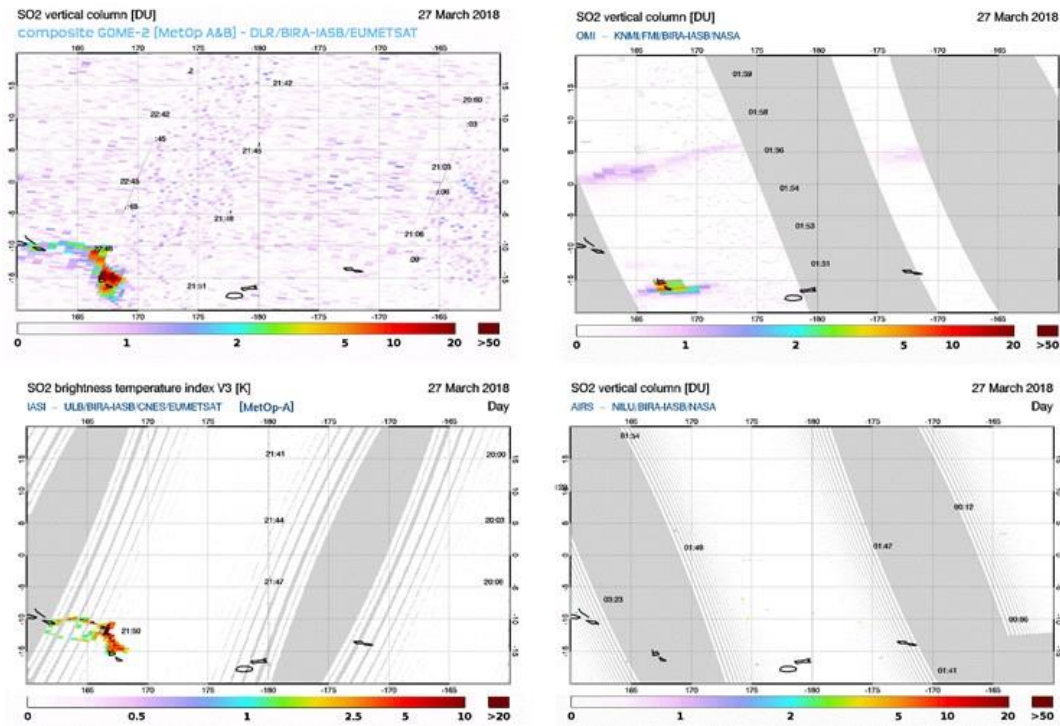


Figure 7.26. Illustration of the SACS region 312 around Vanatou island for 27 March 2018 as seen by GOME-2A and GOME-2B (composite), OMI, IASI-A, and AIRS instruments.

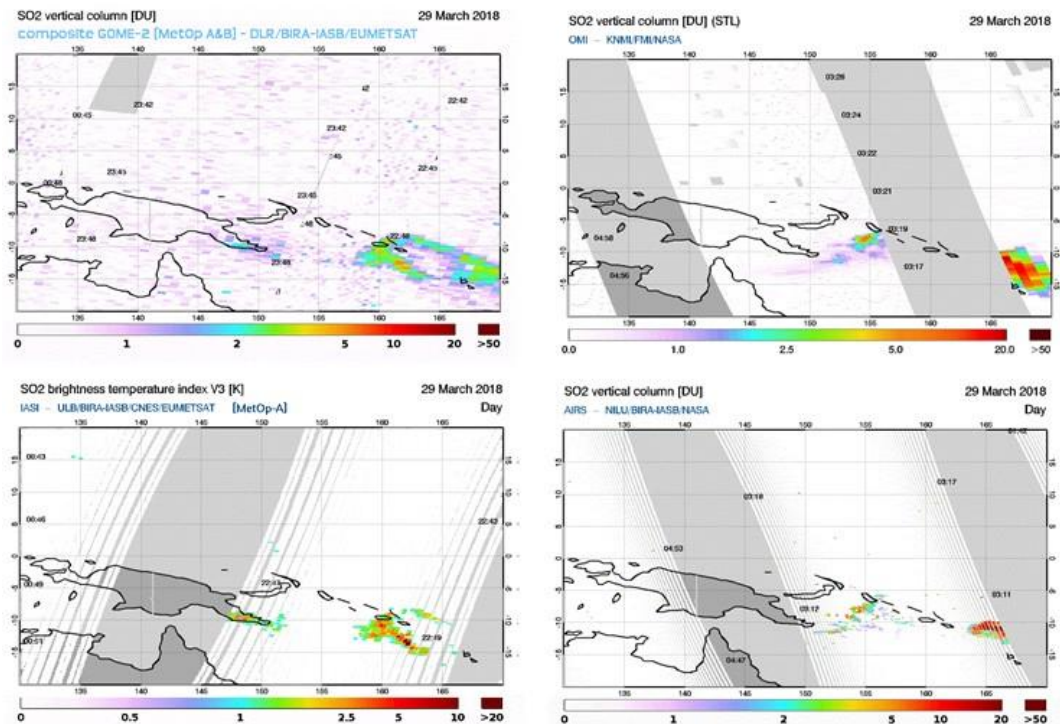


Figure 7.27. Illustration of the SACS region 311 around Vanatou island for 29 March 2018 as seen by GOME-2A and GOME-2B (composite), OMI, IASI-A, and AIRS instruments.

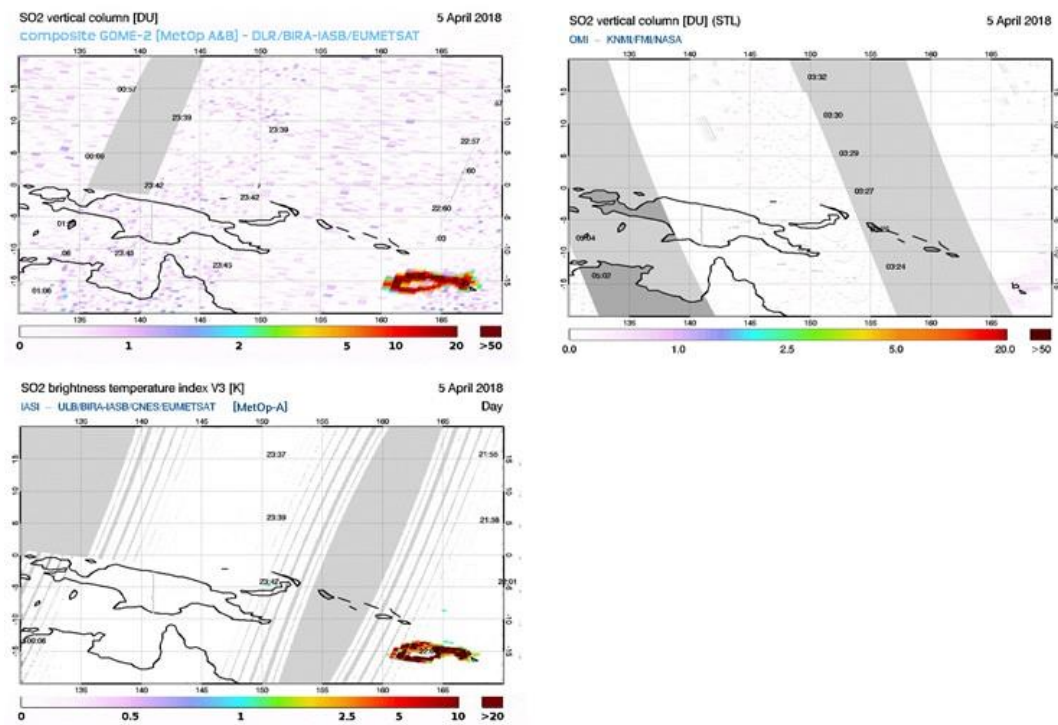


Figure 7.28. Illustration of the SACs region 311 around Vanatou island for 5 April 2018 as seen by GOME-2A and GOME-2B (composite), OMI, IASI-A, and AIRS instruments.

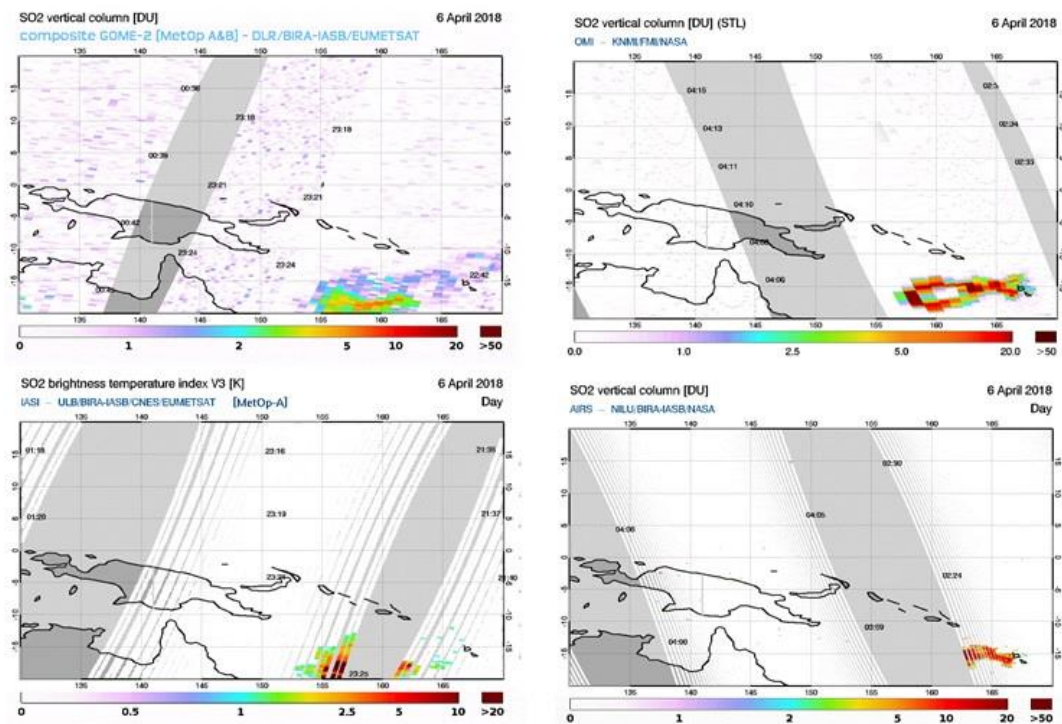


Figure 7.29. Illustration of the SACs region 311 around Vanatou island for 6 April 2018 as seen by GOME-2A and GOME-2B (composite), OMI, IASI-A, and AIRS instruments.

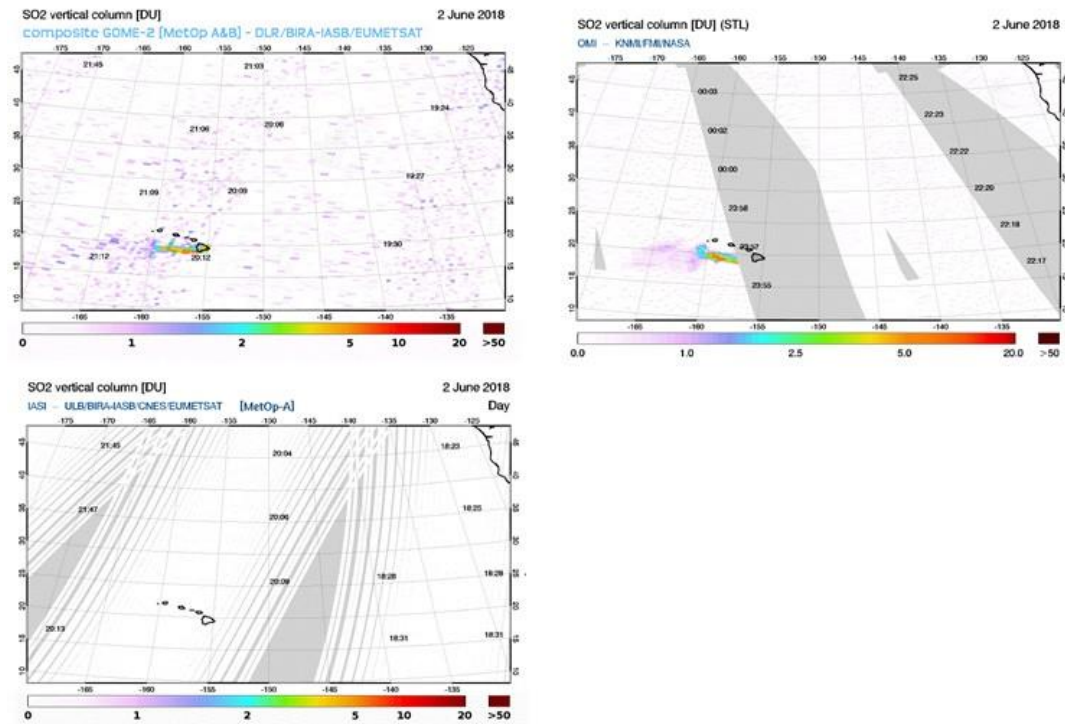


Figure 7.30. Illustration of the SACS region 201 around Hawaii for 2 June 2018 as seen by GOME-2A and GOME-2B (composite), OMI, IASI-A, and AIRS instruments.

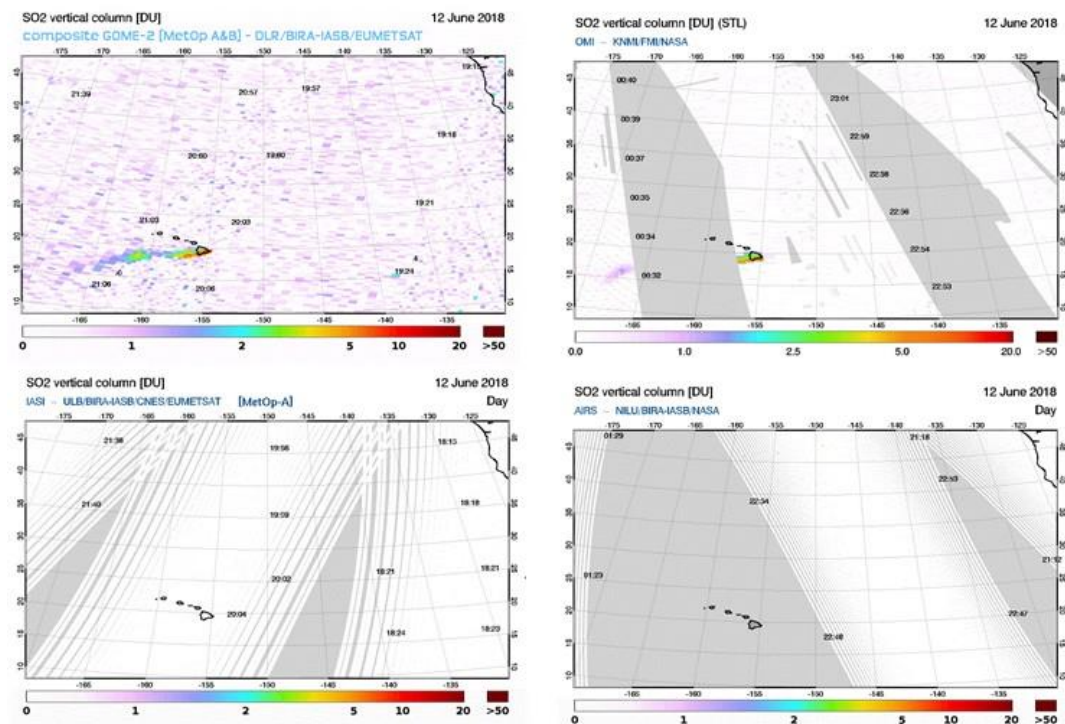


Figure 7.31. Illustration of the SACS region 201 around Hawaii for 12 June 2018 as seen by GOME-2A and GOME-2B (composite), OMI, IASI-A, and AIRS instruments.

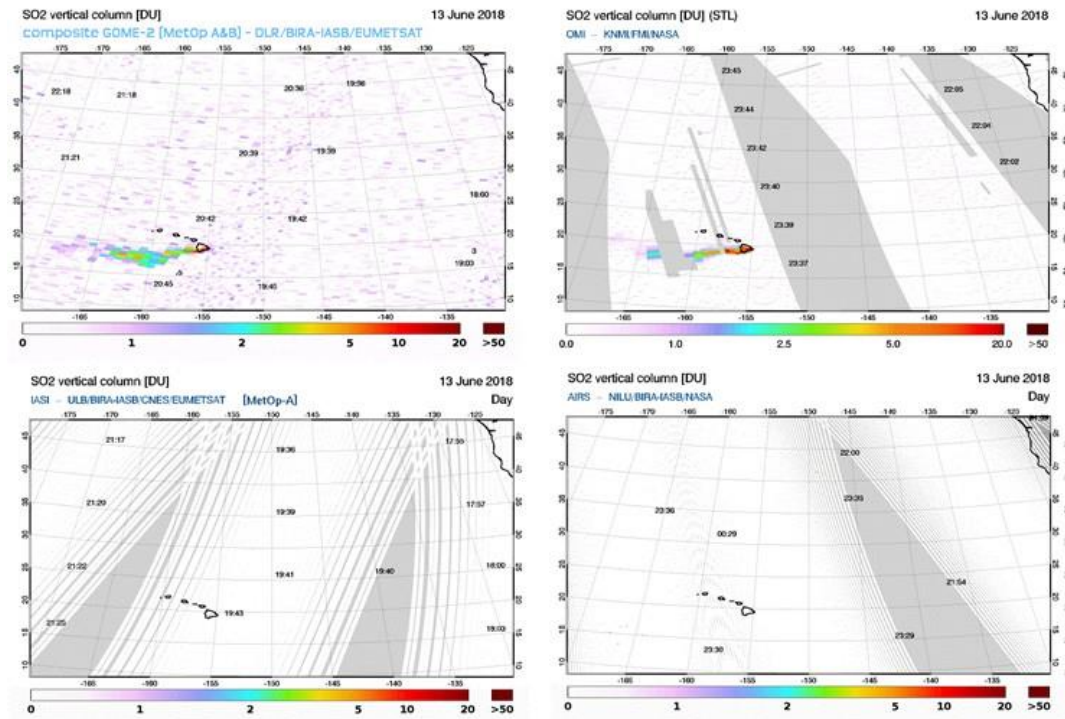


Figure 7.32. Illustration of the SACS region 201 around Hawaii for 13 June 2018 as seen by GOME-2A and GOME-2B (composite), OMI, IASI-A, and AIRS instruments.

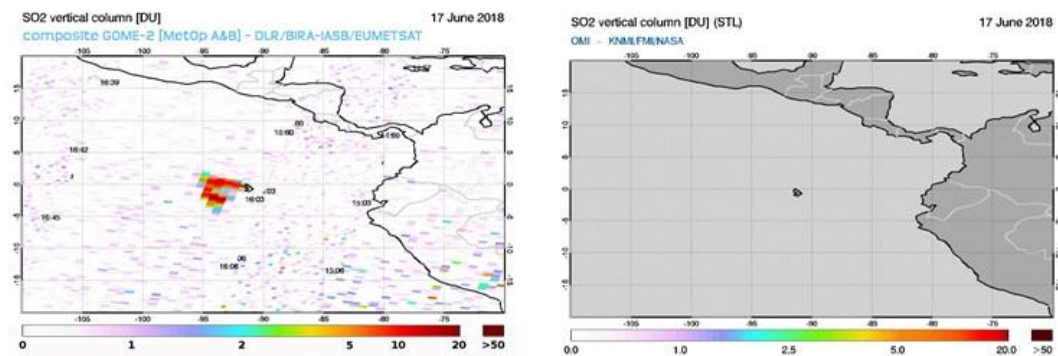


Figure 7.33. Illustration of the SACS region 303 around Galapagos for 17 June 2018 as seen by GOME-2A and GOME-2B (composite), OMI, IASI-A, and AIRS instruments.

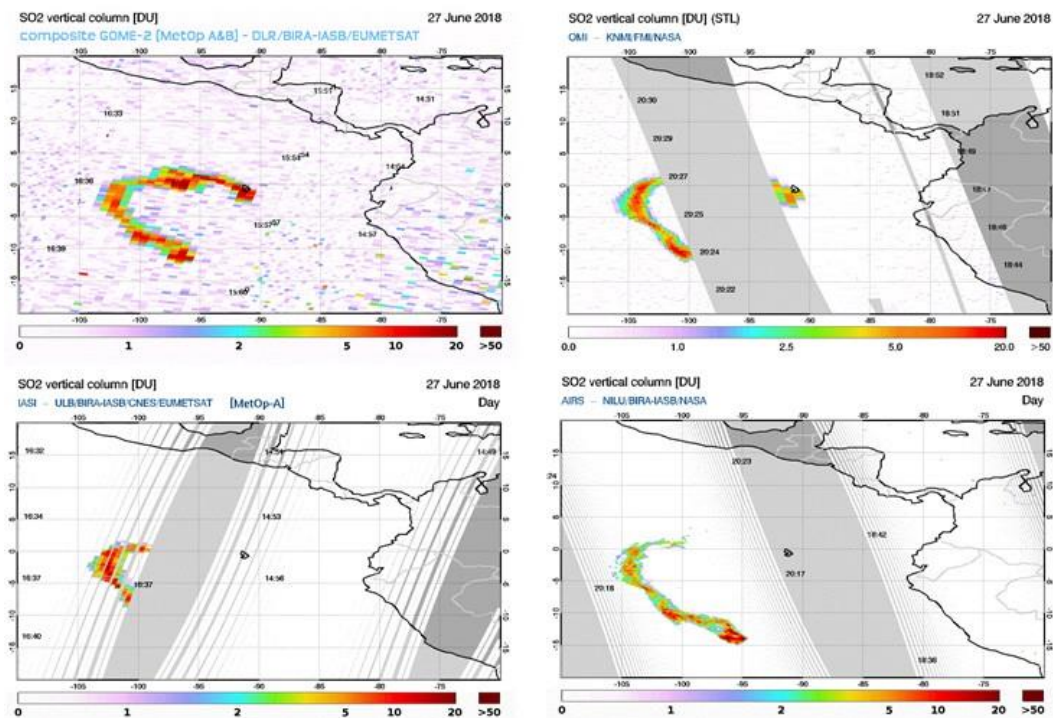


Figure 7.34. Illustration of the SACS region 303 around Galapagos for 27 June 2018 as seen by GOME-2A and GOME-2B (composite), OMI, IASI-A, and AIRS instruments.

GDP-4.8 also contains an anthropogenic SO₂ product that can be compared with ground-based MAXDOAS/DirectSun data from the Xianghe station, similarly to what is done in the SO₂ report (http://acsaf.org/docs/vr/Validation_Report_NTO_OTD_DR_SO2_GDP48_Dec_2015.pdf).

As done in the validation report, clear-sky pixels (i.e., cloud fractions less than 0.3) within a 150 km circle radius around Xianghe and surface height less than 500 m (to exclude observations over clean elevated regions) with solar zenith angles less than 70° and positive cloud albedo are selected. Then, for each pixel, all MAXDOAS data within ± 90 minutes of the overpass time and with SZA < 70° are considered and averaged for the comparison. As described in the validation report, as no averaging kernels are provided with the anthropogenic SO₂ product, the comparisons are expected to be biased due to the profile shape.

Figure 7.35 presents the monthly mean comparisons between MAXDOAS SO₂ VCD and the GOME-2B PBL VCD (SO₂ at 1 km), where the negative trend of the SO₂ columns is nicely seen from both datasets. GOME-2B columns are however very noisy, especially since 2017. For GOME-2A, the anthropogenic SO₂ product has been found to be too noisy to perform a meaningful comparison.

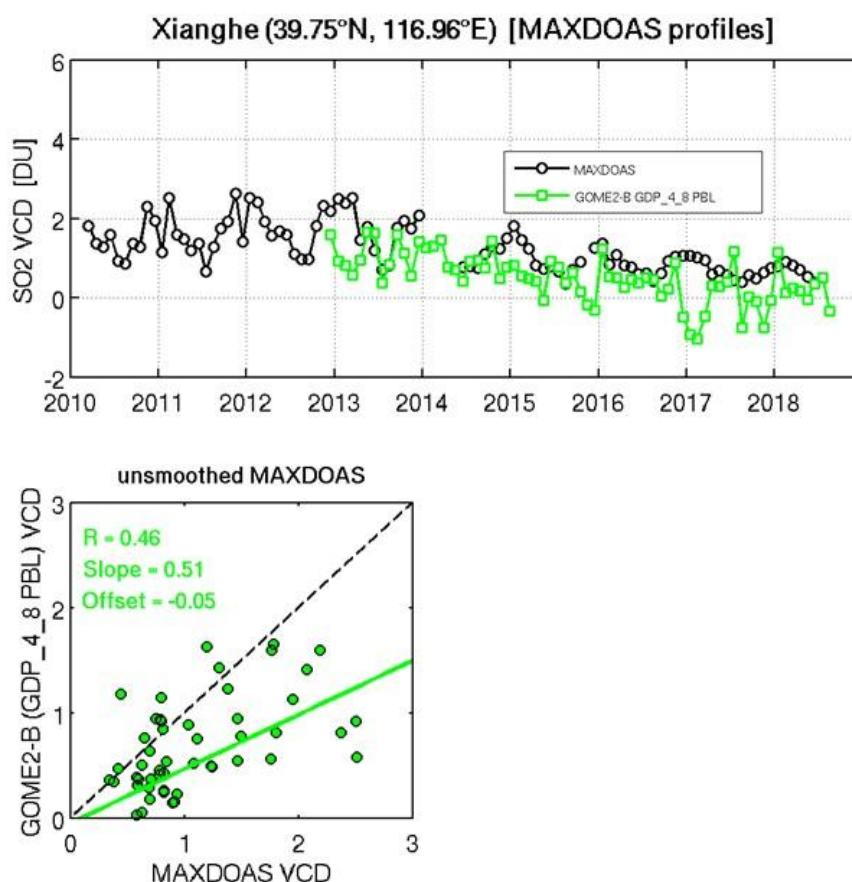


Figure 7.35. Illustration of the anthropogenic SO₂ comparisons in Xianghe. GOME-2B PBL data is compared to the MAXDOAS ground-based data.

As discussed in the last operation report, the plan for the improvement of the SO₂ GOME-2 products is to follow BIRA-IASB recommendations and bring the GDP SO₂ algorithm consistent to the TROPOMI product (Theys *et al.*, 2017). The implementations in the operation chain in DLR should occur in 2019.

References:

- Cl  mer, K., Van Roozendaal, M., Fayt, C., Hendrick, F., Hermans, C., Pinardi, G., Spurr, R., Wang, P., and De Mazi  re, M.: Multiple wavelength retrieval of tropospheric aerosol optical properties from MAXDOAS measurements in Beijing, *Atmos. Meas. Tech.*, 3, 863-878, 2010.
<https://doi.org/10.5194/amt-3-863-2010>
- De Smedt, I., Stavrou, T., Hendrick, F., Danckaert, T., Vlemmix, T., Pinardi, G., Theys, N., Lerot, C., Gielen, C., Vigouroux, C., Hermans, C., Fayt, C., Veefkind, P., M  ller, J.-F., and Van Roozendaal, M.: Diurnal, seasonal and long-term variations of global formaldehyde columns inferred from combined OMI and GOME-2 observations, *Atmos. Chem. Phys.*, 15, 12519-12545, 2015.
<https://doi.org/10.5194/acp-15-12519-2015>
- Gielen, C., Van Roozendaal, M., Hendrick, F., Pinardi, G., Vlemmix, T., De Bock, V., De Backer, H., Fayt, C., Hermans, C., Gillotay, D., and Wang, P.: A simple and versatile cloud-screening method for MAX-DOAS retrievals, *Atmos. Meas. Tech.*, 7, 3509-3527, 2014.
<https://doi.org/10.5194/amt-7-3509-2014>

Hendrick, F.M., Van Roozendael, M., Chipperfield, M.P., Dorf, M., Goutail, F., Yang, X., Fayt, C., Hermans, C., Pfeilsticker, K., Pommereau, J.-P., Pyle, J.A., Theys, N., and De Mazière, M.: Retrieval of stratospheric and tropospheric BrO profiles and columns using ground-based zenith-sky DOAS observations at Harestua, 60° N., Atmos. Chem. Phys., 7, 4869-4885, 2007.

<https://doi.org/10.5194/acp-7-4869-2007>

Hendrick, F., Johnston, P.V., De Mazière, M., Fayt, C., Hermans, C., Kreher, K., Theys, N., Thomas, A., and Van Roozendael, M.: One-decade trend analysis of stratospheric BrO over Harestua (60°N) and Lauder (45°S) reveals a decline, Geophys. Res. Letters, 35, L14801, 2008.

<https://doi.org/10.1029/2008gl034154>

Hendrick, F., Müller, J.-F., Clémer, K., Wang, P., De Mazière, M., Fayt, C., Gielen, C., Hermans, C., Ma, J.Z., Pinardi, G., Stavrakou, T., Vlemmix, T., and Van Roozendael, M.: Four years of ground-based MAX-DOAS observations of HONO and NO₂ in the Beijing area, Atmos. Chem. Phys., 14, 765–781, 2014.

<https://doi.org/10.5194/acp-14-765-2014>

Pinardi, G., Van Roozendael, M., Lambert, J.-C., Granville, J., Hendrick, F., Tack, F., Yu, H., Cede, A., Kanaya, Y., Irie, I., Goutail, F., Pommereau, J.-P., Pazmino, A., Wittrock, F., Richter, A., Wagner, T., Gu, M., Remmers, J., Friess, U., Vlemmix, T., PETERS, A., Hao, N., Tiefengraber, M., Herman, J., Abuhassan, N., Bais, A., Kouremeti, N., Hovila, J., Holla, R., Chong, J., Postylyakov, O., Ma, J.: GOME-2 total and tropospheric NO₂ validation based on zenith-sky, direct-sun and multi-axis DOAS network observations, Proceeding of the EUMETSAT conference, 22-26 September 2014, Geneva, Switzerland.

Richter, A., Behrens, L., Hilboll, A., Munassar, S., Burrows, J.P., Pinardi, G., and Van Roozendael, M.: Cloud effects on satellite retrievals of tropospheric NO₂ over China, oral presentation at the DOAS workshop, September 2017, Yokohama, Japan.

Theys, N., De Smedt, I., Yu, H., Danckaert, T., van Gent, J., Hörmann, C., Wagner, T., Hedelt, P., Bauer, H., Romahn, F., Pederngana, M., Loyola, D., and Van Roozendael, M.: Sulfur dioxide retrievals from TROPOMI onboard Sentinel-5 Precursor: algorithm theoretical basis, Atmos. Meas. Tech., 10, 119-153, 2017.

<https://doi.org/10.5194/amt-10-119-2017>

Vlemmix, T., Hendrick, F., Pinardi, G., Smedt, I., Fayt, C., Hermans, C., PETERS, A., Wang, P., Levelt, P., and Van Roozendael, M.: MAX-DOAS observations of aerosols, formaldehyde and nitrogen dioxide in the Beijing area: comparison of two profile retrieval approaches, Atmos. Meas. Tech., 2, 941–963, 2015.

<https://doi.org/10.5194/amt-8-941-2015>

Wang, T., Hendrick, F., Wang, P., Tang, G., Clémer, K., Yu, H., Fayt, C., Hermans, C., Gielen, C., Müller, J.-F., Pinardi, G., Theys, N., Brenot, H., and Van Roozendael, M.: Evaluation of tropospheric SO₂ retrieved from MAX-DOAS measurements in Xianghe, China, Atmos. Chem. Phys., 14(20), 11149-11164, 2014.

<https://doi.org/10.5194/acp-14-11149-2014>

7.3.1. Online quality monitoring

Before the CDOP-3, the online quality monitoring of the trace gas column products by DLR was limited to the generation of orbital and daily quick look maps of the trace gas columns (NO₂, HCHO, BrO, SO₂ and H₂O) from GOME-2A, GOME-2B, as well as composite maps. A few examples are shown below (see Figure 7.36, Figure 7.37 and Figure 7.38).

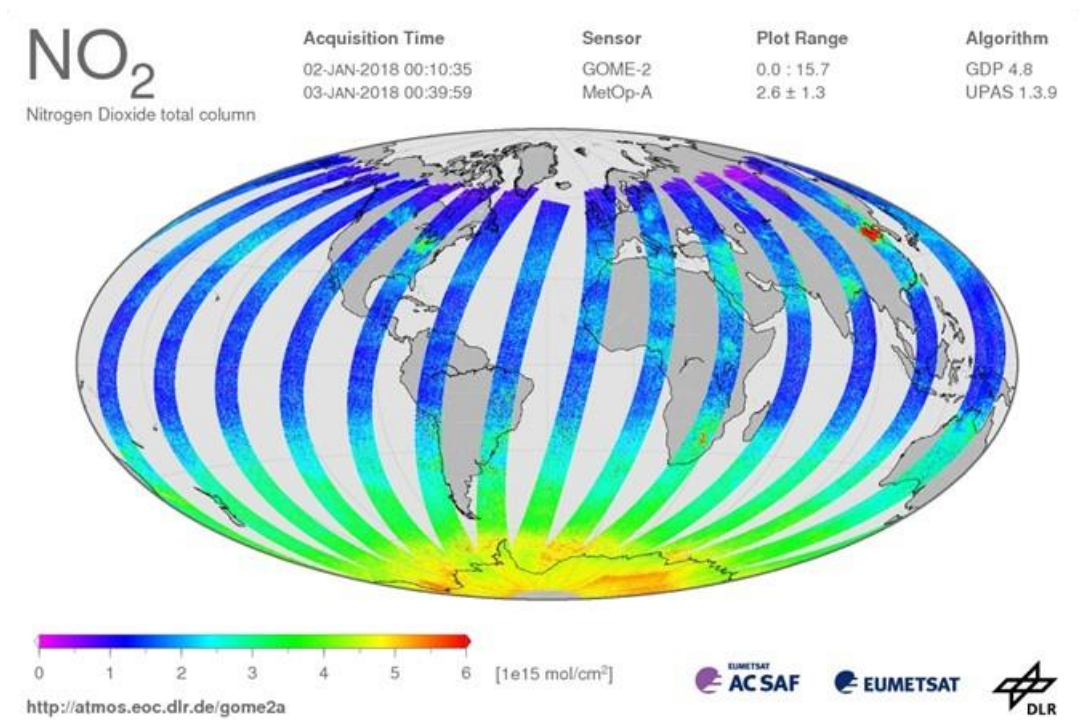


Figure 7.36. Example of daily global map of total NO₂ on January 2, 2018.

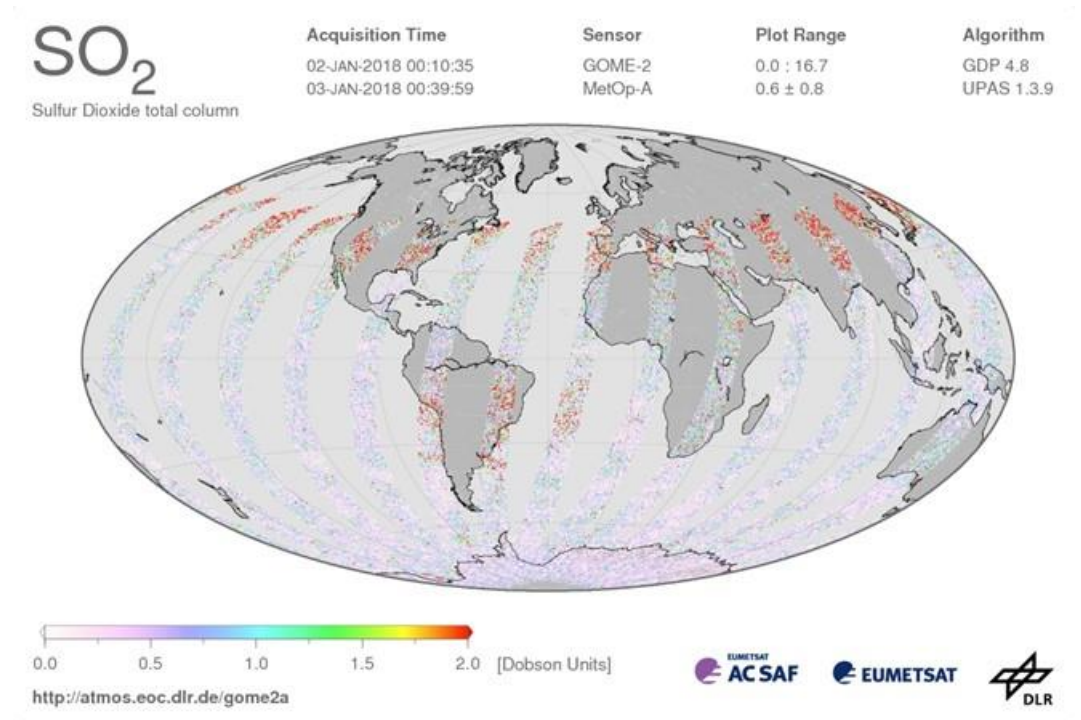


Figure 7.37. Example of daily global map of SO₂ on January 2, 2018.



Date: 10 December 2018

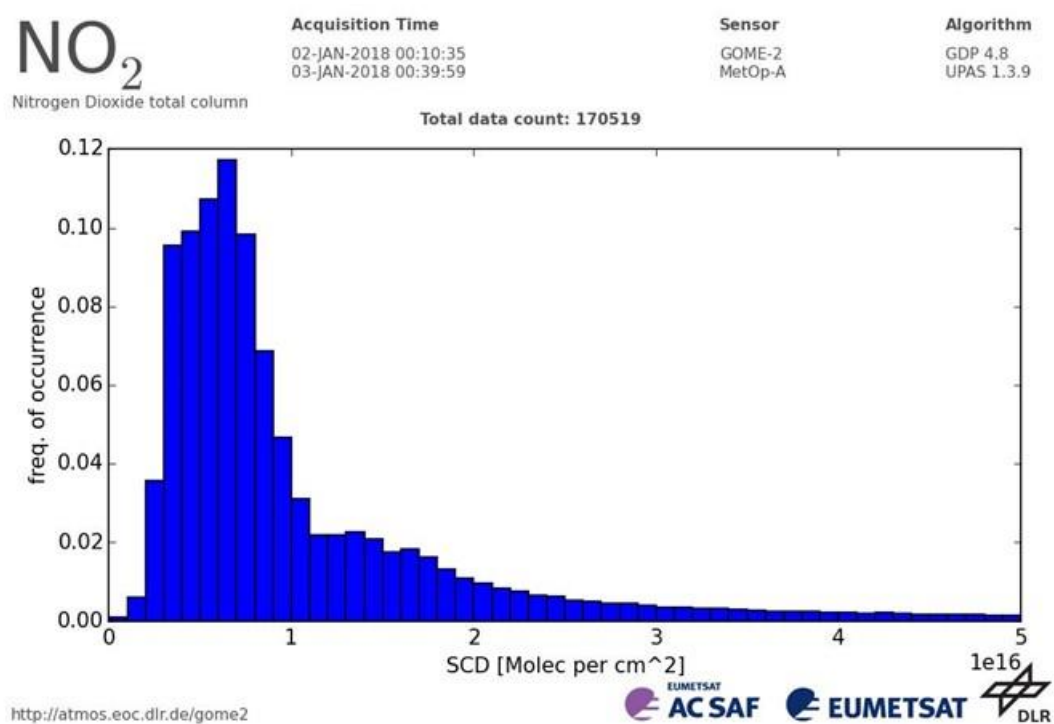


Figure 7.39. Daily distribution map of NO₂ SCDs on January 2, 2018 using the global GOME-2A data.

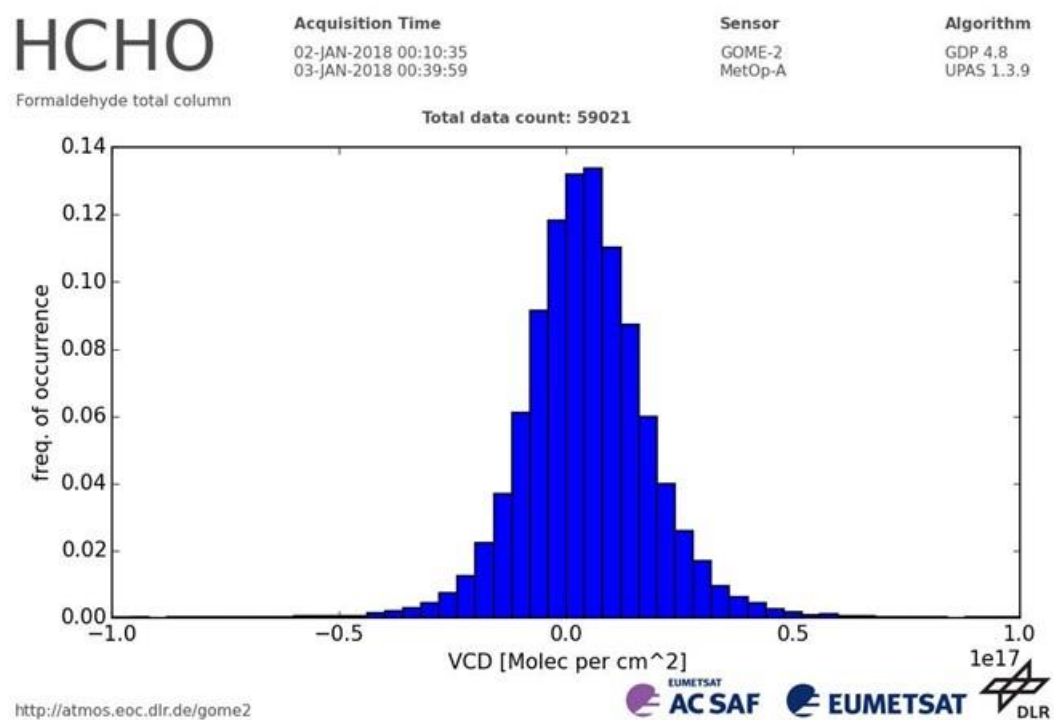


Figure 7.40. Daily distribution of HCHO VCDs on January 2, 2018 using global GOME-2A data.

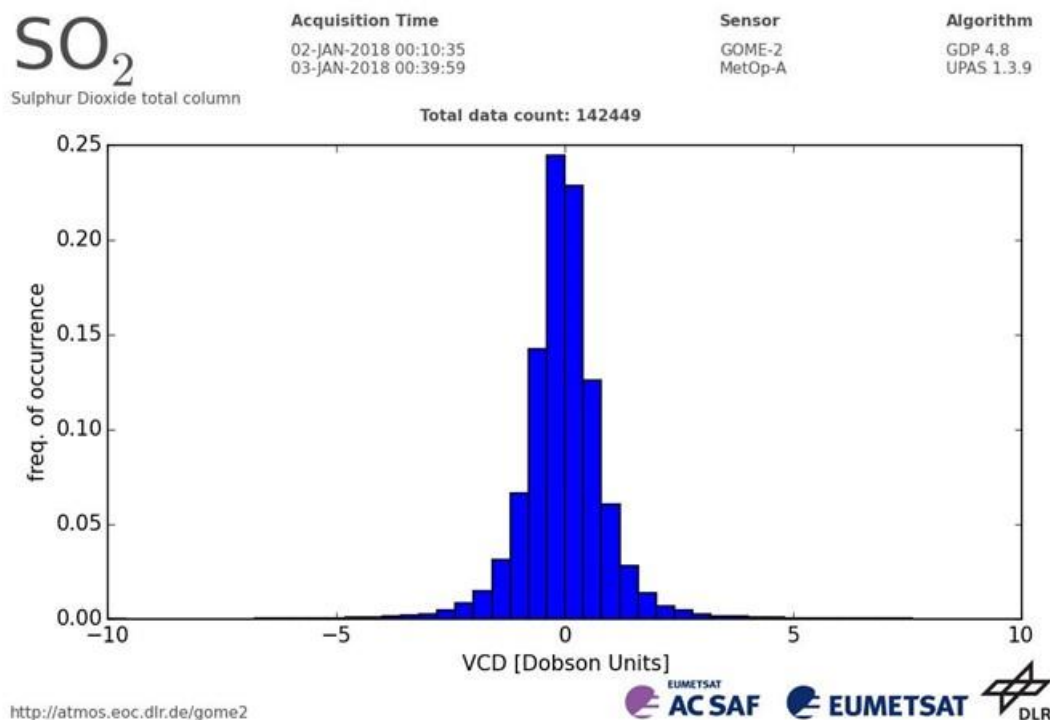


Figure 7.41. Daily distribution of SO₂ VCDs on January 2, 2018 using global GOME-2A data.

In previous reports, BIRA-IASB reported on the development and presentation of quality assessment (QA) pages for NO₂, HCHO, BrO and SO₂ data from the GOME-2A/B sensors. These pages are now operational and have seen only a technical modification in the last period: due to licensing issues, the regional maps are no longer shown by Google Maps, but by the open source Leaflet library.

As a recent edition, a first version now has been created of a new page for the monitoring of volcanic SO₂ from the IASI instruments. This page is in an advanced stage of development but awaits final modifications before it will be added to the operational CDOP website quality assessment section.

In order to provide reliable monitoring of enhanced IASI SO₂ data, the QA system is linked to the alerts for volcanic SO₂ issued by the Support to Aviation Control Service, SACS, hosted at BIRA-IASB (<http://sacs.aeronomie.be>). SACS alerts are issued when clusters of IASI measurements show enhanced SO₂ values. The QA monitoring page graphically displays each of these alerts by showing the average SO₂ total column value of the pixels involved in the alert, as function of measurement time. In addition, the geographical centre of gravity of the involved pixel locations is shown on a map for the alerts of the current month.

A recent example of the map and the graph is depicted in Figure 7.42. As can be seen, the alerts of the current month (August 2018 in this case) that have occurred so far are displayed on the map, color-coded to facilitate their identification with the corresponding symbol in the graph.

Alerts of previous months are not shown on the map (to prevent cluttering), but hovering over an alert symbol in the graph will highlight the map region where the enhanced SO₂ event occurred.

The IASI SO₂ monitoring page is currently undergoing final polishing and is expected to be released on the CDOP website in the next few months.

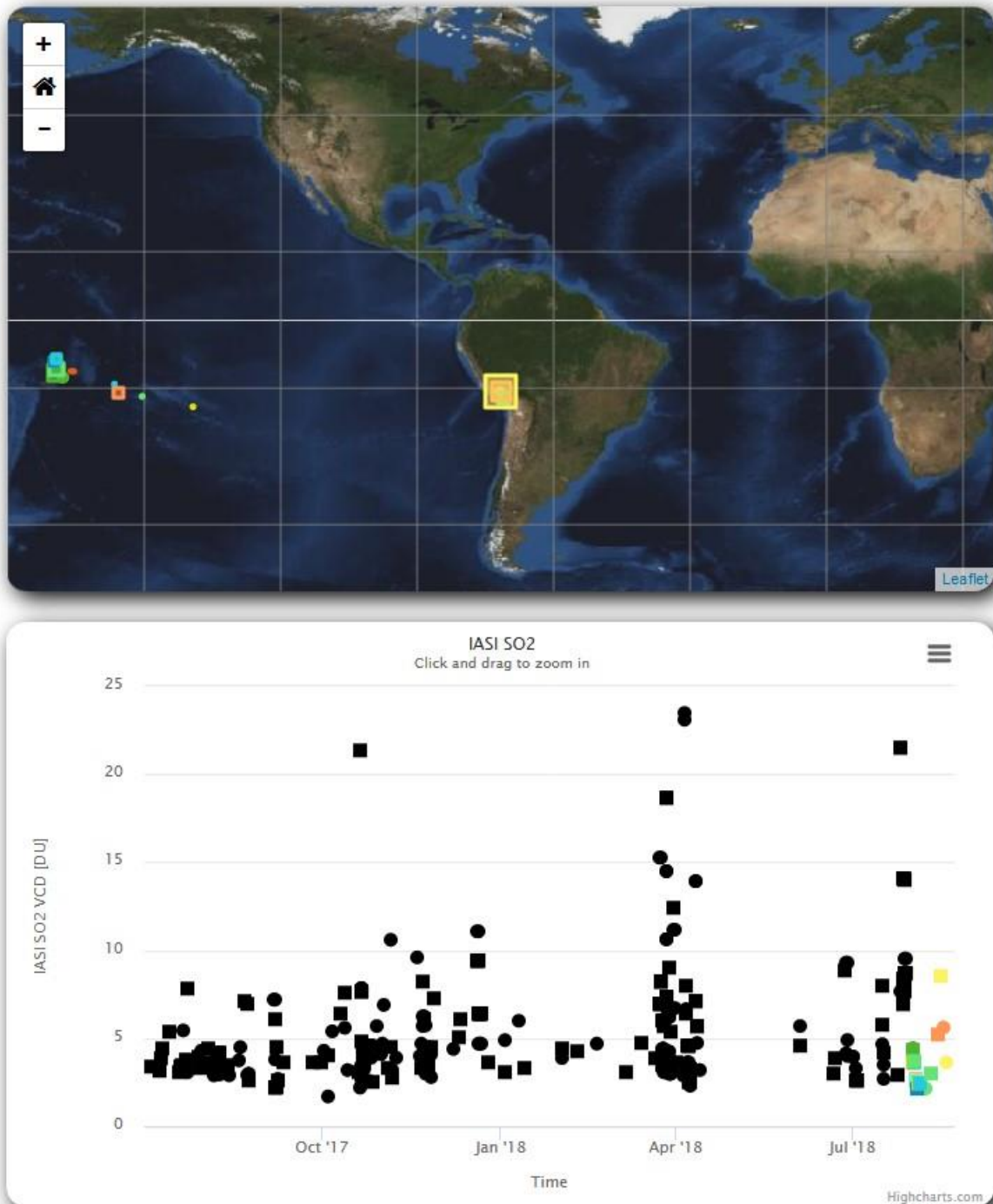


Figure 7.42. Quality monitoring for volcanic IASI SO₂. Colored symbols in the graph correspond to map symbols of the same color. On the map, their size is scaled according to SO₂ vertical column value. Circles denote alerts from IASI-A; squares denote alerts for IASI-B.

7.4. Ozone profile products

Table 7.13. Validation status of ozone profile products

Product Identifier	Product Name	Accuracy	Reference	Validating Institute
O3M-38	NRT high-resolution ozone profile	Fulfil threshold accuracy requirements	RD7	KMI DWD
O3M-47			RD8	
O3M-39	Offline high-resolution ozone profile	Fulfil threshold accuracy requirements	RD7	KMI DWD
O3M-48			RD8	

Validation results can be found in more detail on the AC SAF validation & quality assessment website at http://lap3.physics.auth.gr/eumetsat/ozone_profiles.

Validation activities summary:

This summary contains validation results of the GOME-2A and GOME-2B high resolution (HR) ozone profile products, retrieved by the Ozone Profile Retrieval Algorithm (OPERA) at KNMI. It covers the time period July 2016 until June 2018 for four different latitude belts for the upper stratosphere statistics. For the lower stratosphere statistics, the time period July 2017 – June 2018 has been taken into account for five different latitude belts.

The authors of this summary are Dr. Andy Delcloo from KMI and Dr. Wolfgang Steinbrecht from DWD. More information on how these values are extracted is available in the validation report (https://acsaf.org/docs/vr/Validation_Report_NOP_NHP_OOP_OHP_Feb_2012.pdf).

To report the skill scores of GOME-2 ozone profile products in a more condensed way, the statistics for the different output levels of GOME-2 are reduced to two layers: Lower Stratosphere (until an altitude of 30 km) and Upper Stratosphere (until an altitude of 50 km). Table 7.14 gives an overview on how we define the ranges in height for the different belts for lower stratosphere and upper stratosphere.

The collocation data used for the validation using ozonesonde data are shown in Figure 7.43. The validation for the lower and upper stratosphere is made with lidar and/or microwave data. The stations used in this validation for the lidar/microwave data are the Network for the Detection of Atmospheric Composition Change (NDACC) stations of Ny-Alesund (microwave), Hohenpeissenberg (lidar), Bern (microwave), Payerne (microwave) Haute-Provence (lidar), Table Mountain (lidar), Mauna Loa (lidar and microwave) and Lauder (lidar and microwave).

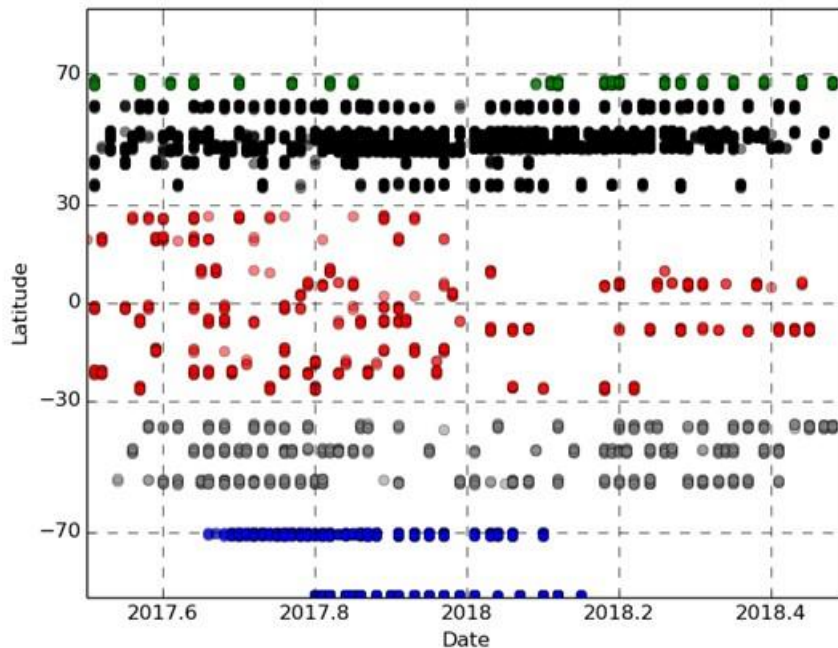


Figure 7.43. Collocation data for the validation with ozonesonde data for the time period July 2017 - June 2018.

Table 7.14. Definition of the ranges in km for lower and higher stratosphere for the different latitude belts

	Lower Stratosphere	Upper Stratosphere
Polar Region	12 km – 30 km	30 km – 50 km
Mid-Latitudes	14 km – 30 km	30 km – 50 km
Tropical Region	18 km – 30 km	30 km – 50 km

Relative differences (Eq. 1) are calculated against sounding data, which is convolved with the averaging kernels (Smoothed Sounding):

$$\frac{(\text{GOME-2} - \text{Smoothed Sounding})}{\text{Smoothed Sounding}} * 100 \quad (1)$$

Table 7.15 shows an overview of the obtained results for the time period July 2017 – June 2018 only for the lower and the higher stratosphere, not taking into account the tropospheric ozone column products since a dedicated product on the ozone profiles is now also operational and the statistics on these products is also mentioned in this report. The statistics for the lower stratosphere are made available by KMI, the statistics for the higher stratosphere by DWD.

Table 7.15. Absolute Differences (AD), Relative Differences (RD) and standard deviation (STDEV) are shown on the accuracy of GOME-2A/B HR ozone profile products for the lower and the higher stratosphere for five different latitude belts for the time period July 2017 - June 2018.

GOME-2A HR						
	Lower Stratosphere			Upper Stratosphere*		
	AD	RD	STDEV	AD	RD	STDEV
	(DU)	(%)	(%)	(DU)	(%)	(%)
Northern Polar Region	-2.8	-4.0	9.8	-17.2	-50.3	16.0
Northern Mid-Latitudes	-0.3	-0.7	8.4	-19.4	-43.0	12.5
Tropical Region	4.3	3.9	6.5	-21.2	-39.9	8.7
Southern Mid-Latitudes	4.1	0.9	7.4	-16.0	-33.7	14.6
Southern Polar Region	-2.6	-1.6	20.1	-	-	-
GOME-2B HR						
	Lower Stratosphere			Upper Stratosphere*		
	AD	RD	STDEV	AD	RD	STDEV
	(DU)	(%)	(%)	(DU)	(%)	(%)
Northern Polar Region	-18.1	-6.1	20.7	-6.1	-24.1	21.8
Northern Mid-Latitudes	-28.5	-10.5	20.4	-3.7	-15.0	16.0
Tropical Region	8.3	6.1	7.3	-7.0	-18.6	7.0
Southern Mid-Latitudes	-12.6	-3.6	16.2	-8.1	-15.7	14.7
Southern Polar Region	-16.3	-1.3	44.9	-	-	-

* For the upper stratosphere, the time period under consideration is July 2016 - June 2018.

The target value is met in the lower stratosphere (15 %) for all belts under consideration. In the upper stratosphere the target and threshold values (15 % and 30 %) are not met any more for the GOME-2A HR products. For GOME-2B HR products in the upper stratosphere, the target value (15 %) is often missed now, but the ozone profile product is generally still within threshold (30 %).

Results can also be consulted on the website at: http://lap3.physics.auth.gr/eumetsat/ozone_profiles

7.4.1. Online quality monitoring

Timeline of the vertically integrated Metop-B ozone profile with respect to time is presented in Figure 7.44.

More information and images at the following web addresses

<http://www.temis.nl/o3msaf/timeseries.php?sat=metopa>

<http://www.temis.nl/o3msaf/timeseries.php?sat=metopb>

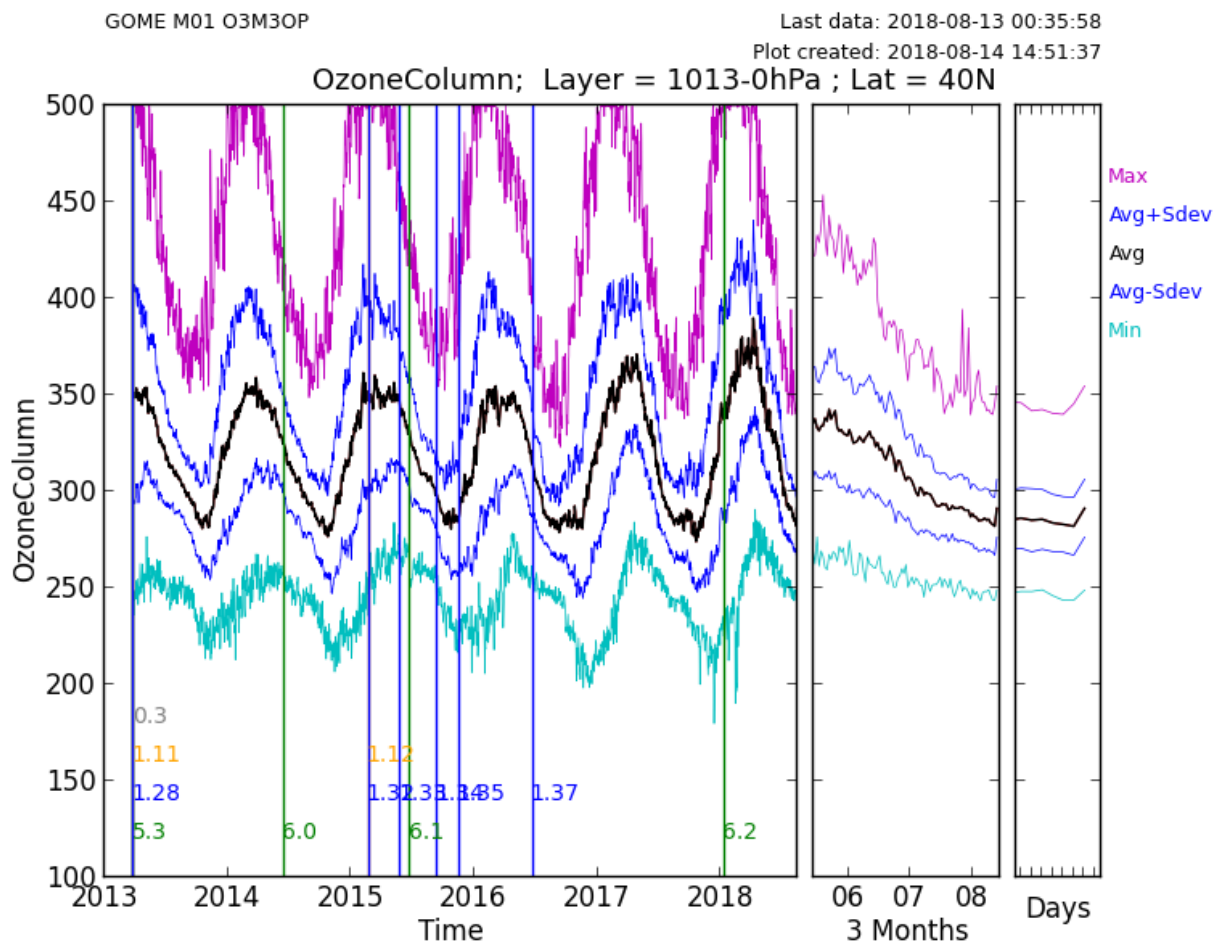


Figure 7.44. Timeline of vertically integrated Metop-B ozone profile.

Legend of the coloured vertical lines:

- Green: PPF version
- Blue: Software version (PGE)
- Orange: Algorithm version
- Grey: Config version

7.5. Aerosol products

Table 7.16. Validation status of aerosol products

Product Identifier	Product Name	Accuracy	Reference	Validating Institute
O3M-61.1	NRT absorbing aerosol index	Fulfil threshold accuracy requirement	RD14	KNMI
O3M-71.1				
O3M-62.1	NRT absorbing aerosol index from PMDs	Fulfil threshold accuracy requirement	RD14	KNMI
O3M-72.1				
O3M-14.1	Offline absorbing aerosol index	Fulfil threshold accuracy requirements	RD14	KNMI
O3M-70.1				
O3M-63.1	Offline absorbing aerosol index from PMDs	Fulfil threshold accuracy requirements	RD14	KNMI
O3M-73.1				

7.5.1. Online quality monitoring

The online quality monitoring of the AAI in this section show (left duo-plot) the radiance corrections for the PMD-AAI at 340 and 380nm, and (right duo-plot) the uncorrected residue, and the corrected residue. The rightmost plot is the result of all the corrections and should stay more or less flat when seasonal cycles and differences are removed.

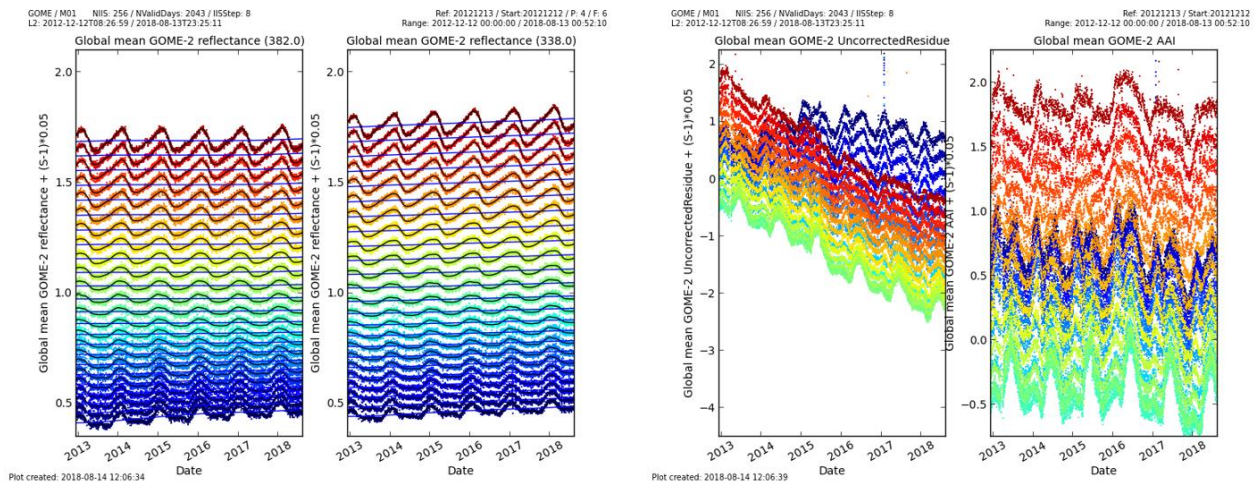


Figure 7.45. Timeline of global mean reflectances at 340 and 380 nm (left) and the uncorrected and corrected AAI from the PMDs of Metop-B.

7.6. UV products

Table 7.17. Validation status of UV products

Product Identifier	Product Name	Accuracy	Reference	Validating Institute
O3M-91	NRT UV index, clear-sky	Fulfil threshold accuracy requirements	RD9	DMI
O3M-92	NRT UV index, cloud-corrected			
O3M-95 – O3M-108	Offline surface UV	Fulfil target accuracy requirements	RD15	FMI

7.6.1. Online quality monitoring

NUV:

There are two daily updated online quality monitoring entries on the NUV web page <http://nuv.dmi.dk/>.

The first one (<http://nuv.dmi.dk/qaqc/nbsp/zonal-mean/>) is showing the zonal mean UV index in five longitude zones. The current zonal mean is compared to the two previous years and problems with data quality will show up in these plots. No problems were seen in the reporting period.

The second one (<http://nuv.dmi.dk/qaqc/nbsp/measured-uv/>) shows a comparison with ground-based measurements for two instruments operated by DMI, one in Copenhagen and one in Greenland. The most recent measurements, preferably only one day old, are shown together with the calculated NUV, details on the comparison can be found on the web page. Problems with the quality of the NUV would show here. Archive page has been included, making it possible to view older data.

OUV:

Online quality monitoring of offline surface UV

(https://acsaf.org/uv_validation/online_quality.html) has not shown any unexpected, permanent changes in the product quality after the latest validation. The latest OUV validation reports were published in February 2009 covering June 2007 – May 2008 (Metop-A data) and in February 2015 covering June 2012 – May 2013 (Metop-B data).

Figure 7.46 presents the long-term monitoring graph of OUV, which illustrates seasonal variation of **global average of erythemal daily dose** (yellow markers). Any sudden changes would indicate

problems with data quality. Additionally, six-month average values (January - June and July - December) are represented by red markers.

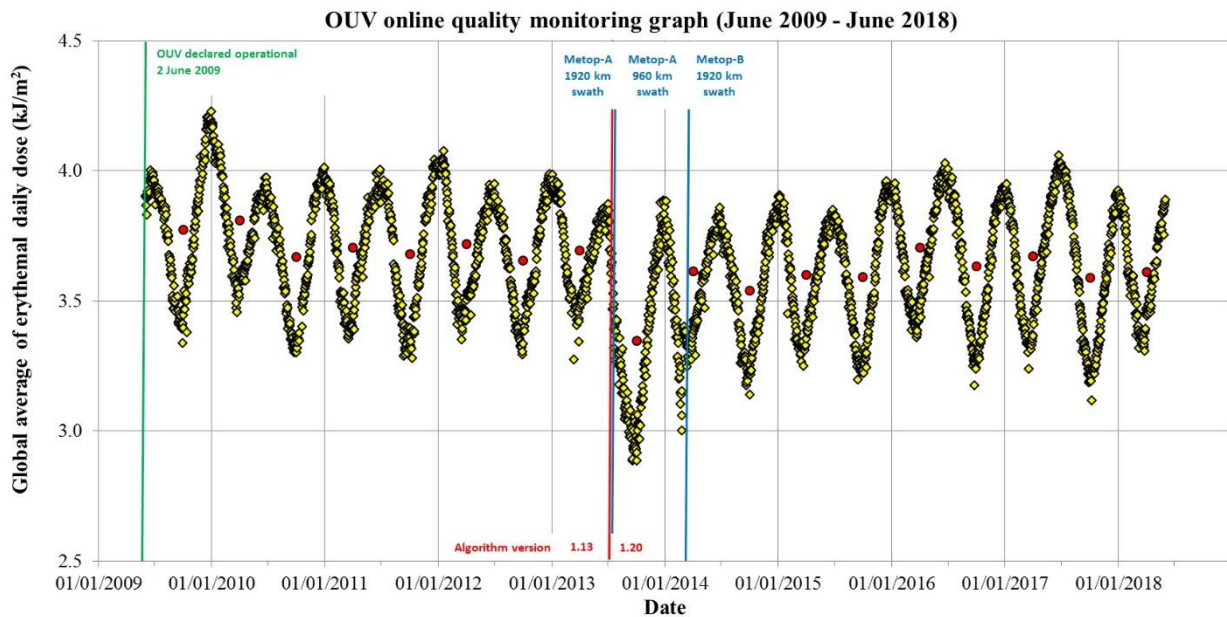


Figure 7.46. OUV long-term monitoring graph.

NOTE: GOME-2A was switched from nominal swath width (1920 km) to reduced swath width (960 km) 15 July 2013. The effect to OUV monitoring values can be clearly seen as more wide-spread global average values of erythemal daily dose. This is due to the dominance of lower EDD values in high latitudes when the satellite coverage near the equator is poor due to narrower swath width.

OUV data processing was switched to use Metop-B data having nominal swath width of 1920 km 1 March 2014.

7.7. IASI NRT products

Table 7.18. Validation status of the IASI CO product

Product Identifier	Product Name	Accuracy	Reference	Validating Institute
O3M-80	IASI NRT CO	Fulfil threshold accuracy requirement	RD20	LATMOS
O3M-57	IASI NRT SO ₂	Fulfil threshold accuracy requirement	RD22	AUTH, BIRA, LATMOS, ULB

Dissemination monitoring activities summary:

IASI CO:

The IASI NRT CO product (v6.3) has been declared operational on 2 March 2017. Here we present statistical results when comparing the EUMETSAT product disseminated by EUMETCast in BUFR format (COX) with the native product produced at ULB (FORLI-CO v20151001) for 6 days representative of 6 months: January 15th, February 15th, March 15th, April 15th, May 15th and June 15th, 2018, for Metop-A and Metop-B. This allows monitoring if any discrepancy occurs

between the two, EUMETSAT and native, products. So far, the discrepancies are found within the numerical errors inherent to the use of different IT infrastructure.

CO total column and profiles are investigated. Statistics between COX data and FORLI-CO data (v20151001) are presented in Table 7.19. Profiles correlation (“Correlation”) score is computed using the discreet cross correlation integral between two profiles, normalized by the square root of the product of their auto-correlation integral. Score of 1 is expected for perfectly matching profiles, 0 for unrelated ones. Absolute and relative differences are calculated for the total columns. These tables are extracted from the Daily Reports from Daniel Hurtmans at ULB.

Figure 7.47 shows the results when plotting the number of common pixels (upper panel) and the total column differences (lower panel) taken from these tables, for the 6 months. A rather stable number of common pixels is shown (a) with the change from version 6.3 to 6.4 in March 2018 and from version 6.4 to 6.4.5 in April 2018 being clearly seen. When zooming into this Figure (b) the constant variations in the number of common pixels and the rather stable column differences for this period are shown.

Table 7.19. Statistics between COX data and FORLI-CO data for 6 days: January 15th, February 15th, March 15th, April 15th, May 15th and June 15th, 2018.

15/01/2018:

		IASI-a		IASI-b	
		Native	COX	Native	COX
Individual Pixels		515822	516032	510347	510526
Common Pixels		515729 (99.94%)		510189 (99.93%)	
Correlation	Mean	1.0000±0.0000		1.0000±0.0000	
	Max	1.0000		1.0000	
	Min	0.9705		0.9776	
Total Column Differences	Mean (10 ¹⁹ mol/cm ²)	-0.0000±0.0002		-0.0000±0.0003	
	Max (10 ¹⁹ mol/cm ²)	0.0518		0.0397	
	Min (10 ¹⁹ mol/cm ²)	-0.0477		-0.1696	
Total Column Relative Differences	Mean (%)	-0.0009±0.0516		-0.0010±0.0834	
	Max (%)	10.5908		16.8891	
	Min (%)	-18.5286		-34.4319	

15/02/2018:

		IASI-a		IASI-b	
		Native	COX	Native	COX
Individual Pixels		509608	509436	515426	515176
Common Pixels		509076 (99.90%)		514869 (99.89%)	
Correlation	Mean	1.0000±0.0000		1.0000±0.0000	
	Max	1.0000		1.0000	
	Min	0.9863		0.9844	
Total Column Differences	Mean (10^{19} mol/cm ²)	-0.0000±0.0015		-0.0000±0.0035	
	Max (10^{19} mol/cm ²)	0.7390		0.3351	
	Min (10^{19} mol/cm ²)	-0.0865		-2.4278	
Total Column Relative Differences	Mean (%)	-0.0011±0.1012		-0.0015±0.0751	
	Max (%)	53.2990		17.6369	
	Min (%)	-13.7237		-28.9453	

15/03/2018:

		IASI-a		IASI-b	
		Native	COX	Native	COX
Individual Pixels		542031	143494	545569	145933
Common Pixels		142074 (26.21%)		145854 (26.73%)	
Correlation	Mean	1.0000±0.0000		1.0000±0.0000	
	Max	1.0000		1.0000	
	Min	0.9939		0.9952	
Total Column Differences	Mean (10^{19} mol/cm ²)	-0.0000±0.0006		-0.0000±0.0001	
	Max (10^{19} mol/cm ²)	0.0114		0.0101	
	Min (10^{19} mol/cm ²)	-0.2134		-0.0331	
Total Column Relative Differences	Mean (%)	-0.0007±0.0623		-0.0005±0.0462	
	Max (%)	3.0819		2.6667	
	Min (%)	-14.2975		-10.8078	

15/04/2018:

		IASI-a		IASI-b	
		Native	COX	Native	COX
Individual Pixels		547156	547277	551170	551763
Common Pixels		547006 (99.95%)		551095 (99.88%)	
Correlation	Mean	1.0000±0.0001		1.0000±0.0000	
	Max	1.0000		1.0000	
	Min	0.9617		0.9877	
Total Column Differences	Mean (10^{19} mol/cm ²)	-0.0000±0.0002		-0.0000±0.0003	
	Max (10^{19} mol/cm ²)	0.0370		0.0897	
	Min (10^{19} mol/cm ²)	-0.0712		-0.0643	
Total Column Relative Differences	Mean (%)	-0.0008±0.0692		-0.0005±0.0595	
	Max (%)	10.9568		15.5197	
	Min (%)	-32.8548		-21.5127	

15/05/2018:

		IASI-a		IASI-b	
		Native	COX	Native	COX
Individual Pixels		532719	532952	526685	526872
Common Pixels		532647 (99.94%)		526603 (99.95%)	
Correlation	Mean	1.0000±0.0001		1.0000±0.0000	
	Max	1.0000		1.0000	
	Min	0.9608		0.9850	
Total Column Differences	Mean (10^{19} mol/cm ²)	-0.0000±0.0002		-0.0000±0.0002	
	Max (10^{19} mol/cm ²)	0.0764		0.0390	
	Min (10^{19} mol/cm ²)	-0.0147		-0.0467	
Total Column Relative Differences	Mean (%)	-0.0007±0.0572		-0.0010±0.0624	
	Max (%)	26.0365		13.0777	
	Min (%)	-6.8825		-18.0399	

15/06/2018:

		IASI-a		IASI-b	
		Native	COX	Native	COX
Individual Pixels		546633	546052	536336	535666
Common Pixels		545724 (99.83%)		535342 (99.81%)	
Correlation	Mean	1.0000±0.0000		1.0000±0.0000	
	Max	1.0000		1.0000	
	Min	0.9903		0.9884	
Total Column Differences	Mean (10^{19} mol/cm ²)	-0.0000±0.0011		-0.0000±0.0003	
	Max (10^{19} mol/cm ²)	0.1053		0.0646	
	Min (10^{19} mol/cm ²)	-0.8002		-0.1222	
Total Column Relative Differences	Mean (%)	-0.0008±0.0641		-0.0009±0.0741	
	Max (%)	21.2169		12.4871	
	Min (%)	-14.0726		-29.2447	

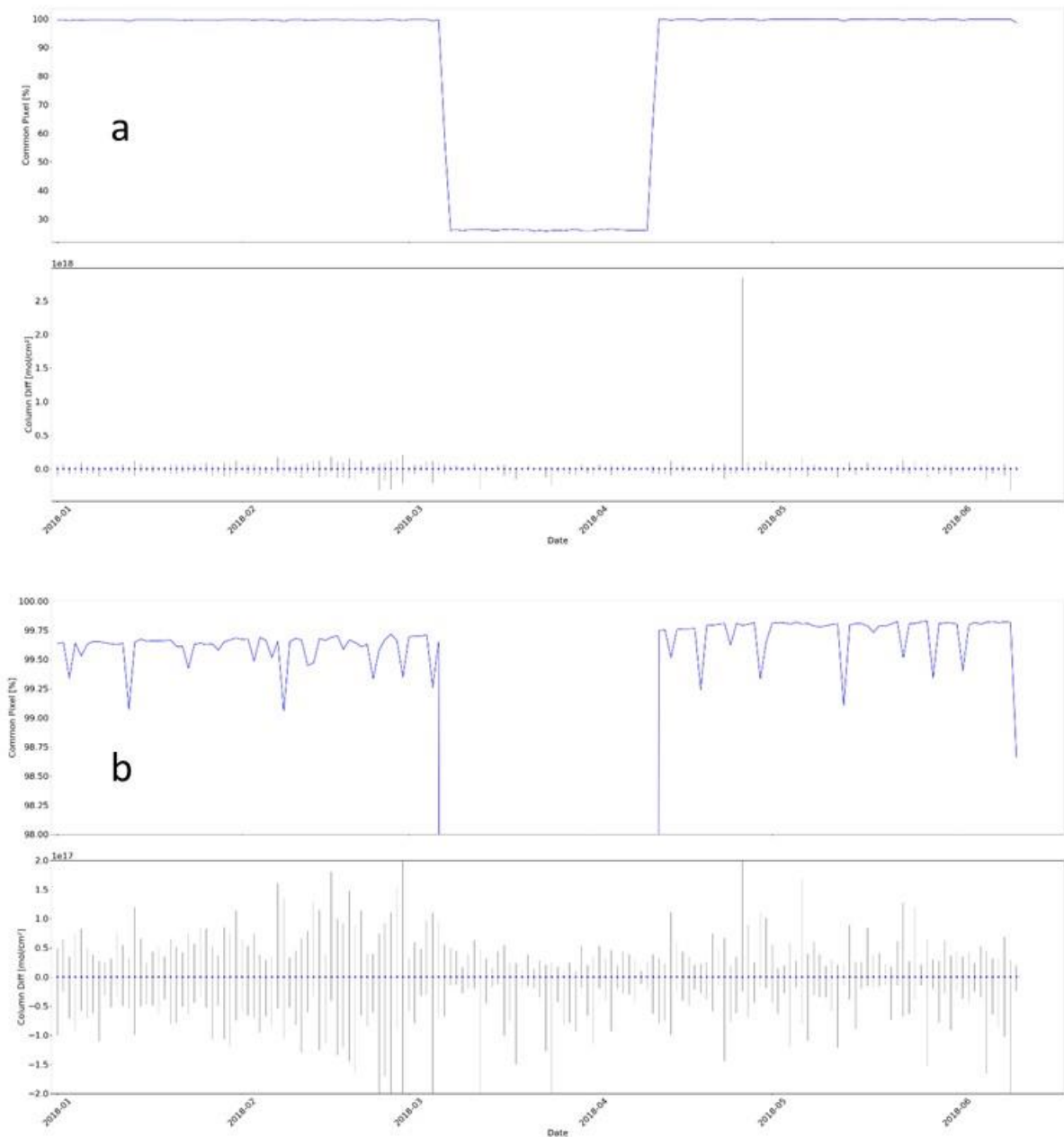


Figure 7.47. Monitoring of IASI CO for 6 months (January - June 2018), upper panel is the number of common pixels and lower panel is the column differences, showing: a) the change of version, from version 6.3 to 6.4 in March 2018 and from version 6.4 to 6.4.5 in April 2018. b) the constant variations in the number of common pixels and the rather stable column differences for this period.

IASI SO₂:

The IASI BRESCIA SO₂ retrieval algorithm has been implemented in the PPF v6.3 at EUMETSAT (operational release on 18/04/2018). Here we compare the EUMETSAT product disseminated by EUMETCast in BUFR format (SO₂ EUMET) with the native product produced at ULB (SO₂ ULB) for 6 days between January and June 2018, for Metop-A. Note that the January to June 2018 period does not include significant volcanic eruptions. We choose to study 10/01/2018, 20/02/2018, 27/03/2018, 12/04/2018, 18/05/2018 and 29/06/2018 as some SO₂ signal is present, but the SO₂ columns are low.

For each of the 6 days, scatterplots for the different estimated altitudes (5, 7, 10, 13 and 25 km) are presented (Figure 7.48 - Figure 7.53). The data have been filtered following the recommendations of the Product User Manual

(https://acsaf.org/docs/pum/Product_User_Manual_IASI_SO2_Mar_2018.pdf, Section 5.2.2): We first keep the pixels with $SO_2_BT_DIFFERENCE > 1K$. Then, we look for more pixels around these pixels: we choose a neighbourhood of ± 10 latitude/longitude, and selected the pixels with $SO_2_BT_DIFFERENCE \geq 0.4K$ (if $SO_2_BT_DIFFERENCE < 0.4K$, there is not enough SO_2 to have a reliable retrieval).

We recall here that when the IASI L2 pressure and temperature profiles are not available, ECMWF forecasts (3h, interpolated in time and space) data are used in the EUMETSAT API. These pixels are flagged with $SO_2_QFLAG = 11$, and are not part of the comparison.

Note that BUFR encoding precision is 0.1 DU (corresponding to the sensibility), explaining the “staircase effect” that can be seen if we when looking at a thinner scale (Figure 7.53b).

Correlation coefficients (in blue) are ~ 1 .

So far, the discrepancies are found within the numerical errors inherent to the use of different IT infrastructure.

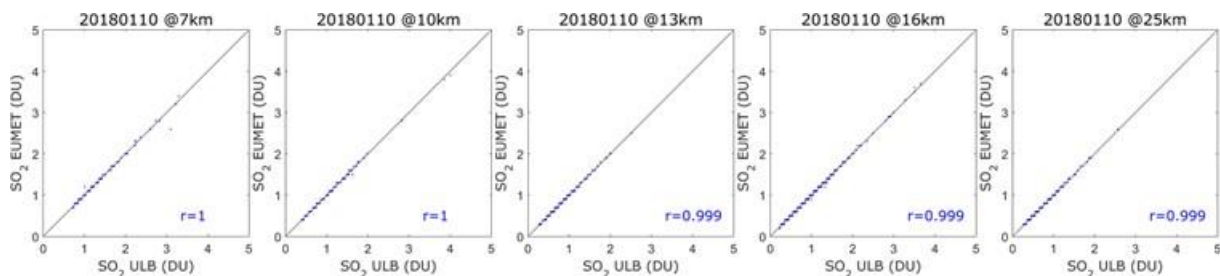


Figure 7.48. Scatterplots (SO₂ EUMET versus SO₂ ULB) for 10/01/2018, for the 5 estimated altitudes (5, 7, 10, 13 and 25 km).

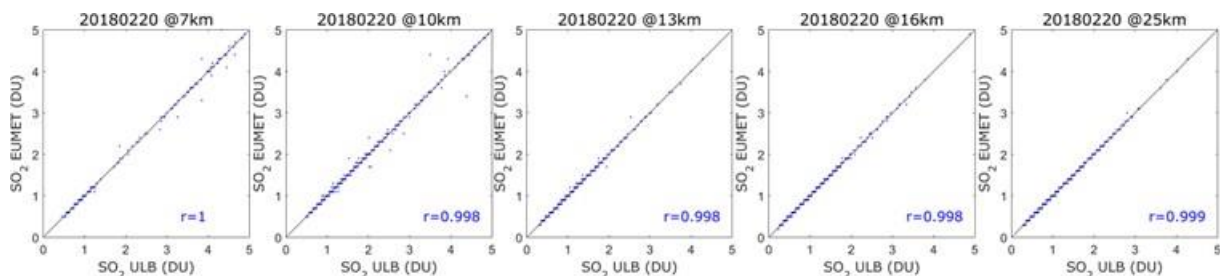


Figure 7.49. Same as Figure 7.48 but for 20/02/2018.

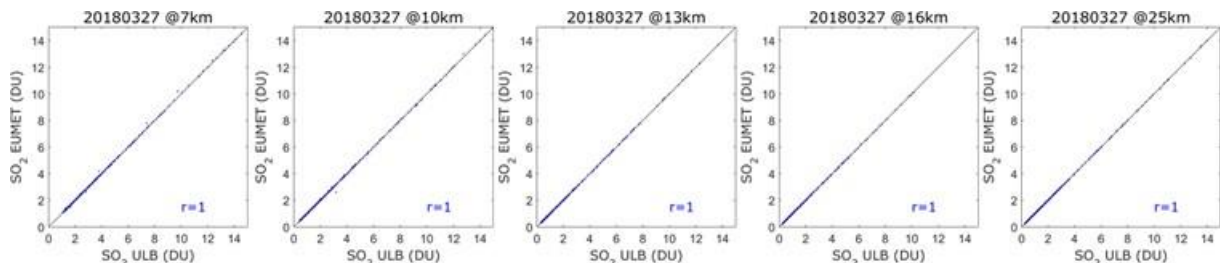


Figure 7.50. Same as Figure 7.48 but for 27/03/2018.

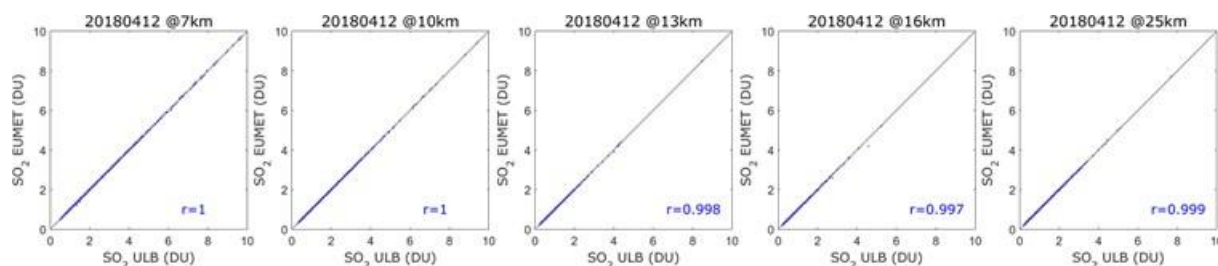


Figure 7.51. Same as Figure 7.48 but for 12/04/2018.

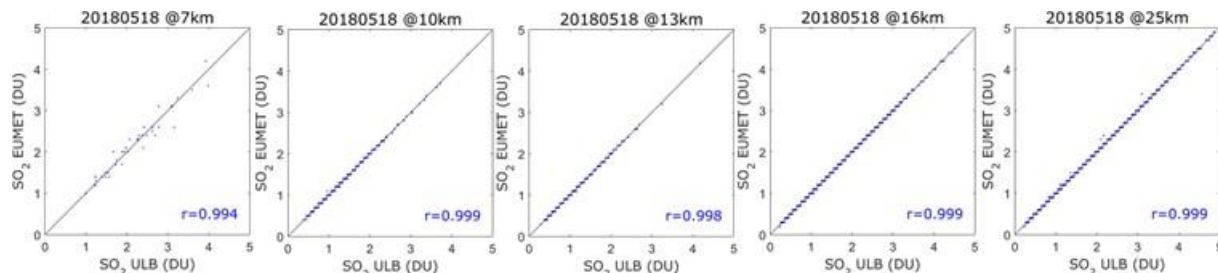


Figure 7.52. Same as Figure 7.48 but for 18/05/2018.

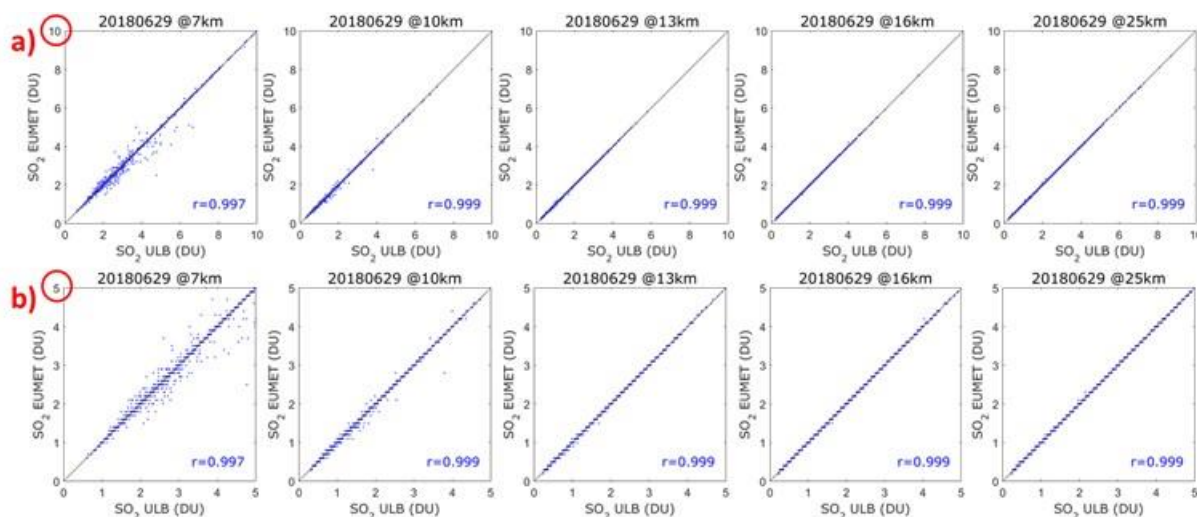


Figure 7.53. a) same as Figure 7.48 but for 29/06/2018, b) same as subplot (a) but with xlim = ylim = 5 DU (Zoom).

Validation with CO FTIR ground-based data

This section presents the work of Bavo Langerock (BIRA-IASB) that compared the CO IASI Metop-A and Metop-B data against FTIR measurement data available from the NDACC (Network for the Detection of Atmospheric Composition Change). The Copernicus Atmosphere Monitoring Service (CAMS) projects supports selected NDACC instruments and PIs for rapid delivery of quality measurements to the NDACC data host (contract CAMS27, <http://cams27.aeronomie.be>). Recent FTIR measurement data is now available for many more sites (in this study we used data from 14 sites).

These ground-based, remote-sensing instruments are sensitive to the CO abundance in the troposphere and lower stratosphere, i.e. between the surface and up to 20 km altitude. CO total columns are validated (surface to 100 km). A description of the FTIR instruments and retrieval methodology can be found at <http://nors.aeronomie.be>. The typical uncertainty on the FTIR CO column is approximately 3 %. Due to the absence of solar light during local winter, the number of

measurements at Arrival Heights in Antarctica (latitude = -77.8°) is limited and is therefore left out from this report.

In this study each FTIR measurement is co-located to each IASI measurements within a time difference of 3 hours, within a latitude difference of 0.5° and a longitude difference of 1.5° . The IASI *a priori* is substituted in the FTIR retrieval and subsequently the FTIR retrieved profile with the IASI *a priori* is smoothed using the IASI averaging kernel, as described in Rodgers *et al.*, 2003. In the plots the relative differences are calculated using the latter FTIR columns (smoothed with the IASI averaging kernels). This validation methodology is described in more detail in Ronsmans *et al.*, 2016.

The correlation coefficients of the Taylor diagrams (Figure 7.54) are generally ranging from ~ 0.8 to nearly 1, showing a very good agreement between the IASI and FTIR data, for both Metop-A and Metop-B. However, some sites show values below 0.8:

1. Ny Alesund and Rikubetsu have only few co-located measurements and are statistically less relevant
2. St. Petersburg has low correlation (0.7 for Metop-A and 0.6 for Metop-B) with a significant number of measurements: this is probably due to underestimation in February - March 2018 (see also below) and some outlying IASI columns in 2018. (See Figure 7.57).

The Taylor diagrams (Figure 7.54) also show that the standard deviations of the FTIR columns values are smaller compared the satellite standard deviation probably due to higher noise on the satellite time series (almost all site points are shifted left of the satellite reference, typically with a factor of 0.75 to 1 of the standard deviation of the satellite CO columns).

Figure 7.55 shows the time-series of bi-weekly mean relative differences for the January 2017 - August 2018 time period. Red indicates a positive bias (IASI > NDACC) while blue indicates an underestimation of the satellite retrievals.

Even if we do not have FTIR data for every month, we can conclude that for most of the 14 stations included in the study, mean relative differences, or biases, are less than 10 % (see Figure 7.56). For the Eureka and Ny Alesund stations, located at high latitudes, biases are larger. A similar bias is found by Buchholz *et al.* (2017) when comparing with MOPITT data. When looking at the stations between -60° and 60° , the Toronto station shows the largest biases (mean bias=13.6 %, see Figure 7.56 and Figure 7.57). The IASI data are generally overestimated. On the contrary, for the stations Garmisch, Zugspitze, St. Petersburg and Rikubetsu in the Northern Hemisphere, the IASI data are underestimated during the winter months. Although the biases are within the total uncertainty (see Figure 7.57, where the time series of the relative differences are plotted for a selected number of sites), the change in bias is remarkable.

Here we present results for one and a half year. A longer time series is required to see if this is recurrent. A more detailed study is required to understand the biases.

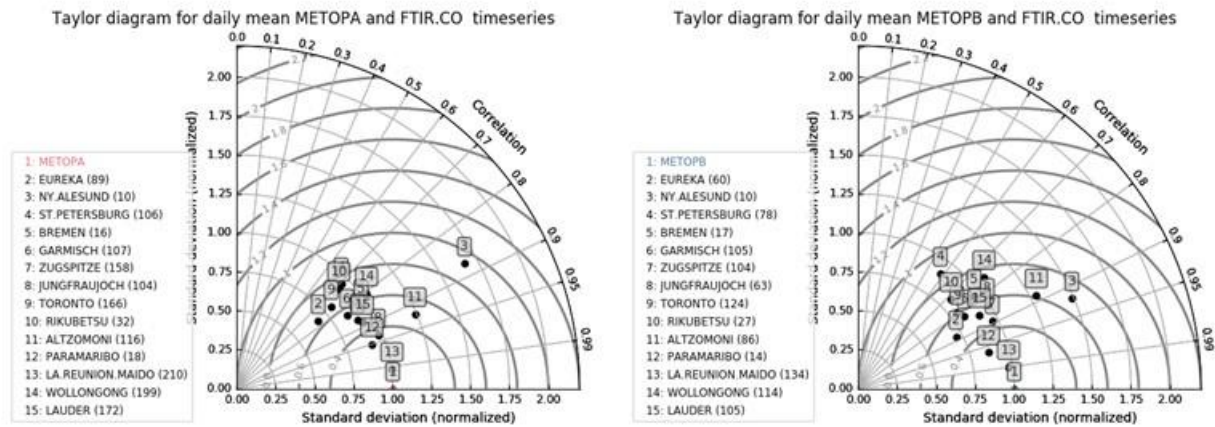


Figure 7.54. Correlation plots for IASI Metop-A (left) and IASI Metop-B (right) CO total columns against 14 NDACC FTIR sites

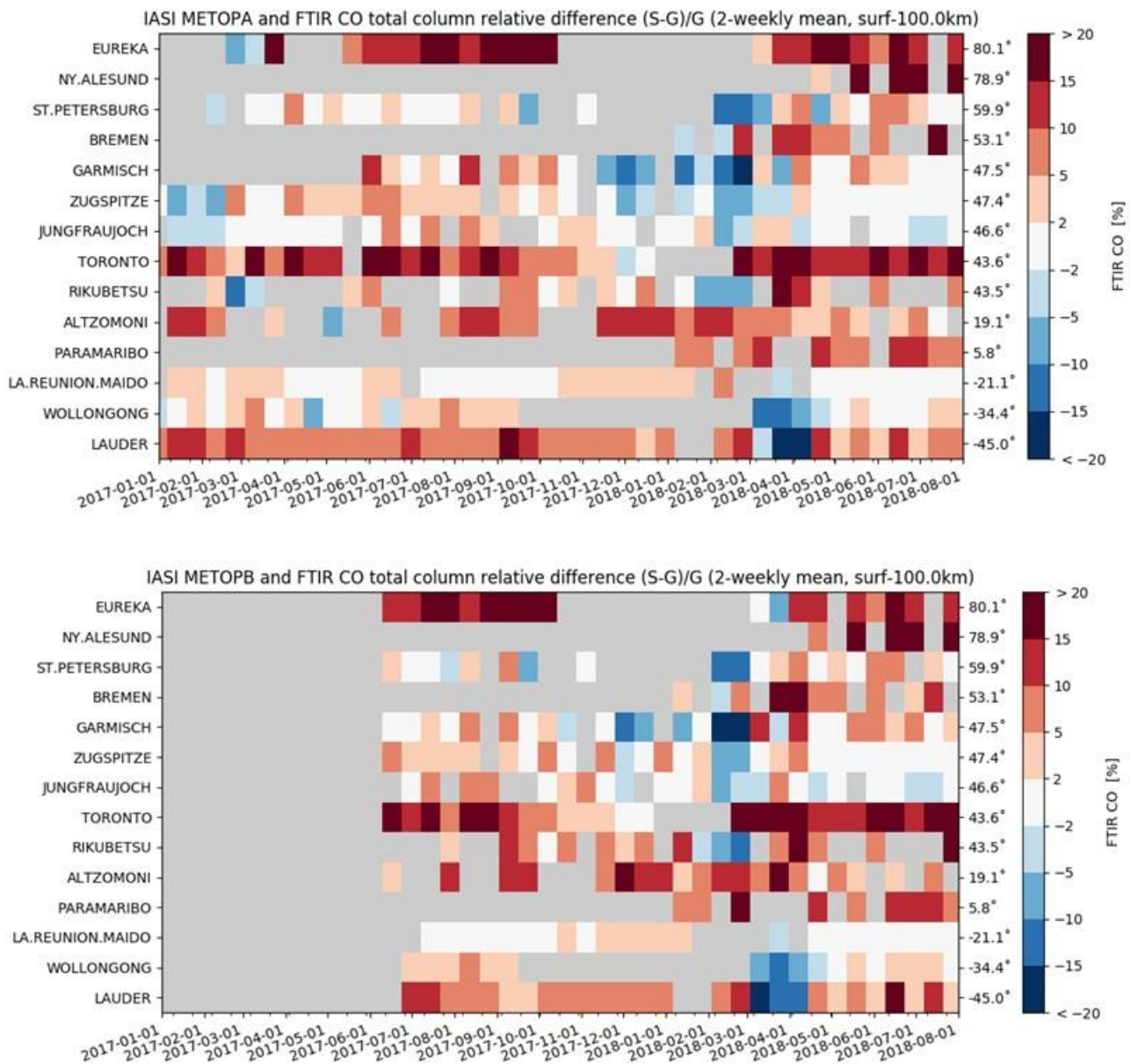


Figure 7.55. Time series of biweekly relative difference for IASI Metop-A (top) and IASI Metop-B (bottom).

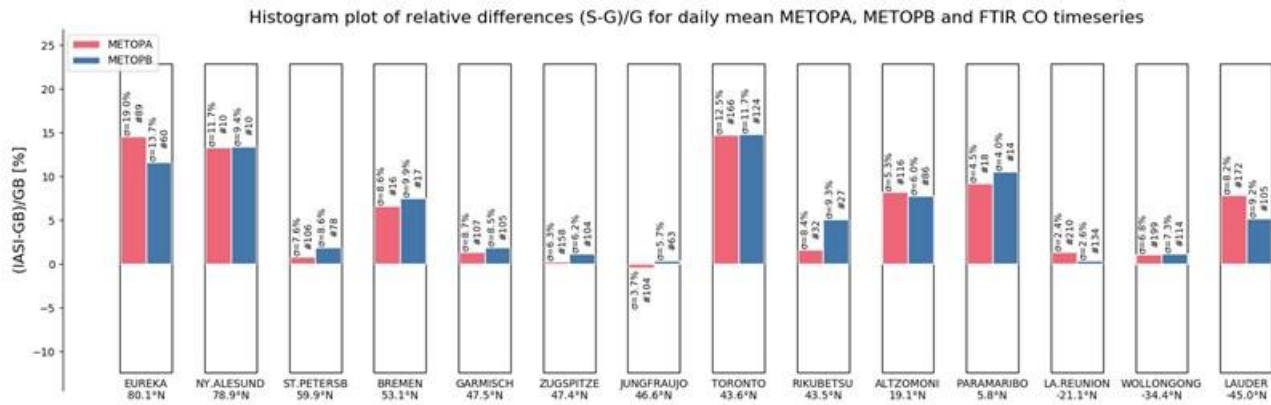


Figure 7.56. Relative mean differences (bias) for IASI Metop-A (red) and Metop-B (blue) CO total columns against 14 NDACC FTIR sites (decreasing latitude). Most sites have biases below 10 %.

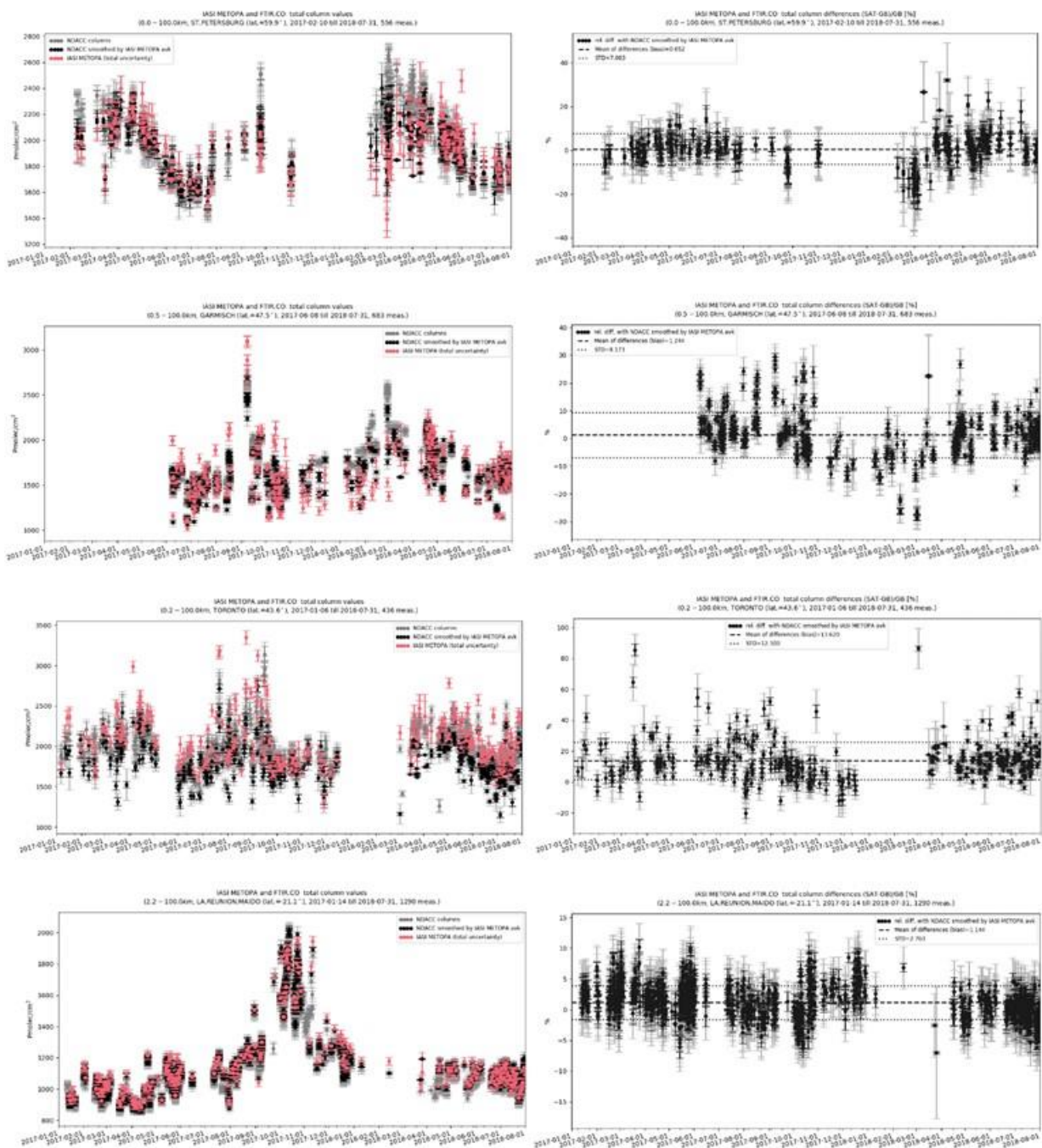


Figure 7.57. Time series of the IASI Metop-A CO total columns against 4 NDACC FTIR sites (from top to bottom: St. Petersburg, Garmisch, Toronto and Reunion Maito). Left: CO total columns time-series. To show the effect of the smoothing operation, the raw NDACC data are plotted in gray. Right: relative differences (in per cent) (the black error bar represents the random uncertainty component of the total error on the difference, the grey is the total (random + systematic) uncertainty on the relative difference).

Acknowledgments: The data used in this publication were obtained as part of the Network for the Detection of Atmospheric Composition Change (NDACC) and are publicly available (see <http://www.ndacc.org>)

Buchholz, R. R., Deeter, M. N., Worden, H. M., Gille, J., Edwards, D. P., Hannigan, J. W., Jones, N. B., Paton-Walsh, C., Griffith, D. W. T., Smale, D., Robinson, J., Strong, K., Conway, S., Sussmann, R., Hase, F., Blumenstock, T., Mahieu, E., and Langerock, B.: Validation of MOPITT carbon monoxide using ground-based Fourier transform infrared spectrometer data from NDACC, *Atmos. Meas. Tech.*, 10, 1927-1956, 2017.

<https://doi.org/10.5194/amt-10-1927-2017>

Ronsmans, G., Langerock, B., Wespes, C., Hannigan, J. W., Hase, F., Kerzenmacher, T., Mahieu, E., Schneider, M., Smale, D., Hurtmans, D., De Mazière, M., Clerbaux, C., and Coheur, P.-F.: First characterization and validation of FORLI-HNO₃ vertical profiles retrieved from IASI/Metop, *Atmos. Meas. Tech.*, 9, 4783-4801, 2016.

<https://doi.org/10.5194/amt-9-4783-2016>

8. List of AC SAF users

The institutes of registered users of AC SAF products are listed below.

FMI archive (orders via web page):

Europe:

- Turkish State Meteorological Service, Turkey (3 users)
- Central Institute for Meteorology and Geodynamics, Austria
- University of Lisbon, Portugal
- Finnish Meteorological Institute, Finland (8 users)
- EUMETSAT, Germany (10 users)
- Tomsk State University of Control Systems and Radioelectronics, Russia
- Rutherford Appleton Lab, UK (2 users)
- University of Trás-os-Montes and Alto Douro, Portugal (2 users)
- Academy of Sciences, Moldova
- University of Extremadura, Spain
- LATMOS/CNRS, France
- KNMI, the Netherlands (3 users)
- University of Oslo, Norway
- S[&]T Corporation, the Netherlands
- Norwegian Institute for Air Research, Norway (2 users)
- Oldenburg University, Germany
- LMD-IPSL-CNRS, France
- University of Lille, France
- Instituto Português do Mar e da Atmosfera, Portugal (2 users)
- Forschungszentrum Jülich GmbH, Germany (2 users)
- Danish Meteorological Institute, Denmark (2 users)
- University of Veterinary Medicine, Austria
- ARPA Valle d'Aosta, Italy
- Belgian Institute for Space Aeronomy, Belgium
- St.Petersburg State University, Russia
- Basque Meteorology Agency, Spain
- DWD, Germany (2 users)
- CNRS, France
- Universidade Nova de Lisboa, Portugal
- Institut Cartografic de Catalunya, Spain
- SMHI, Sweden
- University of Leicester, UK
- Universidade de Aveiro, Portugal
- Czech Hydrometeorological Institute, Czech Republic (3 users)
- Fedorov institute of applied geophysics, Russia
- Centre for Research in Environmental Epidemiology, Spain
- University of Bremen, Germany (4 users)
- LISA-CNRS, France
- Max Planck Institute for Chemistry, Germany (3 users)

- Planeta, Russia (3 users)
- Icelandic Meteorological Office, Iceland
- Hacettepe University, Turkey
- University College London, UK
- Ricardo-AEA, UK
- University of Leeds, UK
- University of Helsinki, Finland (3 users)
- State University, Belarus
- ULB, Belgium (2 users)
- CREAM-CSIC-UAB, Spain
- AUTH, Greece
- Flyby S.r.l., Italy
- Private individual, Germany
- DLR, Germany (2 users)
- Météo France, France (2 users)
- Institute of Global Climate and Ecology, Russia
- University of Athens, Greece
- Kastamonu University, Turkey
- Sistema GmbH, Austria
- Private individual, UK
- INCAS, Romania
- ask – Innovative Visualisierungslösungen GmbH, Germany
- University of Oxford, UK
- Manchester Metropolitan University, UK
- Heuristic Innovations LLC, Armenia
- University of Hamburg, Germany
- Institute of Atmospheric Physics (RAS), Russia
- Research Center of Ecological Safety, Russia
- University of Paris Est Creteil, France
- Satellite Applications Catapult, UK
- The Swedish Defence Research Agency
- Space Research and Technology Institute, Bulgaria
- Bulgarian Academy of Science, Bulgaria
- University of Konstanz, Germany
- Lasem, France
- University of Valencia, Spain
- University of Cologne, Germany
- Hungarian Academy of Sciences, Hungary
- Global Top Systems, Romania
- National Academy of Sciences, Belarus
- National University of Ireland Galway, Ireland
- Eötvös Loránd University, Hungary (2 users)
- University of Granada, Spain
- University of Alicante, Spain
- Federal Office for Radiation Protection, Germany
- Space Research and Technology Institute, Bulgaria

- Federal Research Center Krasnoyarsk Scientific Center of the Siberian Branch of the RAS, Russia
- National Meteorological Administration, Romania
- Parthenope University of Naples, Italy

Asia:

- The Energy and Resources Institute, India
- Science University of Malaysia, Malaysia
- Fudan University, China
- Indian Institute of Tropical Meteorology, India (2 users)
- China Meteorological Administration, China
- Nanjing University, China
- Asian Institute of Technology, Thailand
- China Academy of Sciences, China (5 users)
- Beijing Normal University, China
- Indian Space Research Organization, India
- National Atmospheric Research Laboratory, India (3 users)
- National Meteorological Satellite Center, South Korea
- Indian Institute of Technology Kanpur, India
- Anhui Institute of Meteorological Sciences, China
- Masdar Institute, United Arab Emirates
- The Chinese University of Hong Kong, China
- Zhejiang University, China (2 users)
- Meteorological Research Institute, Japan
- Peking University, China (2 users)
- Malaviya National Institute of Technology Jaipur, India
- University of Electronic Science and Technology of China, China
- Savitribai Phule Pune University, India
- University of Kalyani, India
- Jiangsu Meteorological Observatory, China
- Nanjing University of Information Science & Technology, China (2 users)
- Jawaharlal Nehru University, India
- Chinese Academy of Meteorological Sciences, China (3 users)
- National Central University, Taiwan
- Yonsei University, South Korea (3 users)
- Gwangju Institute of Science and Technology, South Korea (2 users)
- Anna University, India
- Indian Institute of Technology Roorkee, India
- Indian Space Research Organisation, India
- Chiba University, Japan
- Vikram Sarabhai Space Centre, India
- University of the Punjab, Pakistan
- Institute of Remote Sensing and Digital Earth, China
- Sun Yat-Sen University, China
- Indian Institute of Technology Kharagpur, India

Middle East:

- Tel Aviv University, Israel (3 users)
- Sultan Qaboos University, Oman
- Islamic Azad University, Iran (2 users)
- Private individual, Saudi Arabia

North America:

- University of Toronto, Canada
- NASA, USA (3 users)
- ADNET Systems Inc., USA
- Colorado State University, USA
- State of Wyoming, USA
- NOAA Air Resources Laboratory, USA
- Dartmouth College, USA
- Florida State University, USA
- NOAA/NESDIS, USA
- Michigan Technological University, USA (2 users)
- Trinity Consultants Inc., USA
- Environment Canada, Canada (2 users)
- Massachusetts Institute of Technology, USA
- Harvard-Smithsonian Center for Astrophysics, USA
- Dalhousie University, Canada
- University of Alaska, USA (2 users)
- Princeton University, USA
- U.S. Environmental Protection Agency, USA
- Naval Research Laboratory, USA
- University of California, USA
- University of Washington, USA
- University of Texas at Dallas, USA
- University of California, Riverside, USA
- SpaceKnow Inc., USA

South America:

- Universidad Nacional de Córdoba, Argentina
- Instituto Politecnico Nacional, Mexico
- Universidade Federal de Alagoas, Brazil
- LAPIS, Brazil
- Universidad EAFIT, Colombia
- Universidad de la República, Uruguay

Australia:

- University of Southern Queensland
- Australian National University
- University of Melbourne (2 users)

Africa:

- EMA, Egypt

- Addis Ababa University, Ethiopia

Registered users: **227**

FMI archive (orders via EUMETSAT Data Centre):

Europe:

- EUMETSAT, Germany (5 users)
- Hungarian Meteorological Service, Hungary
- DLR, Germany
- Rutherford Appleton Laboratory, UK
- Norwegian Institute for Air Research, Norway
- Royal Meteorological Institute, Belgium
- University of Wrocław, Poland
- Centre for Solar Energy and Hydrogen Research Baden-Württemberg, Germany
- CNRS, France
- AUTH, Greece
- BIRA-IASB, Belgium
- Private individual, Poland
- Météo-France, France
- Technical University of Denmark, Denmark
- Institute of Global Climate and Ecology, Russia
- Vilnius University, Lithuania
- Private individual, Austria
- École Polytechnique, France
- Czech Hydrometeorological Institute, Czech Republic
- University of Valencia, Spain
- University of Reading, UK
- Hungarian Academy of Sciences, Hungary
- Private individual, UK
- University of Bremen, Germany
- Max Planck Institute for Chemistry, Germany (2 users)
- Institute of Atmospheric Sciences and Climate, Italy
- CREA – Council for agricultural research and agricultural economics analysis, Italy
- “University/Research Institute”, Austria
- University of Cologne, Germany
- Hacettepe University, Turkey
- “Education”, Hungary
- University of Lille, France
- Satavia Ltd., UK
- Ministry of the Environment, Estonia
- “Researcher”, Russia

North America:

- Colorado State University, USA
- Harvard University, USA

South America:

- “Education”, Peru

Middle East:

- Private individual, Saudi Arabia
- Private individual, Israel
- “National Institution”, Iran
- “Researcher”, Iran

Asia:

- National Central University, Taiwan
- Yonsei University, South Korea
- Indian Institute of Technology Madras, India
- “Researcher”, South Korea
- “Researcher”, Iran
- China Meteorological Administration, China
- Nanjing University, China
- Centre for Earth and Space Sciences, India
- Sun Yat-Sen University, China
- “Education”, China (2 users)

Africa:

- “Education”, Kenya
- “Education”, Algeria
- Al-Azhar University, Egypt
- “Researcher”, Morocco
- Addis Ababa University, Ethiopia
- “Education”, Morocco
- “Education”, Niger

Registered users: **74**

DLR archive (orders via ATMOS ftp service):

Europe:

- BIRA-IASB, Belgium (5 users)
- DLR, Germany (3 users)
- KNMI, the Netherlands (3 users)
- FMI, Finland (5 users)
- AUTH, Greece (2 users)
- DWD, Germany
- WMO, Switzerland
- University of Extremadura, Spain (2 users)
- Forschungszentrum Jülich, Germany (2 users)
- ECMWF, UK (3 users)
- CNRS, France
- EUMETSAT, Germany (9 users)

- University of Leicester, UK
- University of Bremen, Germany (4 users)
- University of Hannover, Germany
- Heidelberg University, Germany
- Science and Technology Facilities Council, UK
- KMI, Belgium
- Max Planck Institute for Chemistry, Germany (3 users)
- MetOffice, UK
- University of Valencia, Spain
- SMHI, Sweden
- CREA-FCIC, Spain
- Instituto Português do Mar e da Atmosfera, Portugal
- Czech Hydrometeorological Institute, Czech Republic (2 users)
- Laboratoire Interuniversitaire des Systèmes Atmosphériques, France
- Planeta, Russia
- Private individual, Iceland
- Mapographics AS, Norway
- Hacettepe University, Turkey
- University of Cologne, Germany
- Universitat Politècnica de València, Spain
- Private individual, Germany
- Ricardo-AEA, UK
- University of Leeds, UK
- Flyby S.r.l., Italy
- Météo France, France
- Institute of Global Climate and Ecology, Russia
- University of Athens, Greece
- ULB, Belgium
- LATMOS, France
- Kastamonu University, Turkey
- Sistema GmbH, Austria
- Private individual, UK
- ask – Innovative Visualisierungslösungen GmbH, Germany
- University of the Basque Country, Spain
- Satellite Applications Catapult, UK
- The Swedish Defence Research Agency (3 users)
- Space Research and Technology Institute, Bulgaria
- Lasem, France
- University of Cologne, Germany
- Global Top Systems, Romania
- University of Trás-os-Montes and Alto Douro, Portugal
- National Academy of Sciences, Belarus
- National University of Ireland Galway, Ireland
- Turkish State Meteorological Service, Turkey
- University of Granada, Spain (2 users)
- University of Alicante, Spain

- Space Research and Technology Institute, Bulgaria
- University of Helsinki, Finland (2 users)
- National Meteorological Administration, Romania

Asia:

- Peking University, China (2 users)
- China Academy of Sciences, China (6 users)
- Indian Space Research Organization, India
- Seoul National University, South Korea (2 users)
- National Meteorological Satellite Center, South Korea
- Anhui Institute of Meteorological Sciences, China
- The Chinese University of Hong Kong, China
- Zhejiang University, China
- Japan Meteorological Agency, Japan
- Indian Institute of Tropical Meteorology, India
- Malaviya National Institute of Technology Jaipur, India
- Savitribai Phule Pune University, India
- University of Kalyani, India
- Jiangsu Meteorological Observatory, China
- State Environmental Protection Key Lab of Satellite Remote Sensing, China
- Zhejiang Academy of Agricultural Sciences, China
- Anhui Institute of Optics and Fine Mechanics, China
- Jawaharlal Nehru University, India
- Yonsei University, South Korea (2 users)
- Gwangju Institute of Science and Technology, South Korea (2 users)
- Anna University, India
- Indian Institute of Technology Roorkee, India
- Indian Space Research Organisation, India
- Chiba University, Japan
- Chinese Academy of Meteorological Sciences, China
- Nanjing University, China
- University of the Punjab, Pakistan
- Institute of Remote Sensing and Digital Earth, China
- Kyushu University, Japan
- Indian Institute of Technology Kharagpur, India

Middle East:

- Islamic Azad University, Iran
- Masdar Institute, United Arab Emirates
- University of Tehran, Iran
- Khavaran Institute of Higher Education, Iran
- Private individual, Iran
- Private individual, Saudi Arabia

North America:

- NASA, USA (6 users)
- Environment and Climate Change Canada, Canada (5 users)

- NOAA, USA (3 users)
- University of Houston, USA
- Harvard University, USA (2 users)
- Florida State University, USA
- University of Minnesota, USA
- Michigan Technological University, USA
- Trinity Consultants Inc., USA
- Massachusetts Institute of Technology, USA
- University of Wisconsin-Madison, USA
- Johns Hopkins University, USA
- University of North Carolina at Chapel Hill, USA
- University of Alaska, USA (2 users)
- Princeton University, USA
- U.S. Environmental Protection Agency, USA
- University of California, USA
- University of Washington, USA
- University of Maryland, USA
- SpaceKnow Inc., USA

South America:

- Instituto Politecnico Nacional, Mexico
- Universidade Federal de Alagoas, Brazil
- LAPIS, Brazil
- University of São Paulo, Brazil
- Universidad EAFIT, Colombia
- Universidad de la República, Uruguay

Australia:

- Environmental Systems & Services
- University of Southern Queensland
- University of Melbourne (2 users)

Africa:

- National Center for Meteorological Research, Morocco
- EMA, Egypt
- Imo State University, Nigeria

Registered users: **190**

DMI (NUV/CLEAR product via ftp):

- Meteorological Institute of Romania
⇒ Several commercial companies obtain the data from MIR
- Danish Meteorological Institute, Denmark
- TrygFonden, Denmark
- Department for Health, Greenland Homerule
- The Danish Cancer Society, Denmark
- Libraries of Hjørring Community
- RayMio
- Richard McKenzie, New Zealand
- Elian Wolfram, Laser Research Center and Applications, Argentina

Registered users: **8****KNMI (unofficial NRT AAI via ftp):**

- FMI, Finland
- William B. Hanson Center for Space Science, USA
- University of Leicester, UK

Registered users: **3****Known international projects that use EUMETCast or WMO/GTS:**

- MACC project
- SACS service
- Temis WWW service
- ESA GlobVapour
- ESA CCI Ozone project

EUMETCast: (users by country)

Albania	4	Iran, Islamic Republic of	31	Portugal	4
Algeria	4	Iraq	2	Qatar	3
Angola	1	Ireland	4	Romania	5
Armenia	1	Isle of Man	1	Russian Federation	7
Austria	15	Israel	5	Rwanda	1
Azerbaijan	3	Italy	255	San Marino	1
Belgium	9	Ivory Coast	1	Saudi Arabia	2
Benin	1	Jordan	1	Senegal	4
Bosnia and Herzegovina	1	Kazakhstan	5	Serbia	2
Botswana	4	Kenya	5	Slovakia	3
Brazil	2	Kuwait	2	Slovenia	1
Bulgaria	2	Kyrgyzstan	1	Somalia	1
Burkina Faso	1	Latvia	1	South Africa	6
Cameroon	1	Lebanon	3	South Sudan	1
Canada	1	Lesotho	2	Spain	38
China	3	Libya	1	Swaziland	1

Congo	1	Lithuania	2	Sweden	3
Congo, Democratic Republic of	1	Luxembourg	1	Switzerland	9
Croatia	1	Macedonia, FYR of	1	Tajikistan	1
Cyprus	1	Madagascar	3	Tanzania, United Republic of	2
Czech Republic	16	Malawi	2	Togo	1
Denmark	5	Mali	1	Tunisia	1
Egypt	2	Malta	2	Turkey	6
Estonia	3	Mauritania	2	Turkmenistan	1
Ethiopia	3	Moldova, Republic of	1	Uganda	2
Finland	4	Morocco	1	Ukraine	2
France	49	Mozambique	2	United Arab Emirates	1
Germany	78	Namibia	1	United Kingdom	94
Ghana	4	The Netherlands	20	United States	2
Greece	13	Niger	1	Uzbekistan	1
Guinea-Bissau	2	Nigeria	3	Vietnam	1
Hungary	10	Norway	2	Yemen	1
Iceland	1	Oman	1	Zambia	3
India	1	Poland	10	Zimbabwe	2
TOTAL (July 2018)	837				

9. Updates during the reporting period

Listed below are the major configuration updates concerning operational data processing and archiving. If new versions of relevant AC SAF documents are released during the reporting period, they should be listed here also.

9.1. Software updates

No software updates.

9.2. Hardware updates

No hardware updates.

9.3. Documentation updates

16 January:	KNMI: OPERA Software release note (software version 1.50)
16 January:	FMI: Software version document (issue 1.1)
7 March:	FMI: AC SAF Operations Report 2/2017 rev.1
26 March:	ULB: NRT IASI SO ₂ Product User Manual (issue 1.2)
29 March:	KNMI: Aerosol product Algorithm Theoretical Basis Document (issue 2.41)
16 April:	KNMI: Ozone profiles Algorithm Theoretical Basis Document (issue 2.0)
19 April:	FMI: AC SAF Service Specification (issue 1.1)
27 June:	FMI: AC SAF Product Requirements Document (issue 1.3)

10. Changes and usage statistics of the web portal

Listed below are the major changes in the appearance and content on the AC SAF main web pages (<https://acsaf.org/>). Additionally some web page usage statistics gathered by Google Analytics are listed.

10.1. Changes in appearance and content

Table 10.1. Changes in appearance and content of the main AC SAF web portal during the reporting period

Date	Description
10 January	AC SAF web portal switched to use secure HTTPS protocol, access is via https://acsaf.org
23 February	GOME-2 NO ₂ and H ₂ O thematic climate data records added to https://acsaf.org/datarecord_access.html Info page for NO ₂ and H ₂ O TCDRs created: https://acsaf.org/datarecords/no2_h2o_tcdr.html
21 March	Visiting Scientist final report from A. Arellano, Jr. added to https://acsaf.org/VSreports.html
12 June	GOME-2 vertical ozone profile quality assessment pages https://acsaf.org/ozone_qa/ republished after OMPS limb profile update to version 2.5

In addition to updates above, following routine updates are conducted whenever necessary:

- The links to public AC SAF user documents are updated whenever new documents or new versions of existing documents become available
- The “top story” on the front page is updated
- News list on the front page is updated

10.2. Web page statistics

Google Analytics tracking service continuously monitors AC SAF web portal usage. Following diagrams and tables present some statistics gathered during the reporting period.

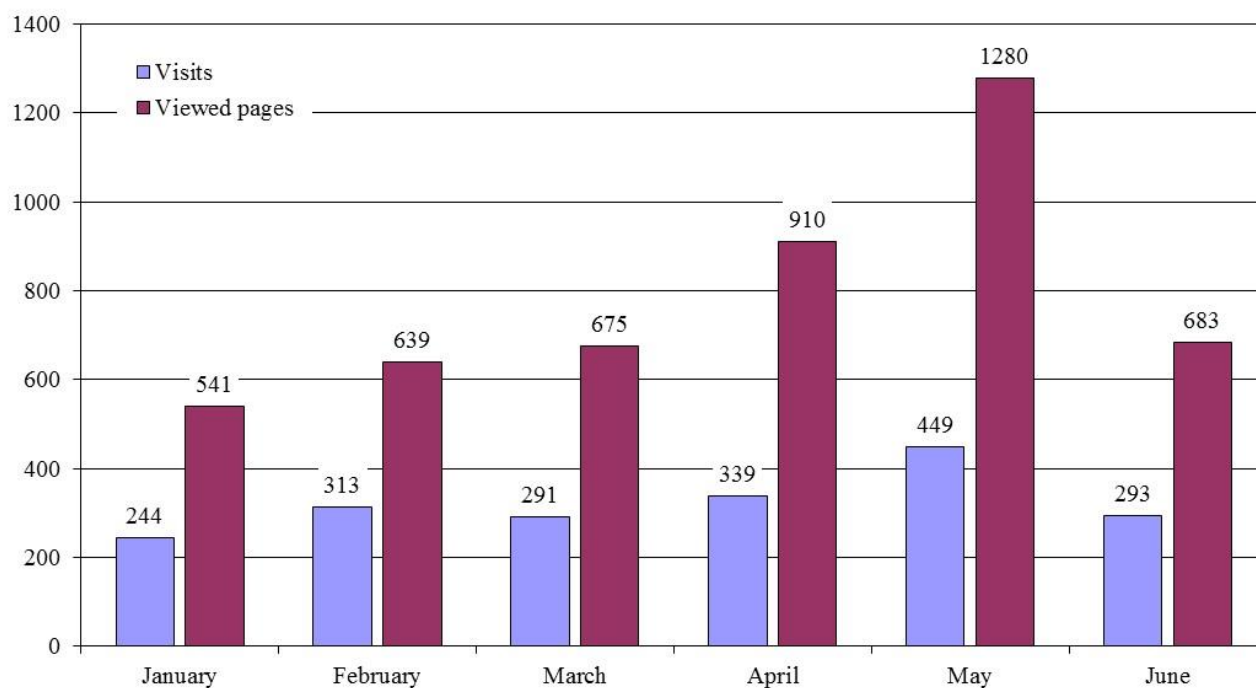


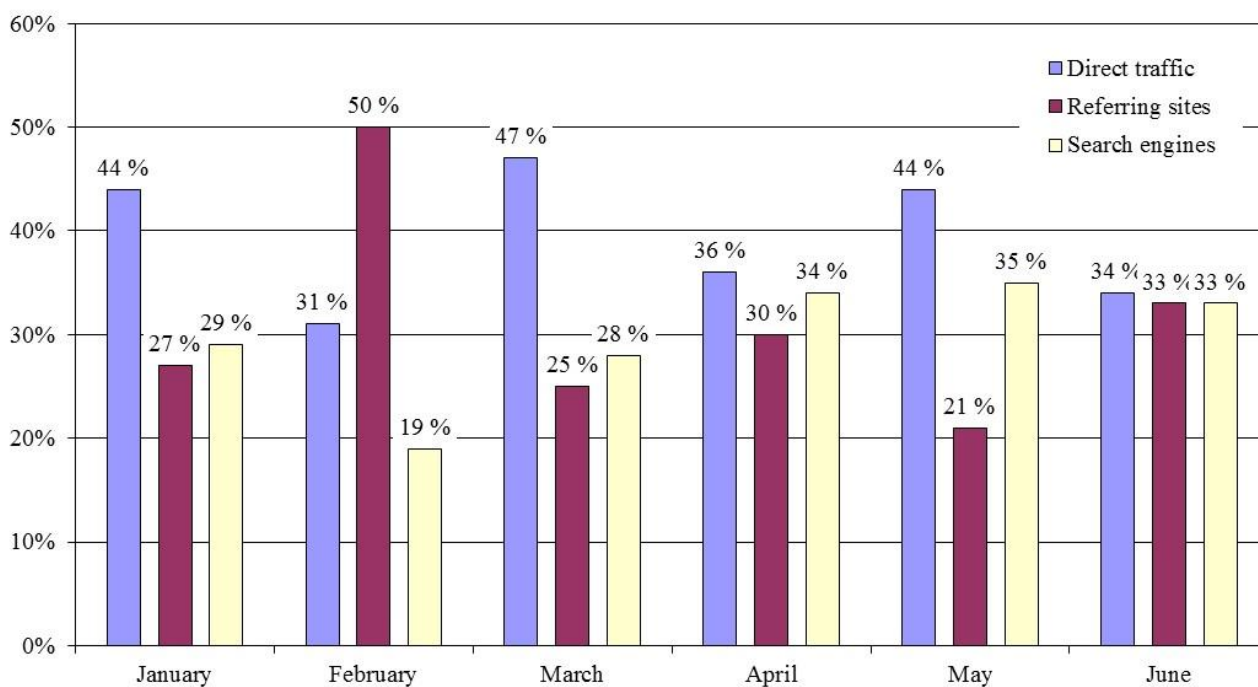
Figure 10.1. Individual visits to the web portal and number of viewed pages

Table 10.2. TOP 5 visiting countries (number of visits in brackets)

January	Germany (20)	USA (18)	Finland (12)	China (10)	Belgium (9)
February	USA (67)	Germany (37)	UK (11)	Netherlands (11)	Finland (8)
March	Germany (27)	USA (26)	Finland (23)	China (9)	Czechia (6)
April	Germany (24)	Finland (18)	USA (18)	Belgium (16)	China (14)
May	Germany (32)	USA (32)	Finland (25)	Greece (12)	Belgium (11)
June	Germany (28)	USA (25)	Finland (12)	Belgium (9)	Netherlands (8)
Σ	USA (182)	Germany (130)	Finland (66)	China (47)	UK (37)

Table 10.3. TOP 5 pages (number of views in brackets)

January	index (218)	offline_access (53)	datarecord_access (25)	nrt_access (23)	products_nap (20)
February	index (247)	nrt_access (52)	offline_access (38)	datarecord_access (22)	index (247)
March	index (226)	offline_access (105)	products/nto_o3 (37)	product_list (36)	index (226)
April	index (262)	offline_access (90)	nrt_access (60)	products/nhp (37)	datarecord_access (33)
May	index (304)	offline_access (120)	nrt_access (110)	products/nhp (80)	datarecord_access (63)
June	index (177)	nrt_access (63)	offline_access (37)	products/nhp (33)	products/iasi_co (30)
Σ	index (1434)	offline_access (443)	nrt_access (330)	datarecord_access (194)	products/nhp (186)

**Figure 10.2. Traffic sources by type**

APPENDIX 1

Table A.1 presents the overall summary of orders from AC SAF archive at FMI, sorted by product types, during the reporting period

Table A.2 presents a detailed summary of product orders from AC SAF archive at FMI during the reporting period.

Table A.1. Overall summary of product orders, by product type, during the reporting period

Product type	Number of orders	Number of users	Number of products	Total size
OOP-A	3	3	1320	43.7 GB
OOP-B	2	2	68	2.26 GB
OHP-A	25	9	15705	3.97 TB
OHP-B	8	6	1043	262 GB
ARS-A	12	6	2148	1.86 GB
ARS-B	9	6	3954	3.60 GB
ARP-A	60	17	7064	43.7 GB
ARP-B	51	23	1533	9.65 GB
OUV-A	2	2	880	36.5 GB
OUV-B	7	5	384	1.95 GB
LER-MSC-A	0	-	-	-
LER-PMD-A	0	-	-	-
LER-MSC-B	0	-	-	-
LER-PMD-B	0	-	-	-

Table A.2. More detailed summary of product orders during the reporting period

JANUARY				
Product type	Number of products	Order size	Order source	Institute / company
ARS-A ARS-B	14 15	26.2 MB	EDC	“Education”, Niger
ARS-A ARS-B	15 15	26.3 MB	EDC	“Education”, Niger
ARS-A ARS-B	15 15	26.3 MB	EDC	“Education”, Niger
OHP-A OHP-B	2 2	1.01 GB	EDC	“Researcher”, Morocco
ARP-A	29	180 MB	WWW	FMI, Finland
ARP-B	29	181 MB	WWW	FMI, Finland

ARP-A	14	86.5 MB	WWW	FMI, Finland
ARP-B	15	93.5 MB	WWW	FMI, Finland
ARP-A-R1	16	90.2 MB	EDC	Max Planck Institute for Chemistry, Germany
ARP-A-R1	16	90.2 MB	EDC	Max Planck Institute for Chemistry, Germany
ARP-A	3	18.8 MB	WWW	FMI, Finland
ARP-B	4	25.0 MB	WWW	FMI, Finland
ARS-A	294	263 MB	WWW	Institute of Remote Sensing and Digital Earth, China
ARS-B	297	271 MB	WWW	Institute of Remote Sensing and Digital Earth, China
ARS-A	438	391 MB	WWW	Institute of Remote Sensing and Digital Earth, China
ARS-A	438	391 MB	WWW	Institute of Remote Sensing and Digital Earth, China
OHP-A OHP-B	67 67	33.8 GB	EDC	Centre for Earth and Space Sciences, India
OHP-A OHP-B	67 67	33.8 GB	EDC	Centre for Earth and Space Sciences, India
OOP-A OOP-B	67 67	4.45 GB	EDC	Centre for Earth and Space Sciences, India
OHP-A OHP-B	2 2	1.01 GB	EDC	Centre for Earth and Space Sciences, India
FEBRUARY				
Product type	Number of products	Order size	Order source	Institute / company
ARP-B	14	86.5 MB	WWW	FMI, Finland
ARP-A	15	92.6 MB	WWW	FMI, Finland
OUV-B	7	334 MB	EDC	“Education”, Peru
OUV-B	7	334 MB	EDC	“Education”, Peru
OUV-B	1	47.7 MB	EDC	“Education”, Peru
OUV-B	1	47.7 MB	EDC	“Education”, Hungary
OUV-B	1	47.7 MB	EDC	University of Lille, France
ARP-A ARP-B	13 14	167 MB	EDC	University of Lille, France
OHP-A OHP-B	13 14	6.79 GB	EDC	University of Lille, France
MARCH				
Product type	Number of products	Order size	Order source	Institute / company
ARP-A	30	186 MB	WWW	FMI, Finland

ARP-B	31	196 MB	WWW	FMI, Finland
ARP-B	1	6.15 MB	WWW	FMI, Finland
ARP-A	1	6.30 MB	WWW	FMI, Finland
ARP-A	31	191 MB	WWW	FMI, Finland
ARP-B	32	203 MB	WWW	FMI, Finland
ARP-A	4	24.6 MB	WWW	FMI, Finland
ARP-B	4	25.5 MB	WWW	FMI, Finland
OOP-A	19	713 MB	EDC	Sun Yat-Sen University, China
ARP-A	14	86.5 MB	WWW	FMI, Finland
ARP-B	14	88.1 MB	WWW	FMI, Finland
ARP-B	6	38.8 MB	WWW	FMI, Finland
ARP-A	5	31.4 MB	WWW	FMI, Finland
ARP-B	41	263 MB	WWW	FMI, Finland
ARP-A	42	260 MB	WWW	FMI, Finland
ARP-B	12	77.1 MB	WWW	FMI, Finland
ARP-A	12	74.1 MB	WWW	FMI, Finland
APRIL				
Product type	Number of products	Order size	Order source	Institute / company
OHP-A	425	106 GB	EDC	“Education”, China
OOP-A	1234	40.8 GB	EDC	“Education”, China
OHP-A OHP-B	19 18	9.28 GB	EDC	Forschungszentrum Jülich, Germany
ARS-B	1	948 kB	EDC	Forschungszentrum Jülich, Germany
ARP-B	1	6.69 MB	EDC	Forschungszentrum Jülich, Germany
OOP-B	1	33.1 MB	EDC	Forschungszentrum Jülich, Germany
ARP-B	411	2.59 GB	WWW	FMI, Finland
ARP-A	413	2.55 GB	WWW	FMI, Finland
ARP-A-R1	182	1.03 GB	WWW	FMI, Finland
ARP-A-R1	98	618 MB	WWW	FMI, Finland
ARP-A ARP-B	4 3	43.4 MB	EDC	Satavia Ltd., UK
ARP-A ARP-B	13 13	163 MB	EDC	Satavia Ltd., UK
ARP-B	27	172 MB	WWW	FMI, Finland

ARP-A	28	175 MB	WWW	FMI, Finland
ARS-A ARS-B	10 9	17.2 MB	EDC	“Researcher”, Morocco
ARS-A ARS-B	4 4	7.34 MB	EDC	“Researcher”, Morocco
ARP-A	1	6.25 MB	WWW	University of Helsinki, Finland
ARP-A-R1	1	5.62 MB	WWW	University of Helsinki, Finland
ARP-A-R1	1	5.69 MB	WWW	University of Helsinki, Finland
ARP-A-R1	5	28.2 MB	WWW	University of Helsinki, Finland
MAY				
Product type	Number of products	Order size	Order source	Institute / company
ARP-A-R1	2	11.4 MB	WWW	University of Helsinki, Finland
ARP-A-R1	2	11.4 MB	WWW	University of Helsinki, Finland
ARP-A-R1	2	11.4 MB	WWW	University of Helsinki, Finland
ARP-A-R1	2	11.4 MB	WWW	University of Helsinki, Finland
ARP-A-R1	2	11.4 MB	WWW	University of Helsinki, Finland
ARP-A-R1	2	11.4 MB	WWW	University of Helsinki, Finland
ARP-A-R1	2	11.4 MB	WWW	University of Helsinki, Finland
ARP-A-R1	3	17.0 MB	WWW	University of Helsinki, Finland
ARP-B	14	89.0 MB	WWW	FMI, Finland
ARP-A	13	80.9 MB	WWW	FMI, Finland
ARP-A	43	268 MB	WWW	FMI, Finland
ARP-B	84	533 MB	WWW	FMI, Finland
ARP-A	42	262 MB	WWW	FMI, Finland
OUV-B	366	1.14 GB	WWW	University of California, Riverside, USA
ARP-B	55	349 MB	WWW	FMI, Finland
ARP-A	55	341 MB	WWW	FMI, Finland
ARP-A	100	616 MB	WWW	FMI, Finland
ARP-B	99	618 MB	WWW	FMI, Finland
OHP-B	863	216 GB	WWW	Jiangsu Meteorological Observatory, China
OHP-A	877	218 GB	WWW	Jiangsu Meteorological Observatory, China
OHP-A	865	216 GB	WWW	Jiangsu Meteorological Observatory, China
ARS-A-R1	438	365 MB	EDC	Ministry of the Environment, Estonia
ARS-A-R1	438	365 MB	EDC	Ministry of the Environment, Estonia

ARP-B-R1	27	154 MB	WWW	Naval Research Laboratory, USA
ARP-B	112	710 MB	WWW	FMI, Finland
ARP-A	5277	32.7 GB	WWW	FMI, Finland
OHP-A OHP-B	10 10	4.99 GB	EDC	“Private individual”, USA
OHP-A	1	250 MB	WWW	University of Helsinki, Finland
ARP-B	27	172 MB	WWW	FMI, Finland
OHP-A	862	213 GB	WWW	Jiangsu Meteorological Observatory, China
OHP-A	426	106 GB	WWW	Jiangsu Meteorological Observatory, China
OHP-A	439	110 GB	WWW	Jiangsu Meteorological Observatory, China
OHP-A	864	214 GB	WWW	Jiangsu Meteorological Observatory, China
OHP-A	877	219 GB	WWW	Jiangsu Meteorological Observatory, China
ARP-A	70	435 MB	WWW	FMI, Finland
OHP-A	1728	432 GB	WWW	Jiangsu Meteorological Observatory, China
OHP-A	1302	314 GB	WWW	Jiangsu Meteorological Observatory, China
JUNE				
Product type	Number of products	Order size	Order source	Institute / company
OHP-A	1742	492 GB	WWW	Jiangsu Meteorological Observatory, China
OHP-A	861	207 GB	WWW	Jiangsu Meteorological Observatory, China
ARP-B	181	1.15 GB	WWW	FMI, Finland
ARP-A	195	1.22 GB	WWW	FMI, Finland
OHP-A	426	106 GB	WWW	Jiangsu Meteorological Observatory, China
OHP-A	833	208 GB	WWW	Jiangsu Meteorological Observatory, China
OHP-A	849	213 GB	WWW	Jiangsu Meteorological Observatory, China
OHP-A	1724	432 GB	WWW	Jiangsu Meteorological Observatory, China
ARP-A	84	525 MB	WWW	FMI, Finland
ARP-B	85	543 MB	WWW	FMI, Finland
OUV-A	879	36.5 GB	EDC	“Researcher”, Russia
ARS-B	3597	3.27 GB	WWW	Indian Institute of Technology Kharagpur, India
ARP-A	99	619 MB	WWW	FMI, Finland
ARP-B	100	635 MB	WWW	FMI, Finland
ARP-A	1	6.30 MB	WWW	FMI, Finland
ARP-B	2	12.5 MB	WWW	FMI, Finland

ARP-A	15	93.8 MB	WWW	FMI, Finland
ARP-B	14	89.3 MB	WWW	FMI, Finland
OHP-A	424	115 GB	WWW	Jiangsu Meteorological Observatory, China
OUV-B	1 Selected subset: UVI Region: 20-32E, 58-70N (43.2 kB in total)		WWW	FMI, Finland
ARP-A	14	87.9 MB	WWW	FMI, Finland
ARP-B	14	89.3 MB	WWW	FMI, Finland
ARP-A	14	87.9 MB	WWW	FMI, Finland
ARP-B	14	89.3 MB	WWW	FMI, Finland
OUV-A	1 Region: 18-33E, 59-71N (227 kB in total)		WWW	FMI, Finland

APPENDIX 2

Table A.3 presents a detailed summary of failed product orders from AC SAF archive at FMI during the reporting period. The middle column indicates whether the failure was related to problems with AC SAF archive and/or ordering system or was the problem on the user's side.

Table A.3. Summary of failed product orders during the reporting period

Date	Error type	Failure description and details
	N/A	Origin: Order ID: User institute: Order contents: Ordering log error message: ‘ Failure description: Corrective action: Final outcome: